



Spatial heterogeneity in microglial ultrastructural alterations in the APP-PS1 mouse model of Alzheimer's disease amyloid pathology

Mémoire

Hassan El Hajj

Maîtrise en neurobiologie - avec mémoire
Maître ès sciences (M. Sc.)

Québec, Canada

© Hassan El Hajj, 2019

Résumé

Les principales caractéristiques de la maladie d'Alzheimer (MA) sont le dépôt de plaques amyloïdes ($A\beta$) extracellulaires et les enchevêtrements neurofibrillaires intracellulaires composés de protéines tau. À mesure que la maladie progresse, la mort neuronale et une diminution de la densité synaptique sont observées, parallèlement à une augmentation de la neuroinflammation et du dysfonctionnement immunitaire. Le processus de neuroinflammation est étroitement lié à la présence de plaques $A\beta$ et peut affecter les interactions microgliales avec les structures neuronales tout au long de la progression de la maladie. L'activation substantielle et chronique des microglies déclenchée par la présence d' $A\beta$ est supposée affecter l'homéostasie cérébrale en raison d'une altération des actions physiologiques microgliales, notamment au niveau des synapses. Ici, nous visons à générer de nouvelles connaissances sur l'implication microgliale dans la physiopathologie de la MA en combinant la microscopie optique et électronique pour étudier l'ultrastructure microgliale et les interactions neuronales / synaptiques en relation avec le dépôt de plaques $A\beta$. Des souris APP-PS1 âgées de 14 mois ont été étudiées en même temps que des témoins appariés selon l'âge. En outre, des sections de la MA humaine post-mortem ont également été examinées dans notre étude. Dans nos expériences, les plaques $A\beta$ ont été visualisées en utilisant du méthoxy-XO4 qui se lie sélectivement et irréversiblement aux feuilles d' $A\beta$ et permet leur détection en microscopie optique. De plus, l'immunocoloration post-mortem de la microglie avec le marqueur de la molécule adaptatrice de fixation du calcium ionisée (IBA1) et un traitement supplémentaire pour la microscopie électronique à transmission ont permis d'étudier la microglie à différentes proximités des plaques. Nos analyses ultrastructurelles ont révélé des différences significatives dans les activités phagocytaires et les caractéristiques morphologiques. Les corps cellulaires microgliaux de l'APP-PS1 avaient une surface et un périmètre significativement supérieurs à ceux des témoins de type sauvage et présentaient des signes de stress et une activité phagocytaire diminuée. Ces signes de stress et de phagocytose altérée ont également été observés dans les prolongements microgliaux des échantillons APP-PS1. De plus, les microglies présentaient divers phénotypes morphologiques et réactions cellulaires physiologiques selon leur proximité des plaques. Les corps des cellules microgliales proches des plaques étaient plus

larges en surface et en périmètre que les témoins de type sauvage et les autres régions APP-PS1 situées plus loin des plaques. Les microglies proches des plaques étaient plus susceptibles de contenir des dépôts A β et moins susceptibles de contenir ou d'encercler des éléments neuronaux. En outre, elles présentaient des signes de stress caractérisés par des corps cellulaires assombris et un réticulum endoplasmique dilaté. Tous ces résultats définissent les changements radicaux qui se produisent au niveau ultrastructural dans le cerveau en réponse à la déposition A β .

Abstract

The main hallmarks of Alzheimer's disease (AD) are the deposition of extracellular amyloid (A β) plaques and intracellular neurofibrillary tangles composed of tau protein. As the disease progresses, neuronal death and decreased synaptic density is observed, concurrent with an increase of neuroinflammation and immune dysfunction. The process of neuroinflammation is tightly linked to the presence of A β plaques and may affect microglial interactions with neuronal structures throughout disease progression. Substantial and chronic microglial activation triggered by the presence of A β is suspected to affect brain homeostasis due to an alteration of microglial physiological actions, notably at synapses. Here we aim to generate new insights regarding microglial implication in AD pathophysiology by combining light and electron microscopy to study microglial ultrastructure and neuronal/synaptic interactions with relation to A β plaque deposition. 14 months old APP-PS1 mice were studied alongside age-matched controls. Also, post-mortem human AD sections were examined in our study. In our experiments, A β plaques were visualized using Methoxy-XO4 which binds selectively and irreversibly to A β sheets and allows their detection under light microscopy. Furthermore, post-mortem immunostaining of microglia with the ionized calcium-binding adapter molecule 1 (IBA1) marker and additional processing for transmission electron microscopy allowed the study of microglia at different proximities to the plaques. Our ultrastructural analyses revealed significant differences in phagocytic activities and morphological features. Microglial cell bodies in APP-PS1 were significantly larger in area and perimeter compared to wild-type controls and displayed signs of stress and decreased phagocytic activity. These signs of stress and impaired phagocytosis were also found in microglial processes in the APP-PS1 samples. Additionally, microglia showed diverse morphological phenotypes and physiological cell reactions dependent on their proximity to plaques. Microglial cell bodies near plaques were larger in area and perimeter compared to wild-type controls and other APP-PS1 regions located farther from plaques. Microglia near plaques were more likely to contain A β and less likely to contain or encircle neuronal elements. Also, they presented signs of stress characterized by darkened cell bodies and dilated

endoplasmic reticulum. All these findings define the drastic changes that are taking place at ultrastructural level in the brain in response to A β deposition.

Table of contents

RÉSUMÉ.....	II
ABSTRACT.....	IV
TABLE OF CONTENTS.....	VI
LIST OF TABLES.....	IX
LIST OF FIGURES.....	X
ABBREVIATIONS.....	XII
ACKNOWLEDGMENTS.....	XV
FOREWORD.....	XVII
1. INTRODUCTION.....	1
1.1. ALZHEIMER’S DISEASE.....	1
1.1.1 Neurofibrillary tangles.....	3
1.1.2 Amyloid beta.....	4
1.1.3 Oxidative stress.....	7
1.1.4 Neuronal calcium homeostasis.....	8
1.2 APP MICE MODELS IN AD.....	8
1.3 AMYLOID CASCADE HYPOTHESIS.....	9
1.4 NEUROINFLAMMATION INVOLVEMENT IN AD.....	11
1.5 INNATE IMMUNE RESPONSE IN CNS.....	13
1.6 MICROGLIA.....	14
1.6.1 Microglia during brain development.....	15
1.6.2 Microglia in the adult healthy brain.....	18
1.6.3 Microglia in aging and Alzheimer’s disease.....	20
1.6.4 Chronic stress effects on microglia in AD.....	24
1.7 HYPOTHESIS AND OBJECTIVES.....	25
2. STUDYING MICROGLIAL INTERACTIONS WITH THE PLAQUES OF AMYLOID-β USING CORRELATIVE LIGHT AND ELECTRON MICROSCOPY.....	26
RESUMÉ.....	28
2.2 KEYWORDS:.....	29
2.3 SHORT ABSTRACT:.....	29
2.4 LONG ABSTRACT:.....	29
2.5 INTRODUCTION:.....	30
2.6 PROTOCOL:.....	31
2.6.2 Methoxy-X04 solution injection:.....	32
2.6.3 Transcardial perfusion of the injected mice.....	32
2.6.4 Brain sectioning using a vibratome.....	34
2.6.5 Section screening for the presence of methoxy-X04-stained plaques:.....	35
2.6.6 Pre-embedding immunostaining for IBA1:.....	36
2.6.7 Processing for electron microscopy:.....	38
2.7 REPRESENTATIVE RESULTS:.....	40
2.8 FIGURE LEGENDS:.....	42
Figure 2.8.1 Visualization of A β plaques in 21-month old APP-PS1 mice using light microscopy, following systemic injection of the fluorescent dye methoxy-X04.....	42

Figure 2.8.2 Visualization of microglial cell body and fine processes in 21-month old APP-PS1 mice by IBA1 staining at the light microscopic level.	43
Figure 2.8.3 Dual visualization of A β plaques and IBA1-immunostaining in 6-month old APP-PS1 mice at the ultrastructural level.	46
Figure 2.8.4 Additional examples of IBA1-immunostained microglia in 6-month old APP-PS1 mice as observed with transmission electron microscopy.....	46
2.9 DISCUSSION:.....	47
2.10 ACKNOWLEDGEMENTS	48

3.SPATIAL HETEROGENEITY OF MICROGLIAL ULTRASTRUCTURAL AND FUNCTIONAL ALTERATIONS WITH RELATION TO A β PLAQUES AND NEURONAL DYSTROPHY IN ALZHEIMER'S DISEASE MOUSE MODEL AND HUMAN HIPPOCAMPUS..... 49

3.1 ACKNOWLEDGEMENTS	50
3.2 CONFLICT OF INTEREST STATEMENT	50
3.3 RESUMÉ	51
3.4 ABSTRACT.....	52
3.5 INTRODUCTION	53
3.6 MATERIALS AND METHODS.....	56
3.6.1 Animals.....	56
3.6.2 Brain sections screening for Methoxy-X04-labeled plaques	56
3.6.3 Human tissue.....	57
3.6.4 Brain sections immunostaining and processing for electron microscopy.....	57
3.6.5 Transmission electron microscopy (TEM) imaging	58
3.6.6 Quantitative ultrastructural analysis of microglia.....	59
3.6.7 Statistical analysis	60
3.7 RESULTS	61
3.7.1 Microglial ultrastructure is altered in proximity to fA β	61
3.7.2 Microglial phagocytosis and extracellular degradation is reduced in AD animals	63
3.7.3 Effects of A β on microglial cell stress	65
3.7.4 Microglial ultrastructure in human cases of AD	66
3.8 DISCUSSION	67
3.9 FIGURE & LEGENDS.....	70
Figure 3.9.1 Defining healthy, dystrophic, and plaque-associated neuropil.	71
Figure 3.9.2 Microglial ultrastructure is changed by proximity to fA β plaques.	72
Figure 3.9.3 Microglial processes lose arborization in the presence of dystrophic neurons in APP-PS1 mice.....	73
Figure 3.9.4 Distinct changes in process encirclement in APP-PS1 animals.....	74
Figure 3.9.5 Microglial cell bodies in APP-PS1 animals show reduced phagocytosis in areas far from plaque deposition.	76
Figure 3.9.6 Microglial processes are less phagocytic and display poorer digestion of inclusions in APP-PS1 animals, even in regions far from A β deposition	78
Figure 3.9.7 Microglia in APP-PS1 mice perform less extracellular degradation regardless of their proximity to plaques.....	79
Figure 3.9.8 Microglia in dystrophic and plaque-associated neuropil have reduced numbers of tertiary lysosomes.	81
Figure 3.9.9 Proximity to A β plaques correlates with increased ER dilation.	82
Figure 3.9.10 Microglial ultrastructure in post-mortem samples from human AD patient(s).	84
Table 3.9.11 Mean comparison of ultrastructural analysis of microglial cell bodies in wild-type and APP-PS1 mice with the depiction of its p values. n is number per microglial cell body.....	85
Table 3.9.12 Mean comparison of ultrastructural analysis of microglial processes in wild-type and APP-PS1 mice with the depiction of its p values. n is number per microglial process	86
Wild-type.....	86
APP-PS1	86

4. DISCUSSION:	87
5. REFERENCES.....	93

List of tables

Table 3.9.11 Mean comparison of ultrastructural analysis of microglial cell bodies in wild-type and APP-PS1 mice with the depiction of its p values. n is number per microglial cell body.....	74
Table 3.9.12 Mean comparison of ultrastructural analysis of microglial processes in wild-type and APP-PS1 mice with the depiction of its p values. n is number per microglial process.....	75

List of figures

Figure 1.1 Comparison of a healthy brain to a AD brain, where we can see volume loss and thinning in the cortex which are features of advanced AD.....	2
Figure 1.2 Sequential cleavage of APP by two pathways where cleavage by β -secretase followed by γ -secretase leads to the cleavage of A β peptide and favors the amyloidogenic pathway.....	5
Figure 1.3 Successive pathogenic phenomena triggered by the amyloid cascade hypothesis.....	11
Figure 2.8.1 Visualization of A β plaques in 21-month old APP-PS1 mice using light microscopy, following systemic injection of the fluorescent dye methoxy-X04.....	35
Figure 2.8.2 Visualization of microglial cell body and fine processes in 21-month old APP-PS1 mice by IBA1 staining at the light microscopic level.....	36
Figure 2.8.3 Dual visualization of A β plaques and IBA1-immunostaining in 6-month old APP-PS1 mice at the ultrastructural level.....	37
Figure 2.8.4 Additional examples of IBA1-immunostained microglia in 6-month old APP-PS1 mice as observed with transmission electron microscopy.....	39
Figure 3.9.1 Defining healthy, dystrophic, and plaque-associated neuropil.....	61
Figure 3.9.2 Microglial ultrastructure is changed by proximity to fA β plaques.....	62
Figure 3.9.3 Microglial processes lose arborization in the presence of dystrophic neurons in APP-PS1 mice.....	63
Figure 3.9.4 Distinct changes in process encirclement in APP-PS1 animals.....	64
Figure 3.9.5 Microglial cell bodies in APP-PS1 animals show reduced phagocytosis in areas far from plaque deposition.....	65
Figure 3.9.6 Microglial processes are less phagocytic and display poorer digestion of inclusions in APP-PS1 animals, even in regions far from A β deposition.....	67
Figure 3.9.7 Microglia in APP-PS1 mice perform less extracellular degradation regardless of their proximity to plaques.....	68
Figure 3.9.8 Microglia in dystrophic and plaque-associated neuropil have reduced numbers of tertiary lysosomes.....	69
Figure 3.9.9 Proximity to A β plaques correlates with increased ER dilation.....	71
Figure 3.9.10 Microglial ultrastructure in post-mortem samples from human AD patient(s).....	73

Abbreviations

A β	Amyloid beta
AD	Alzheimer's disease
AMPA	α -amino-3-hydroxy-5-methyl-4-isoxazolepropionic acid receptor
APOE E4	Apolipoprotein E E4 gene
APP	Amyloid protein precursor
ATP	Adenosine triphosphate
BBB	Blood brain barrier
BDNF	Brain-derived neurotrophic factor
CNS	Central nervous system
Ca ⁺²	Calcium ion
CSF	Cerebrospinal fluid
DAMPS	Damage associated molecular patterns
dLGN	Dorsal lateral geniculate nucleus
EMP	Erythromyeloid precursor
EM	Electron microscopy
fAD	familial Alzheimer's disease

GABA	Gamma-Aminobutyric acid
GR	Glucocorticoid receptor
GWAS	Genome-wide association study
HAPP	Human amyloid protein precursor
HPA	Hypothalamic pituitary adrenal
IBA1	Ionized calcium binding adaptor molecule 1
IDE	Insulin degrading enzyme
IL-1 β	Interleukin 1 beta
IL-10	Interleukin 10
IL-6	Interleukin 6
ISF	Interstitial fluid
LRP-1	Lipoprotein receptor-related protein-1
LTD	Long-term depression
LTP	Long-term potentiation
MHC1	Major histocompatibility complex 1
MR	Mineralocorticoid receptor
MTBR	Microtubule binding region
NADPH	Nicotinamide adenine dinucleotide phosphate
NEP	Nepriylsin

NFTs	Neurofibrillary tangles
NK	Killer cells
NMDA	N-methyl-D-aspartate
NPC	Neuronal precursor cell
NSAIDs	Non-steroidal anti-inflammatory drugs
OS	Oxidative stress
PAMPS	Pathogen associated molecular patterns
PCD	Programed cell death
PRRs	Pattern recognition receptors
PSEN	Presinilin
PSEN1	Presinilin 1
PSEN2	Presinilin 2
ROS	Reactive oxygen species
SGZ	Subgranular zone
Tg	Transgenic
TGF- β	Transforming growth factor beta
TNF α	Tumor necrosis factor alpha
TLRs	Toll-like receptors
5HT	Serotonin

Acknowledgments

I want to thank Dr. Marie-Éve Tremblay for giving me the opportunity to enter the world of research, this opportunity granted by Dr. Tremblay was significant in my learning journey in different aspects of life. Her patience, vitality, flexibility, scientific leadership skills, enthusiasm and scientific knowledge, added a lot to me on the personal and scientific level. I wish her, and her lab all the success and prosperity.

A special thanks to the director of the neurobiology program Dr. Katalin Toth and for the committee members Dr. Claude Rouillard and Dr. Denis Soulet of my thesis evaluation for taking from their precious time to examine my thesis.

Also, I would like to thank all my team members especially Julie, Kanchan, Kaushik, Thomas, Cynthia and Nathalie for every piece of information they provided me during my stay at the lab.

I want to take the opportunity to thank all the people working in CHUL who helped me during my master's especially professors, students, and employees of the neuroscience axe. Also, special thanks to the employees of the animal facility at CHUL and Julie-Christine Levesque for her technical support for the TEM platform.

To my parents: any achievement in my life whether big or small would not be possible without all the physical, emotional and financial sacrifices that you granted me from the day I was born. Even now, though I am an adult, I can still feel that your contribution is still present and still has the same impact on my life. No words can serve even to describe your love, mercy and inspiring presence. The same words go to my second father, my eldest brother Ali, all that you did to me will always be carved in my memory, and I will still be grateful to your sacrifices that made me grow.

To my family: thank you, my brothers, Zoulfikar, Haidar and my sister Fatima for being kind and tolerant to your youngest brother and to every bit of help and consideration you offered me. Also, a big thanks to all my relatives.

To my wife: Yara you are the kindest person I ever met, you never stop giving, all that you provide is unconditional. You were everything good during this journey. My journey without you is impossible. Thank you for being the joyful, kind, patient and sincere part of my life. Also, I want to thank your father Essam for all what he adds to my life.

To my daughter Mennat-Allah: thank you for all the fun, life, energy and love you add to my life. I wish you will lead a happy and meaningful life.

To my son Mohamad-Ali: Welcome to life, for now, you propagate peace and serenity to all the house. Can't wait to see you grow to become a right person.

To my friends: Thank you Dany for all the support and all the serious and fun conversations that always made me feel better. Shady thank you for being a good friend for all these years. I would also like to thank Hassan Hawilo, Hassan Khatib, Mahmoud,

Mazen, Feyiz, Bader, Maher, Wissam, Nadhir and Joe Abdo for all the help, support, inspiration and friendship moments.

Finally, Thank you God for showing us the way and giving us a choice to awarely seek what we want. All the gratitude for your infinite mercy and compassion.

“So whoever does an atom’s weight of good will see it.”

“And whoever does an atom’s weight of evil will see it.”

Foreword

The methodological paper represented in chapter 2 and titled *Correlative Light and Electron Microscopy to Study Microglial Interactions with β -Amyloid Plaques* (Bisht K, El Hajj H, Savage JC, Sánchez MG, Tremblay MÈ) was published in the *Journal of Visualized Experiments (JoVE)* in 1st of June 2016. During this project, I carried out most of the experiments and I participated in writing the material and methods section and the introduction which were all corrected by Marie-Ève Tremblay. The project itself was designed and supervised by Marie-Ève Tremblay.

The article titled Spatial heterogeneity of microglial ultrastructural and functional alterations with relation to A β plaques and neuronal dystrophy in Alzheimer's disease mouse model and human hippocampus represents chapter 3 of this thesis. This article is submitted to the *journal of Neuroinflammation*. In this project I carried all the experiments, imaged all the samples, collected and analyzed all the data, and prepared all the figures and tables that were included. I also participated in writing of the manuscript, I wrote the introduction and the materials and methods and they were corrected Julie Savage and Marie-Ève Tremblay. This project was designed and supervised by Marie-Ève Tremblay.

During my master's study, I also contributed to other projects in the lab. In the article *Dark microglia: A new phenotype predominantly associated with pathological states* (Bisht K, Sharma KP, Lecours C, Sánchez MG, El Hajj H, Milior G, Olmos-Alonso A, Gómez-Nicola D, Luheshi G, Vallières L, Branchi I, Maggi L, Limatola C, Butovsky O, Tremblay MÈ) that was published May 2016 in the journal of *Glia*. I provided brain tissue samples from APP-PS1 mice that were used in this study.

In the article Fluoxetine treatment affects the inflammatory response and microglial function according to the quality of the living environment (Alboni S, Poggini S, Garofalo S, Milior G, El Hajj H, Lecours C, Girard I, Gagnon S, Boisjoly-Villeneuve S, Brunello N, Wolfer DP, Limatola C, Tremblay MÈ, Maggi L, Branchi I) that was published in November 2016 in the journal of *Brain Behavior Immunity*, I was responsible of the light microscopy section of the study, the other team provided the slides and I arranged and imaged the samples, as well as supervised and revised the analysis that was done in this section.

In the article *Identification and Localization of the Cyclic Nucleotide Phosphodiesterase 10A in Bovine Testis and Mature Spermatozoa* (Goupil S, Maréchal L, El Hajj H, Tremblay MÈ, Richard FJ, Leclerc P) that was published in August 2016 in the journal *PLoS One*, I designed the protocol of sperm immunostaining and processing for electron microscopy (EM) with the help of Loïze Maréchal. I carried on the experiments, prepared the samples for EM and imaged them using transmission electron microscopy.

In the article *Prenatal Immune Challenge in Mice Leads to Partly Sex-Dependent Behavioral, Microglial, and Molecular Abnormalities Associated with Schizophrenia* (Hui

CW, St-Pierre A, El Hajj H, Remy Y, Hébert SS, Luheshi GN, Srivastava LK, Tremblay MÈ) that was published in February 2018 in Frontiers Molecular Neuroscience, I helped in the immunostaining and the processing of samples for electron microscopy. Also, I helped in cutting the samples and imaging them.

1. Introduction

1.1. Alzheimer's Disease

Alzheimer's disease (AD) was first identified over a century ago by Alois Alzheimer where he reported an atrophic brain with neurofibrillary deposits and areas resistant to staining in the case of 51 year-old demented patient (1)(2). Alzheimer's disease, being the most common cause of dementia as well as the major cause of death, accounts for 60-80% of dementia cases (3). There are nearly 46 million patients worldwide (world Alzheimer's report). The progression of AD leads to deterioration of cognitive functions including memory, speech, language, judgment, reasoning, planning and other thinking abilities. AD has a clinical duration ranging from 8-10 years (4). The main changes seen at the level of the brain are neuronal death and extensive loss of synapses particularly in the neocortex and hippocampus (5,6,7). Numerous extracellular deposits of amyloid beta ($A\beta$) sheets and intraneuronal fibrillar tangles are the major defining indicators of the disease (8,9). The pathogenesis of AD appears to be extremely complex due to the involvement of multiple cellular and molecular interactions. Currently there are no treatments to stop, slow or reverse the progression of the disease.

Risk factors of the disease are multifactorial. Type 2 diabetes, hypertension, smoking, sedentary lifestyle, obesity, and head injury are mostly preventable risk factors of AD. The age and genetics are the main risk factors that can not be prevented. Most of the AD cases are sporadic, but a rare type of AD which appears in less than 0.5% of cases is also present. This type is the familial form of AD (fAD) which is caused by mutations in three genes, amyloid precursor protein (APP), presenilin 1 (PSEN1) and presenilin 2 (PSEN2). Symptoms in fAD develop early between 30 and 50 years of age (10). Sporadic forms of AD which appear later in the lifespan are driven by a combination of genetic and environmental factors. Apolipoprotein E (APoE) e4 allele is linked to increased risk and earlier onset in AD. People having one copy of the e4 allele of apolipoprotein E (APoE) are in risk in developing AD by 47%, while homozygosity increased the risk to 90%. Also, people not having the e4 allele have a mean age onset of 84.3 years compared to heterozygous that have a mean of 75.5 and the homozygous with a mean of 68.4 years (11). Genome-wide association studies (GWAS) have pinpointed to more than 20 genetic risk

factors related to cholesterol metabolism and inflammatory pathways (12).

Physical exercise and education may have a protective role against AD as shown in epidemiological studies. Midlife hypertension and diabetes in addition to vascular disease negatively impact the risk of developing AD (13).

The pathophysiology of AD is defined by the accumulation of the extracellular amyloid plaques, intracellular neurofibrillary tangles (NFTs) of Tau and neuroinflammation which is mainly orchestrated by microglia, the immune cells of the central nervous system (CNS). Loss of synapses, dystrophic neurites and associated astrogliosis are widely seen as the disease progresses, leading to neuronal death and macroscopic atrophy in the structure and volume of the affected areas of the brain (14) (Figure 1.1).

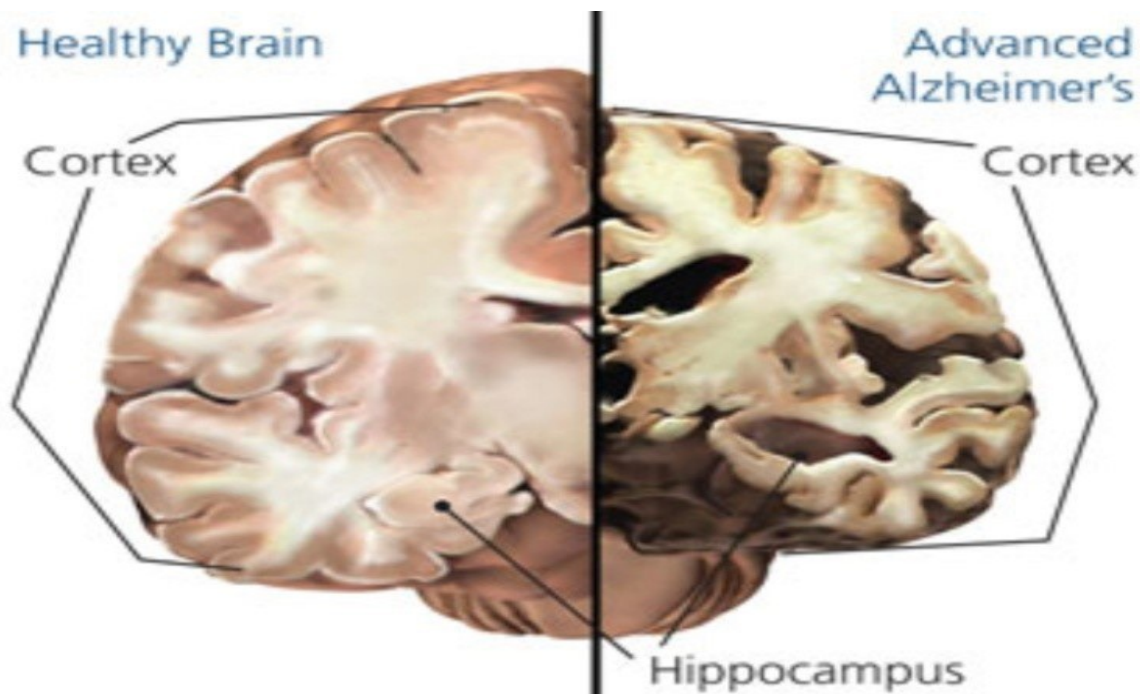


Figure 2.1 Comparison of a healthy brain to a AD brain, where we can see volume loss and thinning in the cortex which are features of advanced AD(15).

1.1.1 Neurofibrillary tangles

One of the major characteristics of AD is the formation of neurofibrillary tangles (NFTs). These tangles contain paired helical filaments of hyperphosphorylated tau protein (16). These inclusions are pathologically linked to a number of neurodegenerative diseases where they are seen with excessive neuronal loss and gliosis. In addition to AD these hallmarks are also present in Down's syndrome, several variants of prion diseases, progressive supranuclear palsy, amyotrophic lateral sclerosis/parkinsonism-dementia complex of Guam (ALS/PDC), Pick's disease, corticobasal degeneration, sporadic frontotemporal dementias, and familial FTDP-17 syndromes (17).

Normally, tau is one of the proteins involved in the microtubule assembly, it plays an important role in cellular structure maintenance and proper axonal transport (18). Also, it is essential to axonal growth and development of neurons. Six isoforms are expressed in the human brain as the result of alternative mRNA splicing that yields tau proteins containing 0–2 acidic N-terminal inserts (0 N, 1 N, or 2 N) and 3 or 4 microtubule binding repeat (MTBR) regions. These regions may adopt pathological oligomers/aggregates preventing normal functions or leading to loss of functions of the tau protein (19,20). The suggested mechanism of tau induced neurodegeneration may include the discontinuity of axonal transport due to aggregates acting as physical blockage and synaptic malfunction (21). In AD, NFTs are mainly associated with amyloid plaques and located mainly in the cell bodies and dendrites of the neurons (18). Tau pathology typically begins in the allocortex of the medial temporal lobe (entorhinal cortex and hippocampus) before spreading to the associative isocortex. Primary sensory, motor and visual areas tend to be relatively spared. The progression of neuronal and synapse loss occurs in parallel to tangle formation (22). While the amyloid cascade hypothesis suggests that the pathology of tau is dependent on A β , studies show that tau can cause neurodegeneration independently of A β . For that reason, it is reasonable to say that both pathologies act in parallel in promoting their toxic effects and exacerbating AD progression (23). A study has shown that tau facilitates A β toxicity by directing the Src kinase Fyn to the N-methyl-d-aspartate (NMDA) receptors, increasing the interactions of Src kinase Fyn with the PSD95 proteins and resulting in

excitotoxicity (24). In transgenic mice carrying mutant APP overexpression of tau led to exaggerated pathogenesis (25). When tau was genetically removed from these mice, pathologic features were reduced suggesting this interrelated process between A β and NFTs (26).

1.1.2 Amyloid beta

A β peptide is the main component of the neuritic plaques in the brain of AD patients (27). It was first sequenced from meningeal blood vessels of individuals with AD or Down's syndrome (9,28). A β deposition is widely believed to be the main driver of AD pathogenesis. Although there is a weak coexistence between accumulation of neuritic plaques and the severity of the clinical symptoms of the disease, studies point out to the important role of soluble A β and its accumulation in different pools in AD progression.

Mainly, A β is formed after sequential cleavage of APP. While the precise physiological function of APP is not known, studies have shown that overexpression of APP has a positive effect on cell health and synaptic functions and is highly expressed in brain regions where synaptic modification occurs (29). A β is produced when APP is sequentially cleaved by β and γ secretases. β -secretase first yields a large derivative sAPP β , which is rapidly cleaved by γ -secretase producing A β (Figure 1.2). Due to γ -secretase imprecise cleaving processes, numerous A β species exist. A β 40 comprises 80-90% of produced A β followed by A β 42 which comprises to 5-10% of A β species. A β 42 species are more hydrophobic and fibrillogenic and they are the main deposited A β form in the brain (31).

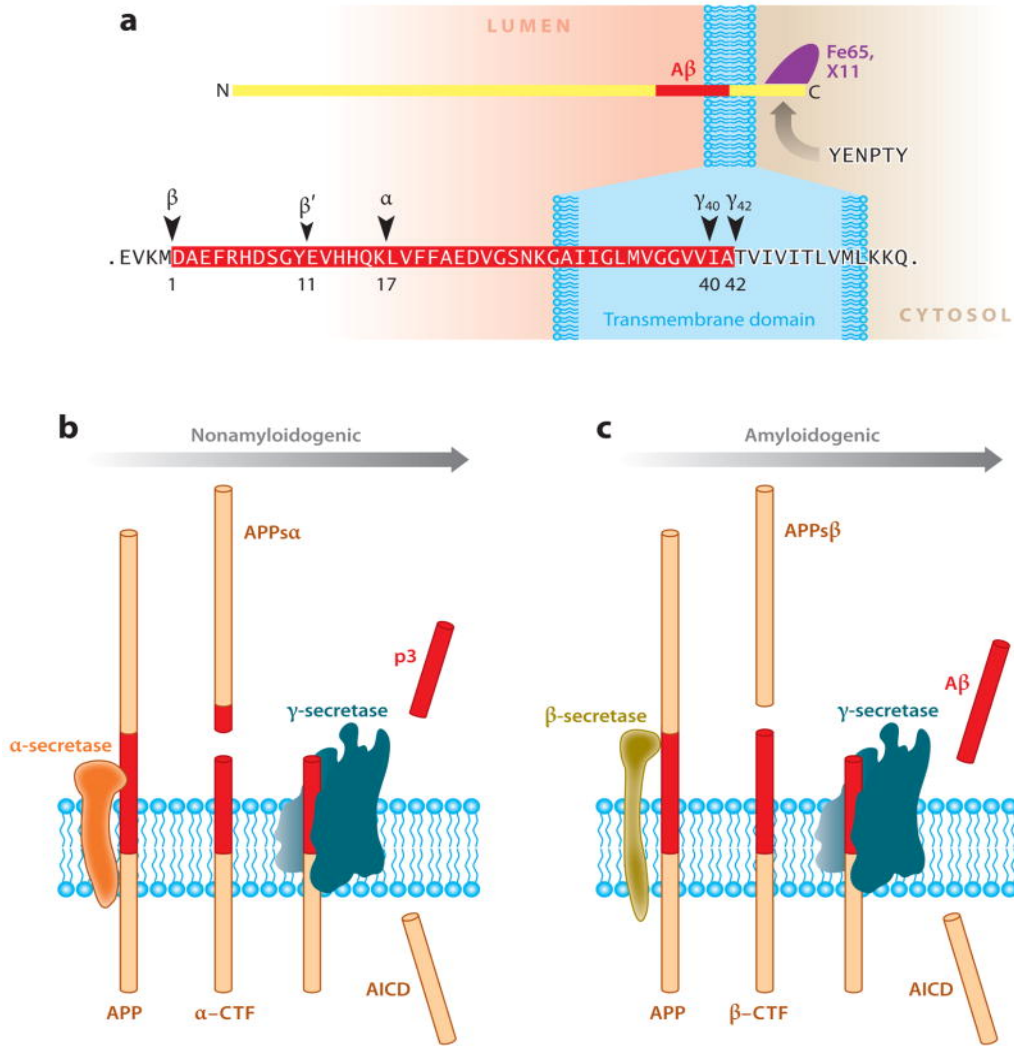


Figure 1.2 Sequential cleavage of APP by two pathways where cleavage by β -secretase followed by γ -secretase leads to the cleavage of A β peptide and favors the amyloidogenic pathway (30).

Genetic cases in AD revealed that the deposition of A β is a general event that characterizes both late sporadic form of AD and the early fAD which is caused by autosomal dominant mutation of APP (32). Autosomal dominant mutations are mainly manifested on APP, PSEN1 and PSEN2 genes. The occurrence of these different mutations individually or combined leads to increase in the production of the more toxic form of A β which is the A β 42 (33). In addition to that, in sporadic AD cases the presence of the APOE E4 allele plays a major role in AD as a significant genetic component which leads to increased A β deposition (34). While ApoE2 and E3 is seen to diminish A β deposition, APOE E4 allele is

strongly associated with increased A β deposition and ApoE4 is found to increase the deposition (35).

The toxicity of A β peptide is considered the main driving force towards the development of AD. A β is considered to be the main trigger to neuroinflammation, oxidative damage and NFTs deposition. In tissue cultures A β fibrils were found to be extremely toxic to neurons (36). Also, in vivo A β was found to cause neuronal alteration and gliosis in the CA1 hippocampus of the PDAPP transgenic mouse model which overexpresses human amyloid precursor protein V717F (PDAPP minigene) (37). Also, multiphoton imaging of GFP-labeled neurons in Tg-2576 AD mouse model revealed loss of synaptic terminals and synaptic function in cortical neurons (38). Another study on PDAPP mice, which show first the highest density of A β in the hippocampus, revealed abnormalities in spatial memory tests (39). Moreover, A β plaques are seen to strongly accumulate early in the hippocampus of CCR2 deficient Tg-2576 mice. CCR2 is a chemokine receptor expressed by microglia and contributes to phagocytes accumulation at site of inflammation, so these mice which have alteration in the accumulation of macrophages at site of inflammation is strongly affected by the pathogenesis of A β deposition. Beside the increased deposition, increased mortality of these mice is also evident. Thus, microglia play an essential role in decreasing the burden of deposits in these mice by their ability to recruit more cells at the site of inflammation (40).

In AD patients, a clearance abnormality leads to the accumulation of A β in the brain. Removal of A β oligomers from the brain takes place with the aid of several pathways (41). These pathways include passive flow through the cerebrospinal fluid and sequestration into the vascular compartments by lipo-protein receptor-related protein-1 (LRP-1), phagocytosis by microglia and astrocytes and proteolytic degradation by neprilysin (NEP) as well as insulin degrading enzyme (IDE) (42). Also, the meningeal lymphatic vessels are another pathway that was recently discovered to be involved in the drainage of macromolecules found in cerebrospinal fluid (CSF) and interstitial fluid (ISF) to the cervical lymph nodes (43). LRP-1 receptors interact with A β in order to transport it from the CNS through the

Blood-Brain Barrier (BBB). The BBB constitutes of compactly closed monolayer of brain endothelial cells that are supported by astrocytic cells end-feet. It is a highly selective semipermeable boundary that separates the brain and the extracellular fluid in CNS from the circulating blood. This barrier limits the entry of neurotoxic molecules, pathogens, red blood cells (RBCs) and leukocytes from entering the brain (44). Increased levels of A β and aging cause a decrease in the expression of LRP-1 leading to A β accumulation in the brain (45). Normally, the proteases NEP and IDE degrade A β in the brain but during aging and AD the expression of NEP and IDE decreases, thus favoring the accumulation of A β in the brain (42,46). The secretion of IDE in the brain is regulated by microglia. IDE and NEP concentration and activity decreases in the AD brain, specifically in the cortex and hippocampus (47).

1.1.3 Oxidative stress

Neuronal death and apoptosis are highly affected by oxidative stress (OS). OS is a common characteristic that appears in neurodegenerative diseases and especially in AD (48). Cell damage occurs in response to an imbalance between the levels of antioxidants and the production of reactive oxygen species (ROS) (49). Accumulation of free radicals and the altered activity of antioxidant enzymes such as superoxide dismutase and catalase promotes OS and are present in AD brain (50). Excessive presence of A β loads leads to increased production of ROS through a mechanism of activation of N-methyl-D-aspartate (NMDA) receptors which are involved in synaptic plasticity and are essential in memory, learning and modification of neuronal circuits (51). Also, reactive microglia in the context of inflammation *in vitro* can produce a variety of free radicals, pro-inflammatory cytokines and neurotoxic prostaglandins. Also, A β fibrils can activate nicotinamide adenine dinucleotide phosphate (NADPH) oxidase enzyme pathway in rat microglia and human phagocytes and neutrophils, enhancing the production of multiple reactive oxygen intermediates. In addition to that, reactive microglia can secrete huge amounts of nitric oxide in the AD brains (52). The A β deposits, hyperphosphorylated tau, neuroinflammation, and OS phenomena were proposed to augment one another in a combined interplay leading to AD development (53). Also, neuronal mitochondria which

are highly vulnerable to OS seem to show metabolic alterations leading to further increase in ROS levels and eventually promoting cell death through caspase activity and apoptosis (54).

1.1.4 Neuronal calcium homeostasis

Memory loss is a result of synaptic elimination that occurs in AD (55). During the stages of disease, calcium (Ca^{2+}) influx and efflux regulation and its subcellular compartmentalization by neurons is disrupted (56). Calcium plays an important role in maintaining the health and integrity of neuronal cells. When Ca^{2+} signaling is deregulated, a negative impact is laid on the health and stability of the dendritic spines which contributes to synaptic loss. Calcium disruption is the result of multiple factors including OS, metabolic impairment due to $\text{A}\beta$ oligomers and presenilin (PSEN) gene mutations (57). The calcium alterations are characterized by abnormal function of ryanodine receptors and store-operated calcium channels (58) and imbalance Ca^{2+} -calmodulin-dependent kinase II and Ca^{2+} -dependent phosphatase calcineurin activities at the synapse (59,60). Also, in AD long-term depression (LTD), a form of activity-dependent reduction mechanism of synaptic transmission that is long-lasting and input-specific, is favored instead of long-term potentiation (LTP), a form of activity-dependent enhancement of synaptic transmission, causing the further elimination of synapses (61).

1.2 APP mice models in AD

In order to mimic the pathogenesis occurring in AD in human subjects, a wide number of transgenic (Tg) mouse models were developed. Tg mice that overexpress APP were generated using different promoters with or without fAD mutations. Transgenic expression of the human APP (hAPP) is the primary, most widely used model in AD. Numerous lines of hAPP exist and these models show strong amyloid deposition, memory deficits and can mimic synaptotoxicity of AD without significant neuronal loss. The most used models of APP-Tg mice include PDAPP (62), Tg2576 (63), APP 23 (64), J20 (65), and TgCRND8 (66). The Swedish mutation (67) is the most commonly used mutation. This mutation leads

to overproduction of total A β from APP. The first generation Tg mice have A β plaques that are similar to the one seen in AD brain but with some differences. Also, these mice have cognitive deficits before A β deposition but they do not exhibit NFTs formation and neuronal loss that is seen in humans.

However, AD pathology was not totally repeated by APP-Tg mice. So, a combination of APP-Tg mice and other mutant mice was performed to recapitulate AD pathogenesis. PS1 contributes to fAD pathogenesis by being a constituent of the cleavage process that generates A β from APP (68). PS1 mutations alone did not induce A β pathology, but combining PS1 mutant mice with APP-overexpressing mutant mice lead to increase in A β pathogenesis where A β deposits were seen as early as 6 months of age in mice. In addition, behavioral deficits and neuronal loss was also present in those mice. Several examples of the double Tg mice are Tg2576 and PS1M146L Tg (69), APPKM670/671NL Tg and PSA246E Tg (70), APP751KM670/671NL-V717I Tg and PSM146L Tg (71), and APP KM670/671NL-V717I and PSEN1M233T/L235P knock-in (72). Those mice are considered adequate to study A β production, deposition, and the neuroinflammation associated with it.

1.3 Amyloid cascade hypothesis

The amyloid cascade hypothesis is still dominant in the AD field 25 years after its introduction (73). The trigger of this cascade is the deposition of A β peptide in the brain due to overproduction and/or abnormal clearance process of the peptide. This event puts a foundation of successive pathogenic developments leading to dementia (Figure 1.3). Since the hypothesis was introduced, numerous studies offered arguments and counterarguments that targeted cellular and molecular mechanism of this hypothesis.

Multiple arguments were presented throughout the years to support the hypothesis. Argumentations state that regions governing memory and cognition in the brain show increased A β deposition, where these depositions are also accompanied by degenerating neurons and activated glial cells in all AD patients (74). Also, genetic abnormalities in the APP gene impact disease progression and mimic its neuropathological features, where

vigorous forms manifestation of fAD are caused by the APP gene mutation. Individuals with Down's syndrome have three copies of the APP gene and they develop AD neuropathology with the same pathogenic sequence proposed by the cascade hypothesis (75). Carriers of missense mutation of APP which causes reduction in the production and aggregation of A β are less prone to AD and cognition deficits linked to aging process (76). Moreover, A β deposition due to alteration of its clearance from the brain of individuals inheriting the APOE E4 allele shows a typical A β linked neuropathology (77). In addition, studying synaptic loss pattern which is a main characteristic of AD progression reveals that synaptic function mainly the LTP processes and the synaptic structures of the dendritic spines show extensive impairment as a result of interaction with A β 42 oligomers (78). A β oligomers diffuse from and are present surrounding the plaque in a haloed pattern. The density of synapses is shown to decrease in the vicinity of these halos while having normal healthy states going farther away from the plaque halos (79). Besides, cultured rat neurons exhibit neurodegeneration and tau hyper phosphorylation as a result of addition of A β oligomers to the culture (80). Finally, the sequence of A β deposition, tangle formation, glial cells activation and neuronal degeneration is evident in imaging and biomarker modeling studies of human AD (81,82).

The counterarguments presented against the amyloid hypothesis indicate the following findings : Studies in Tg-mice overexpressing A β 42 did not show neuronal loss or cognitive impairment due to the presence of A β deposits (83,84). A β antibodies are seen to decrease the deposition A β but without any effect on the tau pathology or disease symptoms (85,86). Also, brain imaging studies in humans showed that healthy individuals may possess A β deposits and AD patients may have few concentration and distribution of these deposits (87,88). Also, aged healthy patients may have numerous widely distributed plaques in the brain mimicking demented patients without having the disease (89). This debate will continue while studies are trying to decipher the relation and primacy of those complex cascades that are taking place in different stages of the disease.

1.4 Neuroinflammation involvement in AD

Numerous complex cellular and molecular mechanisms contribute to the neuroinflammatory responses in AD. While the main initiators of these responses are considered to be A β and tau pathologies, the domination of the amyloid hypothesis is now being questioned due to the multiple failures that are facing the clinical trials targeting this specific hypothesis.

Neuroinflammation is now considered as a new mechanism that could underlie the pathophysiology of the disease. A large body of studies implicate inflammation as a potential contributor in AD progression. The brains of human AD patients and AD mice models have been found to possess increased markers that are linked to innate and adaptive immune system reactions (91,92). Also, although there is still a debate on the exact role of non-steroidal anti-inflammatory (NSAIDs) drugs in AD, studies have shown a decreased risk of developing AD in patients taking NSAIDS in stages before the disease begins to manifest (93). Furthermore, the involvement of neuroinflammation in AD pathophysiology is strongly supported by recent GWAS studies. It was found that 20 variants which are specific to late-onset AD concern genes related to innate and adaptive immune responses. The gene variants were: HLA-DRB5/HLA-DRB1 (94), CD33, MS4A, ABCA7, EPHA1 (95,96), TREM2 (97), TYROBP (98) and CR1, CLU (99,100).

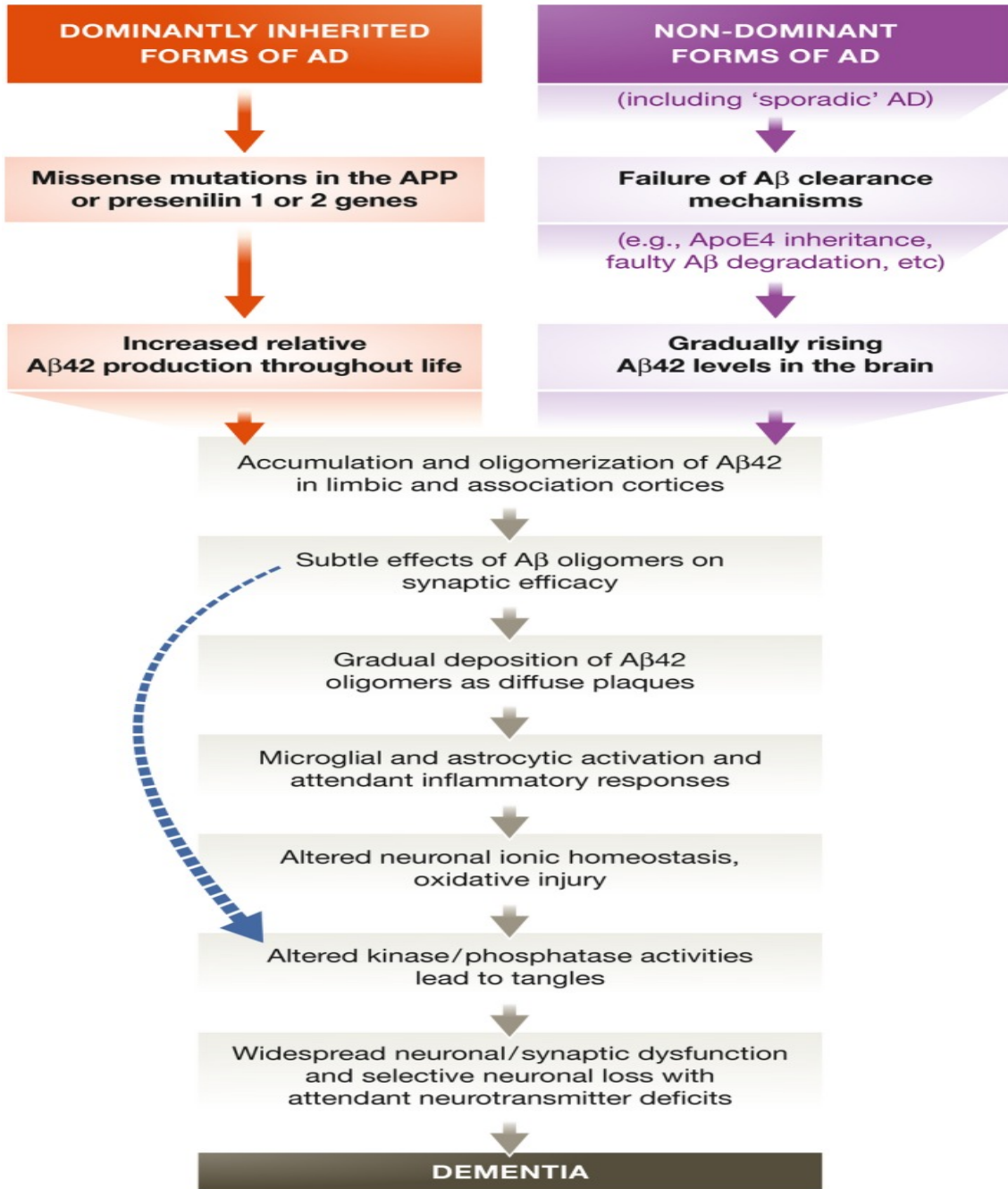


Figure 1.3 Successive pathogenic phenomena triggered by the amyloid cascade hypothesis. (90)

1.5 Innate immune response in CNS

According to the amyloid cascade hypothesis, A β deposits in the brain can trigger a reactive response of microglia, the primary innate immune cells of the brain (101). The innate immunity process is the first line of defense issued by the body against pathogenic and dyshomeostatic challenges. The response is characterized as being rapid and non-specific against those challenges and insults. Dendritic cells, neutrophils, monocytes/macrophages and natural killer cells (NK) cells are the main composition of the innate response family in the body. However, with regard to the CNS and to AD pathology, microglia are considered as the primary immune residents that are key players in neuroinflammation (102). Microglia are thought to engage themselves in the clearance process of the A β deposits over the course of prevention of the cascading events that lead to neuronal loss (103). The neuroinflammatory process taking place in the CNS develops from an acute state to a chronic state in the pathogenesis of AD (104). Scavenger receptors such as toll-like receptors (TLRs) which are expressed on immune cells and help in the induction of immune response by the ability to recognize wide range of molecules derived from pathogens, RAGE and CD36 are found on microglia and other cells from the innate immune system (105,106). These receptors can bind to A β leading to secretion of inflammatory cytokines (107). Moreover, the activation of those receptors leads to production of toxic molecules such as free radicals which promotes the inflammatory process. Overall, the chronic deposition of A β was proposed to result in a sustained state of inflammation leading to microglial functional alteration and eventual neuronal death due to the accumulation of toxic products and irreversible cellular dysfunction (108).

By studying the involvement of the innate immune cells in the pathogenesis of AD, the periphery also has to be considered. Numerous studies on the BBB describe a compromised integrity in mouse models and human (44). This change in integrity allows a less controlled fashion of the peripheral immune cells entry and infiltration to the brain parenchyma. This infiltration is mainly due to cross signaling that is triggered by microglial reactivity after contacting A β , in which microglia adopt a pro-inflammatory profile. The chronic release of cytokines, chemokines and complement factors which may cross the BBB and travel to the periphery can cause activation and recruitment of peripheral immune cells to the site of

insult (108,109). In conclusion, microglia, being the immune cells responsible for the homeostasis of the brain, play a major role in directly responding to an insult and orchestrating and managing the recruitment process of the peripheral immune cells to the brain. Also, microglia act as a supporting guide to those cells in the process of inflammation. Microglia and the innate immune cells using cross signaling can have a beneficial and/or detrimental role in AD.

1.6 Microglia

Since they were characterized, the scientific advancement provided progressive comprehension of microglia role in the CNS. The understanding of this role grows in an exponential pattern offering us a more explicit characterization of the cells' structure and function in the CNS. Early in 1856, glial cells were distinguished from neurons and were considered as a significant part of the whole CNS, which was previously identified solely as made up of neurons (110). Then, glial cells were differentiated, and they were called astrocytes (111). Moreover, Ramón Y Cajal identified a third type of cells and added it to neurons and astrocytes (112). Another cell type which exhibits a rod-like shape and granular features was also identified mainly in brain diseases and injury (113,114,115). It was with Pio del Rio Hortega that the name and distinction of microglia came to light. In addition to astrocytes, microglia and oligodendrocytes are now considered the main types of glial cells in the CNS (116). Microglia are the tissue macrophages of the brain parenchyma, and they constitute around 5-10% of the cellular buildup of the CNS (117). Other types of macrophages are present in the CNS. Perivascular, meningeal and choroid plexus macrophages are mainly situated at sites between parenchyma and circulation, and they are derived from precursor blood monocytes (118). Unlike those macrophages, microglia are derived from the erythro-myeloid precursor (EMP) of the yolk sac (119). In mice, it was shown that precursors cells travel to the brain from the primitive macrophage pool at embryonic day 9.5. After that, the precursors develop to immature microglial cells with an amoeboid morphological features (120). The presence of microglia in the neuroepithelium is temporally concurrent with the development of neurons and before the differentiation of other glial cells. For this reason, microglia are considered as a major player in multiple developmental events that occur in the CNS throughout life (121). Also,

microglia follow a specific sequence where within 48 hours of their residence in the mouse brain at E9.5 they start their process of maturation, proliferation and brain regions' colonization (122,123). Also, in the postnatal and adult periods of life, the proliferation of microglia is seen to be mainly dependent on an intrinsic pool of cells found locally within the brain (122,124).

1.6.1 Microglia during brain development

The contribution of microglia to proper brain development and function is highly essential. Microglial intervention in the brain is not restricted entirely to the context of injury and disease. In response to an insult, microglia are recruited to the damaged site where they attempt to restore brain homeostasis using phagocytosis of debris and apoptotic cells. On the contrary, microglia can induce a pathological neuroinflammatory response by releasing pro-inflammatory cytokines and neurotoxic proteins (125). The contribution of microglia to brain disease is not entirely clear. It is not determined yet if microglia are the mediators in pathologic events and/or if they are affected by the pathology itself. Also, microglia in the healthy brain are considered to be actively surveying the brain parenchyma by retracting and expanding their processes and exhibit a highly dynamic state to achieve their service function (126). Numerous data incorporate microglia in multiple processes required for brain wiring and proper development.

1.6.1.1 *Microglia correlation with programmed cell death (PCD)*

During the early phases of brain development, microglia are directly involved in the shaping of the maturing CNS. Studies revealed that microglia act as both mediator and responder to the process of PCD, which takes place in early postnatal brain development. During that stage, more than half of the neuronal population colonies of the brain are removed (127,128). Microglial participation is evident in the way they follow neural proliferation in the developing regions of the CNS, in addition to their coexistence with dying neurons in those regions (129,130). Also, microglia are temporally and spatially concurrent with the waves of PCD that are seen in multiple brain regions (131). While microglia are strongly correlated to PCD phenomena in the CNS, they are also shaping the brain developmental events by supporting neuronal health, survival and providing trophic

factors for neuronal precursor cells (NPCs) (132,133). Cell cultures from mice lacking microglia showed altered proliferation of NPCs. This effect was reversed when microglial cells derived from wild-type mice were added to the culture (134). Moreover, removing or deactivating microglia at the postnatal stage of brain development resulted in excessive neuronal death in the cerebral cortex. This data suggests that microglia provide trophic support to neurons in this particular stage of development (135). Thus, microglial mediation and response to early brain developmental stages serve as a proof of their multifaceted roles in the CNS.

1.6.1.2 Microglia and the build-up of synaptic networks

In embryonic development, microglial spread in the brain follows a specific and complex pattern (136,137). Microglia gather at high densities along certain developing axonal tracts. For example, microglia in mice at embryonic stage 14.5 control the extension of dopaminergic axons by their phagocytosis with no effect on serotonergic axonal tracts (137). Interestingly, studies suggest that for the development of corpus callosum, microglial contribution is due to trophic factors secretion instead of targeted phagocytosis (138). Also, guiding cues signaled by microglia may be responsible for directing the pattern of interneurons dissemination in the development process of the forebrain (137). During the postnatal period, an overabundance of synaptic contacts occurs. An activity-dependent refinement of those contacts takes place where elimination of specific synapses is favored while maturation of other activity-relevant synapses is implemented (139). Also, in the retinogeniculate system and in the CA1 hippocampus of mouse models, microglia are involved in the removal of less-active synapses and maturation of functional ones. Impairment of this microglial response leads to decrease in synaptic transmission and functional brain connectivity (140,141).

In pathological conditions, microglia strip and eliminate by phagocytosis synaptic terminals showing decreased activity (142). Moreover, microglia in physiological state target synaptic elements and remove synapses that are showing reduced activity (143). Considering those facts, multiple studies were conducted for the aim of elucidating microglial role in synaptic pruning during development. In late postnatal stages in mice, microglia exhibit an

increase in phagocytic inclusions after sensory deprivation performed in the course of visual cortex development (144). Other studies, immune-stained markers of synaptic origins were detected in microglia cytoplasm during hippocampal region development suggesting microglial processes refinement of synaptic contacts by phagocytosis (145). Also, microglia contribute to retinogeniculate system development by phagocytosis of weak synapses (141,146). Microglia interact with unwanted synapses via C1q and C3 complement proteins (147). Also, serotonin (5HT) signaling in the thalamus activates microglial synapse elimination through microglial 5-HT_{2B} receptors (148). Moreover, in the dorsal lateral geniculate nucleus (dLGN), remodeling of axons and synaptic removal processes are regulated by major histocompatibility complex class 1 (MHC1) molecules (149). Microglia are known to express MHC1 receptors, which may link synaptic elimination process in this region to microglia.

In addition to phagocytosis, microglia impact synaptic functions regarding development, functional patterning and maturation by secreting multiple mediators (150,151). The implication of microglia in influencing synaptic formation can also be seen during developmental stages. Activated microglia promote the creation of new filopodia on layers 2 and 3 of pyramidal neurons in the developing cortex (152). Moreover, microglial secretion of mediators and cytokines promotes synapse formation. Addition of microglial interleukin IL-10 to neuronal cultures induced development of new synapses (153). Also, microglial depletion in adults and the third postnatal week showed alteration in activity-dependent synapses formation in motor cortex. Similar results were reproduced by knocking out brain-derived neurotrophic factor (BDNF) from microglia, suggesting a significant role of microglial BDNF in synapse formation and function (154). Hypothetically, activity-dependent mediums summon microglial processes to targeted synapses which participate in a learning process. Microglia then release BDNF which act as a key mediator in the maturation of synapses during development. Accordingly, studies speculate on the role of BDNF in the maturation of thalamocortical synapses during barrel cortex development (155). Another microglial signaling molecule that participates in the maturation of synapses is the tumor necrosis factor alpha (TNF α). TNF α is shown to impact synaptic transmission and plasticity in developing brain

(156). *In vitro*, TNF α increases the expression of α -amino-3-hydroxy-5-methyl-4-isoxazolepropionic acid (AMPA) and NMDA receptors thus favoring excitatory synaptic transmission. Also, the role of gamma-aminobutyric acid (GABA) at synaptic membrane decreases by endocytosis is augmented by the modulatory effect exerted by TNF α , therefore, adjusting inhibitory synaptic transmission (157). An additional mediator expressed by microglia and affecting synaptic function is the pro-inflammatory cytokine interleukin-1 β (IL-1 β). IL-1 β production is increased in pathological conditions. This mediator can modulate excitatory synaptic transmission by down-regulating AMPA receptors (158,159). IL-1 β is an essential component of learning and memory when kept at low physiological levels (160). Fractalkine (CX3CR1) is a protein secreted by neural cells and its receptor is found on microglia, this protein aids in the communication of neural cells with microglia and is important for microglial cell migration. When levels of IL-1 β increase this can disrupt brain plasticity processes. Antagonizing IL-1 β in CX3CR1 knockout mice improved hippocampal synaptic plasticity and cognitive functions (161). Microglia also can influence synapse maturation by relocating astrocytic cells to the site of remodeling activating P2Y1 receptors which enhances synaptic strength by the secretion of astrocytic glutamate (162). Microglia participate directly and indirectly in synaptic maturation and function through the release of multiple mediators that exhibits a modulatory or trophic effect.

1.6.2 Microglia in the adult healthy brain

Microglia in the adult healthy brain are not dormant immune cells that only function in incidents of brain injury or external insult. Microglia are involved using different roles in the brain. These roles are intended to secure brain homeostasis profile throughout the life of the organism. Surveillance, neuromodulation, synaptic pruning and phagocytosis are some of the modes of action of microglia that take place in the healthy adult brain (163).

1.6.2.1 *Microglia-synapse interactions*

Using their numerous ramified processes, microglia can extend these processes to the surrounding extracellular space in order to sample and monitor the neuronal parenchyma every few hours for any signs of homeostatic disruption or brain injury (126,164). Microglia actively interact with neuronal structures including synaptic clefts (165). The increased neuronal activity which is characterized by adenosine triphosphate (ATP) release from NMDA receptors can attract microglial processes by activating purinergic receptors (P2RY12), this receptor is highly expressed by microglia and it is a chemotactic receptor essential for orienting microglial processes towards sites of injury (166). Neuronal loss is present at the level of visual cortex in P2RY12 deficient mice suggesting an essential role for microglia in the process of synaptic plasticity (167). Also, using *in vivo* two-photon imaging of the thalamic and cortical neuron of GFP labeled mice where neurons and microglia were both labeled, microglia contact the surrounding neuronal structures constantly in a systemic pattern where presynaptic and postsynaptic elements are also included in the microglia-synapse interactions (165). Therefore, microglia play a key role in synapse modulation of the adult brain.

Microglia express multiple complement components, which normally are important molecules in the immune response against pathogen insult. Microglia express C1q, CR3 and CR5 in the brain. Besides their role in immune response against bacteria and microorganisms, these complements are involved in synaptic pruning process carried by microglia for the functional development of synapses in both developing and adult brains (147). Also, complement induced synaptic pruning is directly related to synapse loss in disease and to cognitive decline during aging where levels of C1q complement tagging synapses for elimination by microglia are highly increased (168).

1.6.2.2 *Microglial phagocytosis and neurogenesis*

Microglia regulate the density of differentiated neurons by using their phagocytic capacity. Microglia engulf NPCs during embryonic and adult neurogenesis (155,169). An important example of ongoing adult neurogenesis in the brain is found in the hippocampus. The sub-

granular zone (SGZ) of the hippocampal formation is a host for stem and progenitor cells that further differentiate to a mature granule cells which constitute in the hippocampal structure (170). These emerging newborn cells engage in processes of learning, memory and emotional behavior (171). At normal physiological conditions, most of these cells undergo apoptosis and they are extensively and rapidly removed by a ramified phenotype of microglial cells which can clear entire cells and cellular debris from the SGZ (168). Also, microglial phagocytic activity toward apoptotic NPCs is mediated by the expression of receptor tyrosine kinases AXL and MER during perinatal stage (172). Deletion of these kinases results in the differentiation and maturation of NPCs and their progeny without being contacted by microglia, thus making these cells a part of the neuronal architecture. In neurodegenerative disease where microglia are suspected to exhibit a deviant neurotoxic role the expression of AXL is elevated implicating microglia in neurodegeneration leading to disease pathology (172,173).

1.6.3 Microglia in aging and Alzheimer's disease

AD is a neurodegenerative disease that is closely linked to aging. Microglia share some phenotypical similarities in both aging and AD. Microglia, being the resident immune cells in the brain parenchyma, initiate a striking response against the pathophysiology taking place in AD. According to neuropathological studies, microglial “activation” in the face of insult in the brain is characterized by a change of its phenotype from ramified morphology to an amoeboid form. This activation may cause microglia to manifest an M1 pro-inflammatory state or an M2 anti-inflammatory and repair states. This concept of M1/M2 polarization which was originally used to describe macrophage activation is now being challenged (174). Recent studies present microglial “activation” as exhibiting more dynamism and heterogeneity in response to pathological progression stages of the disease (175,176). Traditionally, microglial activation was considered a destructive event due to the neurotoxic activity that the cells present *in vitro*. However, recent data revealed that microglia might be neuroprotective in disease situations. Microglia in the CNS can encourage neurogenesis, tissue repair and decrease inflammation in multiple pathological conditions (177). Microglial secretion of Interleukin 10 (IL-10) and transforming growth factor beta (TGF- β) which play essential roles in controlling the immune response, caused a decrease of neuroinflammatory response in experimental meningitis. However, inducing

microglial inactivation in a multiple sclerosis mouse model showed a delay in the onset of disease and enhanced clinical scores (178).

During normal aging, an insult to the brain may cause cellular distress which leads to activation of microglia; this activation follows a particular mode which is known as priming. This mode is additionally present in multiple neuropathological conditions as a result of chronic neuroinflammation. This state of chronic inflammation place microglia in direct exposure to misfolded proteins and cellular debris of apoptotic and dying cells which renders microglia in a pro-inflammatory state. Also, this extensive response carried by microglia due to dyshomeostasis is characterized by morphological changes causing enlargement in microglial somas and retraction of their processes with increased release of the pro-inflammatory cytokines $\text{TNF}\alpha$, $\text{IL-1}\beta$ and IL-6 (179,180).

One of the main hallmarks of neurodegenerative diseases is the aggregation and deposition of misfolded proteins and cellular debris (181). Microglia respond to the presence of aggregates and debris through the sensing of Damage-Associated Molecular Patterns (DAMPs) which belong to the family of Pattern Recognition Receptors (PRRs) expressed by microglia. Also, microglia react to pathological insult through Pathogen-Associated Molecular Patterns (PAMPs) which are also a part of microglia's PRRs (182). In AD, $\text{A}\beta$ diffusing from the plaques are considered as DAMPs activating microglial PRRs, this activation induces a sustained release of inflammatory factors considered to boost neurodegeneration and disease pathology (178). The PRRs that are expressed in neurodegenerative disease include TLRs and their co-receptors (183). In addition to PRRs microglia can also be activated by ATP and UTP, these molecules bind to purinergic receptors on microglial membranes. Moreover, in disease, microglial phagocytic capacity is regulated by complement cascade molecules and TREM2/TYROBP receptor complex which can induce myeloid cells to initiate an immune response (178).

In adulthood, the capability of microglia to proliferate is still possible although not frequent while depending on certain conditions (184). However, studies show that the number and density of microglial cells in the brain increase with age and their even distribution is lessened in multiple regions of the brain (185,186). There is a gradual build-up in the number of microglial cells with age, suggesting a compensatory mechanism allowing to retain homeostatic responsibilities which may become impaired with age due to senescence that affects long living microglia (187). Also, the proliferation of microglial cells is

increased in AD where these cells accumulate near the formed plaques (188). This act may stress the healthy microglial cells trying to balance the outcome of the burden put from senescent cells which cannot participate effectively in the process of contacting, phagocytizing and clearing A β .

Morphologically, upon activation, microglial processes become less ramified, and they undergo retraction (189). In aging human studies, the morphology of microglia was seen to be dystrophic with tortuous somas and de-ramified processes (190). Also, in aging animals microglia show increased variability in soma size while their process arborization is reduced in size and complexity (186). Microglial processes length, thickness, and ramification are significantly reduced in human brain samples from AD patients (191). Adult APP mice compared to their younger subjects exhibit larger somas with retracted processes and this phenomenon is more prominent near the plaques (192). The morphological changes of microglia taking place in both aging and AD suggest that the cells might diminish their surveillant role for a more reactive one.

Microglia using their highly motile processes can cover the brain parenchyma in a couple of hours, this microglial feature is essential for proper surveillance that enables microglia to rapidly react against any insult or cellular changes which may affect brain homeostasis. Impaired surveillance suspected in aging and AD is concurrent with a decrease in motility of microglial processes seen in the mouse brain (193,194). Also, aged microglia show reduced feedback to exogenous ATP and to focal induced tissue injuries where cell motility and recruitment are affected (195). In Tg mice microglial processes motility is also reduced, aged microglial cells around plaques show impaired process motility compared to microglia in young Tg mice (192). Microglial accumulation and migration toward A β plaques are due to chemokines release by the plaques and the chemokine receptors on microglia causing the cells to be activated and attracted to the site of the plaque. IL-8, MCP-1, MIP-1 α , MIP-1 β , M-CSF, and VEGF are the attracting molecules which induce a chemotactic response against A β (196,197,198). Then, the cells related to the plaques can release chemokines attracting other cells to the site of injury localizing the inflammatory response (199).

Phagocytic capacity of microglial cells is important for fulfilling their multiple roles in the brain. Whether phagocytosis is directed against pathogens, apoptotic cells, aggregated

proteins or aiding in synaptic modulation this feature can allow us to assess microglial health and contribution to the well-being of the brain. Studies in mice over 24 months of age showed microglia accumulating different types of cellular inclusions and condensed debris with lipofuscin bodies (200). The accumulation of those inclusions might suggest that microglia have difficulty digesting and clearing those bodies. While the process of aging might affect phagocytosis of myelin, A β and cellular debris, microglial phagocytic capacity is reduced in late stages of cerebral amyloidosis (201). In AD mouse models, microglia are considered to be more effective in A β phagocytosis and clearance at early stages of disease compared to later stages (202). Moreover, microglia from old APP-PS1 mice exhibit reduced expression of A β binding receptors and degrading enzymes which may affect the phagocytosis of the protein (203).

Protein homeostasis (proteostasis) mechanisms are essential for maintaining healthy cellular processes. Loss of these homeostatic mechanisms can be seen with aging and with disease favoring the aggregation and deposition of proteins in multiple neurodegenerative diseases (204). Microglia are generally linked to neurotoxic A β phagocytosis in AD. However, the question is whether microglia are capable of not only engulfing but also clearing the A β protein, thus allowing them to continue their beneficial phagocytic clearance of chronically accumulating plaques (205). Overwhelming disruption of proteostasis might overwhelm microglia with increased aggregation of plaques and hence alter their cellular mechanisms.

The role of neuroinflammation in the pathophysiology of AD is strongly supported by experimental evidence (206). In particular, the implication of microglia is reported by their presence surrounding A β and their adoption of a pro-inflammatory profile. Also, a number of genes of single nucleotide polymorphisms that were revealed by GWAS and are considered AD risk factors are closely related to microglial functions involved in phagocytosis and cytokine production. Those proteins include TREM2, CD33, CR1, ABCA7, SHIP1, and APOE (207). Mutations in microglial genes encoding TREM2 and CD33 are linked to the reduced phagocytic capacity of microglia around plaques. Moreover, transcriptome reports and genetic mutations of microglia in AD form a connection between the disease pathology and immune response alterations, where microglial secretion of inflammatory cytokines, ROS and chemokines near the plaques induces further inflammatory response.

1.6.4 Chronic stress effects on microglia in AD

In response to unfavorable and challenging situations, our bodies enter in a state of stress. Our internal adaptive mechanisms fight to overcome stressful conditions to regain homeostasis (208). Stress can be advantageous or detrimental depending on the type of stressor and its effects. Also, the duration of exposure to the stressor and its consequences play an important role in determining the nature of the outcome of the stressful situation (209). While the adaptive internal body systems can resolve acute stress, chronic stress creates disruptions in the homeostatic mechanisms of the body. Chronic stress is thus considered a risk factor for several diseases including cardiovascular diseases, depression, and AD (210). As a response to stress, the body activates the hypothalamic-pituitary-adrenocortical (HPA) axis which causes the release of cortisol in the blood of humans or corticosterone in the blood of rodents (211). Glucocorticoids then travel by blood and cross the BBB where they bind to mineralocorticoid receptors (MR) and glucocorticoid receptors (GR) located on the membrane of several cells in the brain (212). Microglia express both MR and GR receptors (213). In chronic stress, the activation of the HPA axis is sustained due to the loss of inhibitory feedback (214). This sustained activation leads to a hippocampal neuronal damage in rats (215), and it may initiate AD pathology (216). AD patients had 83% more cortisol in their CSF when compared to age-matched healthy patients (217). People with a history of early-life depression were also more prone to developing AD later in life, thus suggesting a possible impact of stress on brain functions (218). In animal models, chronic restraint stress led to elevated A β 42 levels and plaque deposition in the hippocampus of female 5xFAD mice (219). Sustained social isolation of adult APP/PS1 transgenic mice mainly influenced AD-like pathology. In the hippocampus of 7 months old mice, A β 42/ A β 40 ratio increased and aggravated the impairment of spatial working memory (220). Also, 3xTgAD mice subjected to chronic mild social stress showed an increase in corticosterone levels matching their controls. The transgenic mice presented a decrease in BDNF levels and an increase in oligomeric and intraneuronal A β in the hippocampus (221). Microglia become reactive when exposed to stress signals (222). Microglia play a vital role as a mediator for brain response to stress. In CX3CR1 knockout mice, microglia are not affected by stress due to the alteration of the fractalkine signaling they receive from the neurons, thus rendering these mice more resistant to stress (223). Prevention of anxiety was seen when microglial depletion was induced in mice subjected to chronic stress (224). Also, in rats treated with minocycline, a drug that modulates microglial phagocytic activity, working memory was improved even after exposure to

chronic restraint stress (225). Chronic stress can affect AD pathology in multiple ways by, stress plays an essential role in enhancing A β deposition, increasing pro-inflammatory cytokines release, reducing the secretion of trophic factors, and triggering neuronal loss similar to aging as well as microglial reactivity which may cause an exaggerated immune response furthering neuroinflammation.

1.7 Hypothesis and objectives

The main objective of this thesis is to study the role that microglia is playing in the pathogenesis of AD. Also, this thesis characterizes the morphological and functional changes that are happening to microglia in an APP-PS1 mouse model and in age-matched control, which enables us to study these changes not only in disease but also during normal aging. We hypothesize that microglial reaction to A β pathology is heterogenous and depend on the context that these cells are in. We also assume that understanding this heterogeneity and their implications in different contexts can offer a better understanding of the contribution of these cells in different neurodegenerative diseases and AD in particular.

2. Studying microglial interactions with the plaques of amyloid- β using correlative light and electron microscopy

AUTHORS:

Bisht, Kanchan*;
Neurosciences Axis
CHU de Québec Research Center
2705, boulevard Laurier
Québec, Québec
G1V 4G2 Canada

El Hajj, Hassan*;
Neurosciences Axis
CHU de Québec Research Center
2705, boulevard Laurier
Québec, Québec
G1V 4G2 Canada

Savage, Julie C;
Neurosciences Axis
CHU de Québec Research Center
2705, boulevard Laurier
Québec, Québec
G1V 4G2 Canada

Sánchez, Maria G;
Neurosciences Axis
CHU de Québec Research Center
2705, boulevard Laurier
Québec, Québec
G1V 4G2 Canada

Tremblay, Marie-Ève
Neurosciences Axis
CHU de Québec Research Center
2705, boulevard Laurier
Québec, Québec
G1V 4G2 Canada

*equal contribution as first authors

CORRESPONDING AUTHOR:

Tremblay, Marie-Ève
Neurosciences Axis
CHU de Québec Research Center
2705, boulevard Laurier
Québec, Québec
G1V 4G2 Canada
Tremblay.Marie-Eve@crchudequebec.ulaval.ca
Tel.: 1-418-525-4444, ext. 46379

Resumé

Un protocole détaillé est fourni ici pour identifier les plaques amyloïdes (A β) dans les coupes cérébrales de modèles murins de la maladie d'Alzheimer avant l'intégration de l'immunocoloration en microscopie électronique (EM), spécifiquement pour la molécule adaptatrice ionique liant le calcium 1 (IBA1). Le méthoxy-X04 est un colorant fluorescent qui traverse la barrière hémato-encéphalique et se lie sélectivement aux feuilles plissées présentes dans les plaques A β . L'injection des animaux avec du méthoxy-X04 avant le sacrifice et la fixation du cerveau permet la présélection et la sélection des coupes de cerveau contenant les plaques pour un traitement ultérieur avec de longues manipulations. Cela est particulièrement utile lorsque l'on étudie une pathologie précoce de la maladie d'Alzheimer au sein de régions spécifiques du cerveau ou de couches pouvant contenir très peu de plaques, où elles sont présentes dans une petite fraction seulement des sections. Le traitement post-mortem des coupes de tissus avec du rouge Congo, de la thioflavine S et de la thioflavine T (ou même avec du méthoxy-X04) permet de marquer les feuilles plissées, mais nécessite un nettoyage intensif à l'éthanol incompatible avec notre protocole de EM. Il serait également inefficace de marquer l'A β (et d'autres marqueurs cellulaires tels que IBA1) sur toutes les sections du cerveau des régions d'intérêt, mais seulement produire une petite fraction contenant des plaques A β au bon endroit. Il est important de noter que les plaques A β sont encore visibles après le traitement des tissus pour le EM, permettant une identification précise des zones (généralement de quelques millimètres carrés) à examiner au microscope électronique.

2.2 KEYWORDS:

Alzheimer's disease, mouse model, amyloid- β , microglia, immunohistochemistry, fluorescence microscopy, electron microscopy

2.3 SHORT ABSTRACT:

This article describes a protocol for visualizing amyloid (A) β plaques in Alzheimer's disease mouse models using methoxy-X04, which crosses the blood-brain barrier and selectively binds to β -pleated sheets found in dense core A β plaques. It allows pre-screening of plaque-containing tissue sections prior to immunostaining and processing for electron microscopy.

2.4 LONG ABSTRACT:

A detailed protocol is provided here to identify amyloid A β plaques in brain sections from Alzheimer's disease mouse models before pre-embedding immunostaining (specifically for ionized calcium-binding adapter molecule 1 (*IBA1*), a calcium binding protein expressed by microglia) and tissue processing for electron microscopy (EM). Methoxy-X04 is a fluorescent dye that crosses the blood-brain barrier and selectively binds to β -pleated sheets found in dense core A β plaques. Injection of the animals with methoxy-X04 prior to sacrifice and brain fixation allows pre-screening and selection of the plaque-containing brain sections for further processing with time-consuming manipulations. This is particularly helpful when studying early AD pathology within specific brain regions or layers that may contain very few plaques, present in only a small fraction of the sections. Post-mortem processing of tissue sections with Congo Red, Thioflavin S and Thioflavin T (or even with methoxy-X04) can label β -pleated sheets, but requires extensive clearing with ethanol to remove excess dye and these procedures are incompatible with ultrastructural preservation. It would also be inefficient to perform labeling for A β (and other cellular markers such as IBA1) on all brain sections from the regions of interest, only to yield a small fraction containing A β plaques at the right location. Importantly, A β plaques are still

visible after tissue processing for EM, allowing for a precise identification of the areas (generally down to a few millimeter-square) to examine with the electron microscope.

2.5 INTRODUCTION:

Amyloid A β plaque formation is the main neuropathological hallmark of Alzheimer's disease (AD). However increasing evidence suggests important roles of the immune system in disease progression (226,227). In particular, new data from preclinical and clinical studies established immune dysfunction as a main driver and contributor to AD pathology. With these findings, central and peripheral immune cells have emerged as promising therapeutic targets for AD (206). The following protocol combines light and electron microscopy (EM) to generate new insights into the relationship between A β plaque deposition and microglial phenotypic alterations in AD. This protocol allows the labeling of A β plaques in mouse models of AD using *in vivo* injection of the fluorescent dye methoxy-X04. Methoxy-X04 is a Congo Red derivative that can easily cross the blood-brain barrier to enter the brain parenchyma and bind β -pleated sheets with high affinity. Since the dye is fluorescent, it can be used for *in vivo* detection of A β plaque deposition with two-photon microscopy (228). Once bound to A β , methoxy-X04 does not dissociate or redistribute away from plaques, and it retains its fluorescence over time. It is generally administered peripherally to allow for non-invasive imaging of brain dynamics (229). The fluorescence also remains following aldehyde fixation, allowing for correlative post-mortem analyses, including investigation of neuronal death in the vicinity of A β plaques (230).

This protocol takes advantage of the properties of methoxy-X04 to select brain sections from APP_{SWE}/ PS1A_{246E} mice (APP-PS1; coexpressing a double mutation at APP gene Lys670Asn/ Met671Leu, and human presenilin PS1-A264E variant) (70) that exhibit A β plaques in specific regions of interest (hippocampus CA1, strata radiatum and lacunosum-moleculare) prior to pre-embedding immunostaining against the microglial marker ionized calcium-binding adapter molecule 1 (IBA1) to visualize microglial cell bodies and processes with EM. The mice are given intraperitoneal injection of methoxy-X04 solution, 24 hours prior to brain fixation through transcardial perfusion. Coronal brain sections are

obtained using a vibratome. Sections containing the hippocampus CA1 are screened under a fluorescent microscope for the presence of A β plaques in strata radiatum and lacunosum-moleculare. Immunostaining for IBA1, osmium tetroxide post-fixation, and plastic resin embedding are then performed on the selected brain sections. At the end of this protocol, the sections can be archived without further ultrastructural degradation, ready for ultrathin sectioning and ultrastructural examination. Importantly, the plaques are still fluorescent after immunostaining with different antibodies, for instance IBA1 as in the present protocol. They become darker than their surrounding neuropil following osmium tetroxide post-fixation, independently of methoxy-X04 staining, which helps to accurately identify the regions of interest, generally down to a few millimeter-square, to be examined with the transmission electron microscope.

This correlative approach offers an efficient way to identify specific brain sections to examine at the ultrastructural level. This is particularly helpful when studying early AD pathology, within specific brain regions or layers that may only contain a few A β plaques, present in only a small fraction of tissue sections. During these times especially, it would be inefficient to use immunostaining for A β (and dual labeling for other cellular markers such as IBA1) on several brain section simply to yield a small fraction containing A β plaques at the right location. In addition, injection of live mice with methoxy-X04 prior to sacrifice and tissue processing does not compromise the ultrastructural preservation. Alternative methods such as post-mortem staining with Congo Red, Thioflavin S, Thioflavin T or methoxy-X04 on fixed tissue sections require staining differentiation in ethanol (231,232,233,234), which causes osmotic stress and disrupts the ultrastructure. Congo Red is also a known human carcinogen (235).

2.6 PROTOCOL:

NOTE: All experiments were approved and performed under the guidelines of the Institutional animal ethics committees, in conformity with the Canadian Council on Animal Care guidelines as administered by the Animal Care Committee of Université Laval. APP-

PS1 male mice between 4 and 21 months of age were used. These animals were housed under a 12-hour light-dark cycle at 22–25°C with free access to food and water.

2.6.1 Methoxy-X04 solution preparation:

2.6.1.1) Prepare a 5mg/ml solution of methoxy-X04 (232) by dissolving methoxy-X04 into a solution containing 10% dimethyl sulfoxide (DMSO), 45% propylene glycol, and 45% sodium phosphate buffered saline (0.9% NaCl in 100mM phosphate buffer, pH 7.4).

2.6.1.2.) Using a microbalance, weigh 5 mg of the methoxy-X04 compound. Under a fume hood, dissolve the methoxy-X04 in DMSO and stir until a clear greenish solution is obtained. Successively add propylene glycol and phosphate buffer saline while stirring with each addition.

2.6.1.3) Stir the solution at 4°C on a rotator overnight. Obtain a yellowish green emulsion. The solution may be stored at 4°C for up to two months without degradation.

2.6.2 Methoxy-X04 solution injection:

2.6.2.1) 24 hours prior to perfusion, weigh the mice and give each mouse an intraperitoneal injection of methoxy-X04 at a dose of 10mg/kg of body weight using a 27 ½-gauge needle.

2.6.3 Transcardial perfusion of the injected mice:

2.6.3.1) On the day before the perfusion, prepare appropriate volumes of phosphate buffered saline (PBS), 3.5% acrolein, and 4% paraformaldehyde (PFA) solutions (236) and store them at 4°C overnight. NOTE: These solutions will be used for both perfusion and pre-embedding immunohistochemistry. Take special care when working with acrolein, it is corrosive and toxic to both researchers and the environment. In addition, since acrolein is corrosive to plastic, always use suitable glassware to prepare acrolein solutions.

2.6.3.2) On the day of perfusion, filter the PFA and acrolein by using coarse filter paper of 25µm particle retention.

2.6.3.3) During the perfusion, use a peristaltic pump to deliver 15ml of PBS, 75ml of acrolein, and 150ml of PFA successively into the mouse circulation, at a flow rate of 25ml/min. **CAUTION!** Perform perfusion strictly inside a fume hood to avoid harmful fumes of PFA and acrolein.

2.6.3.4) To set-up the pump, insert one end into the PBS solution, fill the tubing (holding approximately 15ml) with PBS, and fix a 25-gauge winged blood collection needle to the other end. At all times, ensure that the tubing is free from any trapped air bubbles.

2.6.3.5) Place the tube directly in the acrolein bottle after setting the perfusion pump with the tubing filled with PBS.

2.6.3.6) Anaesthetize one mouse at a time with a 90mg/kg of body weight dose of sodium pentobarbital injected intraperitoneally using a 27 ½-gauge needle. Assess responses to tail/toe pinches. Proceed only if the mouse is unresponsive to such aversive, painful stimuli.

2.6.3.7) Secure the mouse in the supine position (lying on the back with face upward) by taping the forepaws and hindpaws to the work surface and carefully expose the heart without causing damage to other organs. Be sure to work quickly after puncturing the diaphragm.

2.6.3.8) Perform an incision through the skin with surgical scissors along the thoracic midline beginning caudal to the ribcage and proceed rostral to the clavicle.

2.6.3.9) Make two additional lateral incisions along the base of the ventral ribcage. Gently move and pin the two flaps of skin, making sure to expose the entire thoracic cavity.

2.6.3.10) Hold the xiphoid process with blunt forceps to expose the thoracic cavity and steady the pointed scissors. Cut through the diaphragm and ribcage, being careful to avoid puncturing the lungs, and continue the incision rostral to the clavicles. Be sure to work quickly after puncturing the diaphragm.

2.6.3.11) Gently tear the pericardial sac with blunt forceps. Hold the heart steady with blunt forceps, cut the right atrium, and start the infusion of PBS. Immediately insert the blood collection needle into the left ventricle.

2.6.3.12) Perfuse the mouse with PBS (in the tubing) followed by acrolein for 3 minutes (corresponding to 75ml) then switch to PFA for 6 minutes (corresponding to 150ml). Be sure to pause the pump flow before switching solution to prevent bubbles from entering the tube.

2.6.3.13) Decapitate the mouse and extract the fixed brain and place it directly into a glass vial containing 4% PFA for at least 2 hours at 4°C.

2.6.3.14) To extract the brain, use scissors and tweezers to cut through the skin to expose the skull. Carefully break the skull open in between the eyes, and chip off small pieces of it to expose the underlying brain.

2.6.3.15) Carefully remove the exposed brain and post-fix it with 4% PFA for additional 2 hours before proceeding for vibratome sectioning.

2.6.4 Brain sectioning using a vibratome:

2.6.4.1) Wash the fixed brain 3 times with chilled PBS. Using a sharp razor blade, remove the olfactory bulb (unless this region is under investigation) and cut the brain transversally into 2-3 pieces of approximately equal height, all of which can be sectioned simultaneously in order to accelerate the procedure.

2.6.4.2) Glue the pieces of brain tissue vertically onto the specimen plate secured into the tray. Make sure that the smooth cut surface sticks firmly to the specimen plate and does not get dislodged during the sectioning procedure. Add enough PBS solution into the tray until the entire brain surface is completely submerged. It is important to keep the brain pieces and subsequent sections fully immersed in PBS throughout this step.

2.6.4.3) Place the tray in the vibratome, adjust the sectioning speed to 0.5 mm/s, the sectioning frequency to 90 Hz and the feed thickness to 50 μ m in order to yield 50 μ m thick sections. Then transfer the sections into 20ml glass vials containing cryoprotectant solution (40% PBS, 30% ethylene glycol, and 30% glycerol) using a fine paintbrush. Store the vials at -20°C until further use. Alternatively, keep the sections in PBS for immediate screening as described in the following steps.

2.6.5 Section screening for the presence of methoxy-X04-stained plaques:

2.6.5.1) With the aid of a stereotaxic mouse brain atlas (237), select brain sections containing the region of interest, for instance the hippocampus CA1 as used in the present example. Place each section into a well within a 24-well culture plate containing enough cryoprotectant solution so as to prevent the sections from drying out.

2.6.5.2) Examine each section successively, to avoid drying out of the sections, using the following procedure:

2.6.5.3) Add a droplet of PBS to a microscope slide with a disposable pipette, and place the section on the droplet.

2.6.5.4) Examine the section under a fluorescent microscope to identify regions containing methoxy-X04 labeled A β plaques. NOTE: methoxy-X04 can be easily visualized using a fluorescence ultraviolet (UV) filter (excitation 340-380 nm).

2.6.5.5) Capture images of regions of interest (ROI) in bright field as well as in fluorescence mode without moving the microscope stage, since each image must show the same region in both fields in order to correlate the presence of the plaques directly to the structural region of the tissue section.

2.6.5.6) Save and name the images taken according to the animal number, also record the well number in the plate and the field of the pictures taken. For example, Ex: 9978A1B; Animal number: 9978; Well number: A1; Field: Bright. Place the section back to its designated well once the imaging is completed.

NOTE: At the end, for each section examined, two pictures are obtained, one in bright field and another in UV field.

2.6.5.7) Open the two images of the same ROI (one in bright field and the other in UV field) in Image J, and using the “**MosaicJ plugin**” align the edges of the two images and save the aligned and combined image according to the well number it came from.

2.6.5.8) Save the picture in a separate folder with the number of the particular animal. Combine the images to identify and localize the plaques in the tissue section, and have a full view of the whole section in the two different fields (bright and UV).

2.6.5.9) After the screening process is completed, store the examined sections at -20°C in a 24-well culture plate containing cryoprotectant until immunostaining or further processing is carried out.

2.6.6 Pre-embedding immunostaining for IBA1:

NOTE: Perform the immunostaining for IBA1 on freely-floating selected sections by placing the plate on a slowly moving rocker at room temperature.

2.6.6.1) Thoroughly wash the sections 3 times with approximately 1ml PBS, each wash lasting for 10 minutes.

2.6.6.2) Quench endogenous peroxidases with 0.3% hydrogen peroxide in PBS solution for 10 minutes. This step prevents non-specific peroxidase activity, which is important to avoid background staining.

2.6.6.3) Wash the tissue in PBS 3 times for 10 minutes each.

2.6.6.4) Incubate the sections in 0.1% sodium borohydride in PBS solution for 30 minutes. This step is important to reduce any remaining aldehydes from the fixation step, and is especially important if acrolein is used in tissue fixation.

2.6.6.5) Wash the tissue in PBS 3 times for 10 minutes each time and make sure to remove all the bubbles.

2.6.6.6) Block the sections for 1 hour. Different antibodies may require different blocking times and solutions. For IBA1, prepare blocking buffer containing 10% fetal bovine serum, 3% bovine serum albumin, and 0.01% Triton X-100 in 50mM Tris-buffered saline (TBS; pH 7.4).

NOTE: The blocking step is to prevent nonspecific binding of the primary antibody. The low concentration of Triton X-100 allows slight permeabilization of membranes for better staining, and is low enough to preserve most ultrastructural features of tissue under EM.

2.6.6.7) Remove the blocking buffer from the tissue, and incubate in primary antibody solution (rabbit anti-IBA1, diluted [1:1000] prepared in blocking buffer) at 4°C overnight.

2.6.6.8) Wash in TBS 3 times for 10 minutes each time.

2.6.6.9) Incubate in secondary antibody (goat anti rabbit conjugated to biotin) [1:200] in 0.05M TBS for 90 minutes.

2.6.6.10) Wash in TBS 5 times for 5 minutes each time.

2.6.6.11) Incubate in Avidin-Biotin complex solution (Avidin [1:100], Biotin [1:100]) in TBS solution for 1 hour.

2.6.6.12) Wash in TBS 5 times for 5 minutes each time.

2.6.6.13) Reveal the IBA1 staining with 0.05% diaminobenzidine (DAB) and 0.015% hydrogen peroxide in TBS for 8 minutes.

NOTE: The timing of DAB development may vary from protocol to protocol and should be determined by quickly examining the stained sections under a light microscope. Note: for IBA1, one should be able to clearly visualize the cell bodies and processes of the IBA1-stained microglia at 20X (see Figure 2.8.2 for representative example). Be cautious using DAB, as it is a known carcinogen.

2.6.6.14) Avoid over-developing by carefully monitoring the sections (as described above) during this step. Stop the reaction by washing the sections in chilled PB 5 times for 5 minutes each time.

2.6.7 Processing for electron microscopy:

2.6.7.1) Prepare 1% osmium tetroxide solution in PBS in a glass vial. Osmium tetroxide is photosensitive – cover the glass vial with aluminum foil to protect the solution from light. **CAUTION!** Be cautious using osmium tetroxide, it is a very hazardous chemical. Perform this and the following steps inside a fume hood.

2.6.7.2) Remove the PBS from the sections and spread them flat using a fine paintbrush. Perform this step one well at a time to avoid the sections from drying out. Be sure to flatten the sections immediately before adding osmium tetroxide, as any folds in the sections will become permanent and attempting to flatten tissue post osmium fixation will only break the sections.

2.6.7.3) Immerse the sections in osmium tetroxide for 30 minutes at room temperature, adding one drop of osmium tetroxide at a time with a transfer pipette, to prevent the

sections from folding. Cover the well with aluminum foil to protect the sections from light.
NOTE: This step fixes the lipids within the sections and the tissue will appear very dark after osmium post-fixation.

2.6.7.4) While sections are in osmium tetroxide, prepare plastic resin in a disposable beaker by mixing 20g component A, 20g component B, 0.6g component C, and 0.4g component D. Combine the components together in the above order and mix them well using a 10ml serological pipette until a uniform color is obtained.

2.6.7.5) Transfer the prepared mixture to aluminum weighing dishes. They will receive the tissue sections once they have been dehydrated.

2.6.7.6) Dehydrate the sections in increasing concentrations of ethanol for 2 minutes in the following order: 35%, 35%, 50%, 70%, 80%, 90%, 100%, 100%, 100%.

2.6.7.7) To remove residual ethanol, immerse the sections in propylene oxide 3 times for 2 minutes each time. Remove the dehydrated-sections from the 24-well culture plate into 20ml glass vials. Always use glass vials when working with propylene oxide as it dissolves plastic, and maintain caution as it is hazardous.

2.6.7.8) Use a bent glass pipette tip or a fine paintbrush to transfer the sections from propylene oxide solution into the resin and leave overnight for infiltration at room temperature. Be careful not to dilute the resin with propylene oxide.

2.6.7.9) Embed the section with the resin on poly-chloro-tri-fluoro-ethylene (PCTFE) film sheets:

2.6.7.9.1) Place the aluminum weighing dishes containing the specimens into a 50-60°C oven for 10-15 minutes prior to embedding the sections on PCTFE film sheets.

2.6.7.9.2) When embedding sections, work with one aluminum weighing dish at a time. Using a fine paintbrush, paint a thin layer of resin onto one PCTFE film sheet.

2.6.7.9.3) Move one section of tissue at a time from the aluminum weighing dish to the PCTFE film sheet. Remove excess resin from around the tissue, being careful not to disturb it.

2.6.7.9.4) After moving all the sections from one weighing dish to the PCTFE film sheet, place a second PCTFE sheet over the first, creating a sandwich of tissue and resin in between 2 sheets.

2.6.7.10) Polymerize the resin in an incubator for 3 days at 55-60°C temperature.

2.6.7.11) The material is now ready for ultrathin sectioning and ultrastructural examination, specialized techniques which are often performed by EM core facilities. Store the samples between PCTFE film sheets safely at room temperature without ultrastructural degradation.

NOTE: The subsequent steps for ultrathin sectioning and transmission electron microscopy examination are explained in *Preparation of mouse brain tissue for electron microscopy*(236).

2.7 REPRESENTATIVE RESULTS:

This section illustrates the results that can be obtained at different critical steps of the protocol. In particular the results show examples of brain sections containing methoxy-X04 stained plaques in specific region and layers of interest: the hippocampus CA1, strata radiatum and lacunosum-moleculare. The plaques and regional/lamellar organization of the hippocampus are successively visualized using a combination of UV and bright field filters (Figure 2.8.1). The selected brain sections are subsequently immunostained and processed for EM while keeping track of their A β plaques, considering that they are still fluorescent following immunostaining, and become darker than the surrounding neuropil following treatment with osmium tetroxide and embedding (Figure 2.8.1). This allows one to identify

the areas (generally a few millimeter-square) to examine with the electron microscope based on the location of plaques. Furthermore, an improved protocol for pre-embedding immunostaining of microglia with IBA1 is described here. This protocol yields an exceptional visualization of microglial cell bodies, large and small processes (Figure 2.8.2) as well as penetration of the antibodies within the brain sections. It thus facilitates the identification of microglial cell bodies and processes at the ultrastructural level, and the study of their interactions with A β plaques (Figures 2.8.3 and 2.8.4).

2.8 FIGURE LEGENDS:

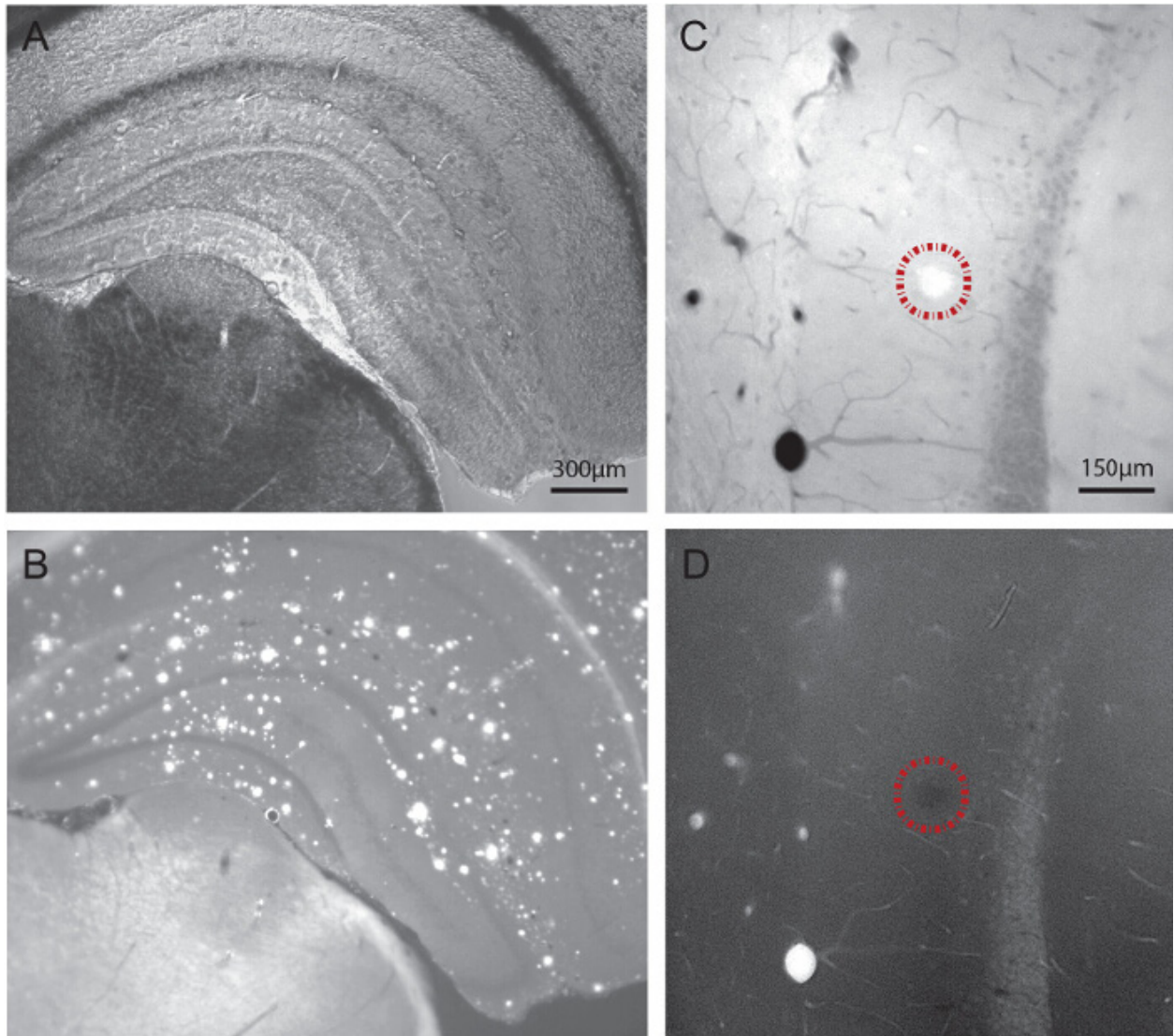


Figure 2.8.1 Visualization of A β plaques in 21-month old APP-PS1 mice using light microscopy, following systemic injection of the fluorescent dye methoxy-X04. A-B: Dual imaging of one hippocampal section using bright field and fluorescence modes. The regions and layers of interest are visualized under bright field (A), and the A β plaques successively localized using an UV filter at a range of 340-380nm (B). C and D: Dual imaging of another hippocampal section before (C) and after (D) pre-embedding immunostaining for IBA1, followed by post-fixation in osmium tetroxide, dehydration in ethanol, and embedding in a plastic resin as required for transmission electron microscopy. To be noted, the plaque (encircled by a dotted line) is still visible upon tissue processing for electron

microscopy. Visualizing the plaques when trimming the tissue blocks allows for a precise selection of the areas to image at high spatial resolution. Scale bars=300 μ m for A and B, 150 μ m for C and D.

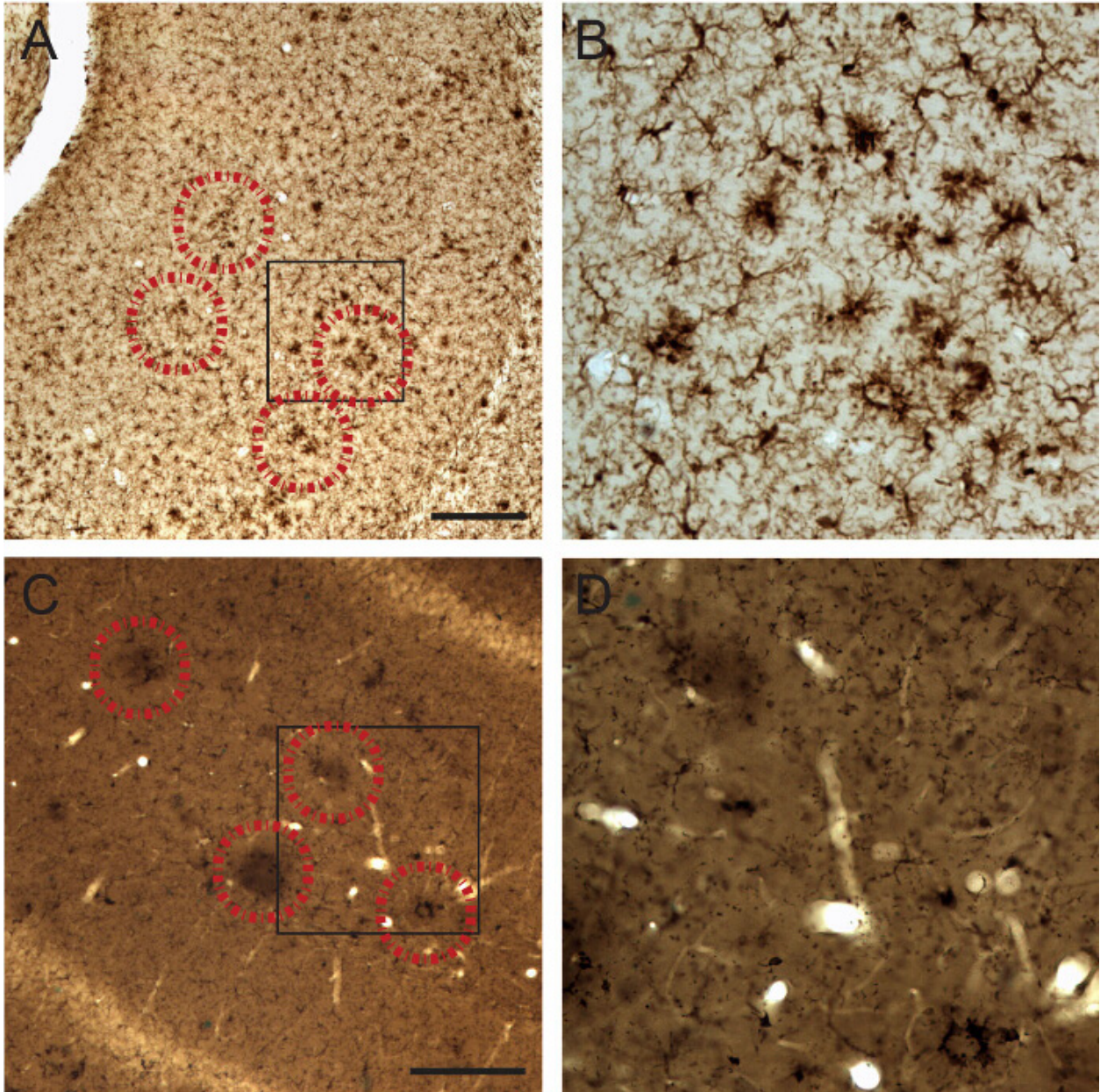


Figure 2.8.2 Visualization of microglial cell body and fine processes in 21-month old APP-PS1 mice by IBA1 staining at the light microscopic level. A-B: Examples of IBA1-stained microglia showing a clustered distribution when they associate with A β plaques (identified by correlative fluorescence imaging of methoxy-X04; encircled by a dotted line) as

observed before osmium tetroxide post-fixation and plastic resin embedding. C-D: Examples of IBA1-stained microglia associated with A β plaques after osmium tetroxide post-fixation and plastic resin embedding. Note that the plaques become darker than their surrounding neuropil following osmium post-fixation, thus allowing keeping track of their location. Scale bar=250 μ m.

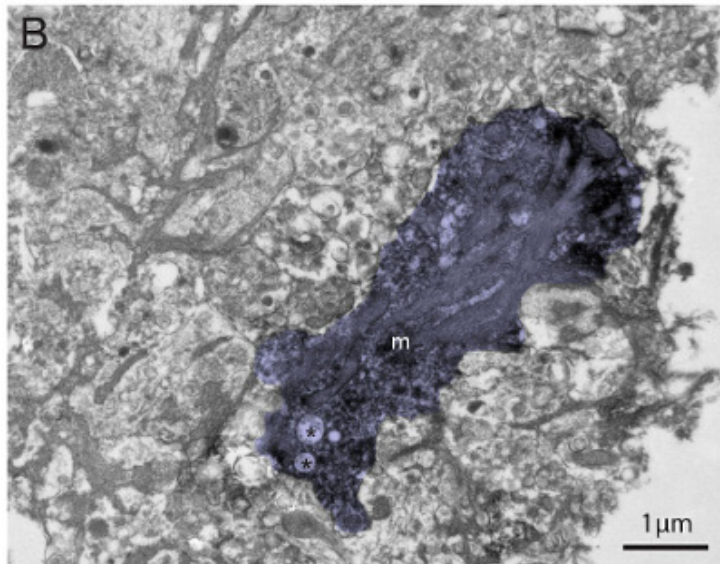
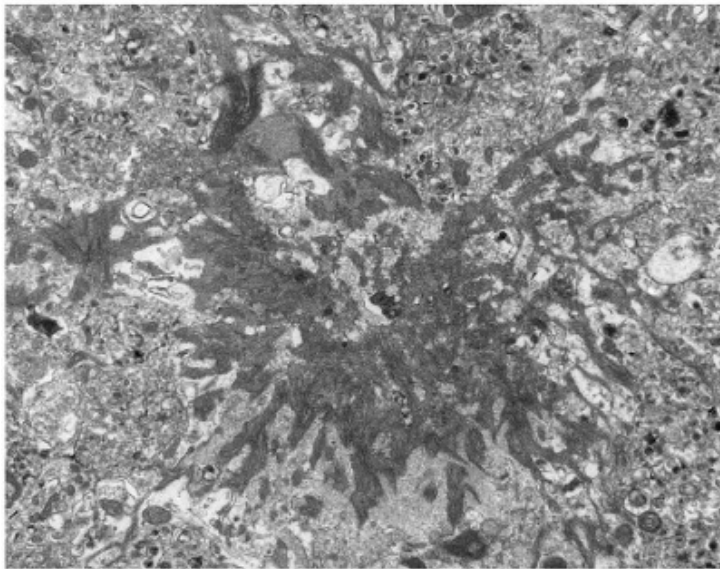
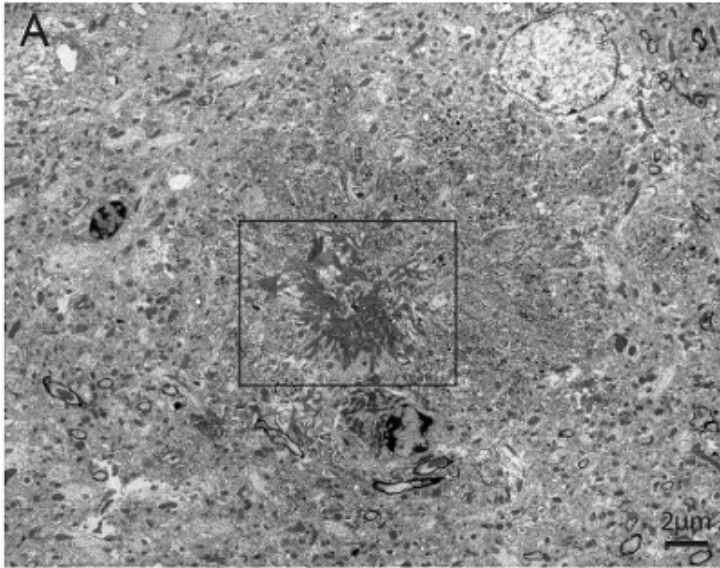


Figure 2.8.3 Dual visualization of A β plaques and IBA1-immunostaining in 6-month old APP-PS1 mice at the ultrastructural level. A: Example of dense core A β plaque recognized by its compact fibrillary structure (see inset) and association with dystrophic neurites with ultrastructural features of autophagy. B: Example of IBA1-stained microglial process (m; colored in violet) found nearby the A β plaque that contains amyloid deposits. Mitochondrial alterations (shown by asterisks) can also be seen within the microglial process. To be noted, this picture was acquired at the tissue-resin border (white, at the right of the picture) where the penetration of antibodies and staining intensity is maximal. Scale bars=2 μ m for A, 1 μ m for B.

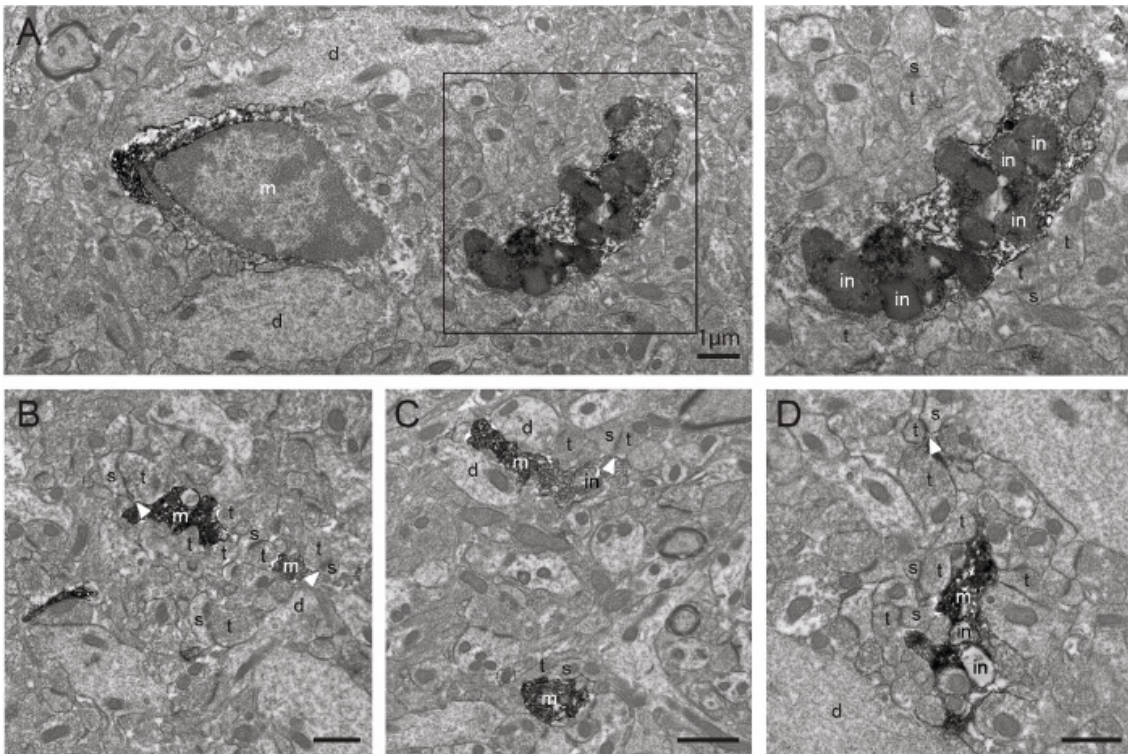


Figure 2.8.4 Additional examples of IBA1-immunostained microglia in 6-month old APP-PS1 mice as observed with transmission electron microscopy. A-D: Examples of IBA1-stained microglial cell body and processes (m) acquired farther from the tissue-resin border, showing an excellent penetration of the antibodies and staining intensity deeper within the section using this protocol. bv=blood vessel, d=dendrite, in=inclusion, s=dendritic spine, t=axon terminal. The arrowheads show synaptic clefts. Scale bars=1 μ m.

2.9 DISCUSSION:

This protocol explains a correlative approach for targeting dense core A β plaques with EM. Methoxy-X04 *in vivo* injection allows rapid selection of brain sections that contain A β plaques within particular regions and layers of interest, for instance the hippocampus CA1, strata radiatum and lacunosum-moleculare. In the present example, methoxy-X04 pre-screening was combined with pre-embedding immunostaining for IBA1 to study how different microglial phenotypes interact with synapses at the ultrastructural level in the presence of dense core A β plaques.

Microglia are incredibly responsive to their surroundings and their inflammatory activity has been long studied in the context of undermining normal brain function and enhancing the advancement of AD. In particular, these cells were implicated in neurodegenerative processes due to their extensive activation and release of pro-inflammatory cytokines, leading to chronic neuroinflammation and disruption of normal brain homeostasis (238). In recent years, however, these resident immune cells were also shown to actively remodel neuronal circuits in the healthy brain, leading to identification of new pathogenic mechanisms (151,143). Their physiological roles at synapses may become dysregulated during neuroinflammation in AD, resulting in exacerbated synaptic loss, currently the best pathological correlate of cognitive decline across various neurodegenerative conditions (7,239).

The modifications made to the previous pre-embedding IBA1 staining method (236) now allow better penetration of antibodies across the brain sections, as well as visualization of microglial cell bodies and fine processes at the ultrastructural level. Overall, the protocol needs to be performed rigorously from mouse perfusion until plastic resin embedding of the tissue sections, considering that ultrastructural degradation occurring at any in-between step could compromise the integrity of cellular membranes, organelles, cytoskeletal elements, etc.

This protocol could be performed without any immunostaining (by omitting section 2.6.6) to solely visualize dense core A β plaques, but it also provides a powerful tool to study the

complex mechanisms of AD pathogenesis with relation to A β deposition, as different antibodies may be used to focus on different cell types, including peripherally-derived macrophages, endogenous microglia, astrocytes, oligodendrocytes and their progenitors, as well as many neuronal subtypes.

Considering the *in vivo* injection of methoxy-X04, this protocol cannot be performed on fixed brain sections, which precludes its use with post-mortem human brain samples. Also, contrarily to immunostaining against A β which labels soluble and insoluble forms of A β , the use of dyes binding to β -pleated sheet protein structures such as methoxy-X04 only allows to visualize dense core plaques, which constitutes another limitation.

Nevertheless, important applications could include studying the roles of microglia and other various cell types, which overlap and augment their activities, and could have direct effects on plaque homeostasis and neuronal function over the course of AD pathology.

2.10 ACKNOWLEDGEMENTS

We are grateful to Dr. Sachiko Sato and Julie-Christine Lévesque at the Bioimaging Platform of the Centre de recherche du CHU de Québec for their technical assistance. Grants from the Natural Sciences and Engineering Research Council of Canada (NSERC) RGPIN-2014-05308, The Banting Research Foundation, and The Scottish Rite Charitable Foundation of Canada to M.E.T supported this work.

H.E.H. is recipient of a scholarship from the Lebanese Ministry of Education and Higher Education, and K.B. from the Faculté de médecine of Université Laval.

3.Spatial heterogeneity of microglial ultrastructural and functional alterations with relation to A β plaques and neuronal dystrophy in Alzheimer's disease mouse model and human hippocampus

Hassan El Hajj¹, Kanchan Bisht¹, Julie Savage*¹, and Marie-Ève Tremblay*^{1,2}

¹ Axe neurosciences, Centre de recherche du CHU de Québec-Université Laval, Québec, QC, Canada.

² Département de médecine moléculaire, Faculté de médecine, Université Laval, Québec, QC, Canada.

* Equal contribution as co-senior authors

Correspondence

Marie-Ève Tremblay

Axe neurosciences, Centre de recherche du CHU de Québec-Université Laval

2705, boulevard Laurier, T2-66

Québec, QC

G1V 4G2

Canada

Phone: +1-418-525-4444 x46379

Fax: +1-418-654-2298

tremblay.marie-eve@crchudequebec.ulaval.ca

3.1 Acknowledgements

We are grateful to Nathalie Vernoux for technical assistance and guidance with the experiments, Julie-Christine Lévesque at the Bio-Imaging platform of the *Infectious Disease Research Centre*, funded by an equipment and infrastructure grant from the Canadian Foundation Innovation (CFI), Luc Vallières and Serge Rivest for providing animals, Martin Parent for human tissue, as well as Martin Fuhrmann and Michael Heneka for discussing some of the findings.

H.E.H. was supported a scholarship from the Lebanese Ministry of Education and Higher Education, K.B. by excellence scholarships from Université Laval and Fondation du CHU de Québec, and J.C.S. by a postdoctoral fellowship from Fonds de recherche en santé du Québec. This work was funded by grants from The Banting Research Foundation, The Scottish Rite Charitable Foundation of Canada, and NEURON-ERANET (TracInflam) awarded to M.E.T.. M.E.T. holds a Canada Research Chair (Tier 2) in *Neuroimmune plasticity in health and therapy*.

3.2 Conflict of interest Statement

The authors declare no competing financial interests.

3.3 Résumé

La maladie d'Alzheimer (AD) est la maladie neurodégénérative la plus fréquente et se caractérise par le dépôt de fibres amyloïdes extracellulaires fibrillaires (fA β) et par des enchevêtrements neurofibrillaires intracellulaires. Au fur et à mesure que la MA progresse, l'amyloïde entraîne une réponse inflammatoire robuste et prolongée via sa reconnaissance par les microglies, les cellules immunitaires résidentes du cerveau. La réactivité microgliale à aux plaques fA β peut affecter leurs interactions avec les structures neuronales, facilitant la perte synaptique et la mort neuronale, la plus connue corrélation avec le déclin cognitif de la MA et d'autres maladies neurodégénératives. Nous avons identifié des phénotypes microgliaux hétérogènes dans des régions spatialement distinctes de l'hippocampe CA1 en utilisant la microscopie optique et électronique corrélative et avons validé nos résultats dans des tissus post-mortem provenant de deux cas humains de MA. Nous avons effectué une analyse ultrastructurale de la microglie dans des tissus sains, des tissus dystrophiques et des tissus proximaux à des plaques fA β dans l'hippocampe ventral de souris APPSwe-PS1e9 âgées de 14 mois par rapport à des souris sauvages. Les corps cellulaires microgliaux des souris AD présentaient des zones de corps cellulaires plus grandes, des périmètres et des signes ultrastructuraux de stress cellulaire au voisinage de fA β . Les corps cellulaires et les prolongements microgliaux dans les tissus apparemment sains et dans les zones de dystrophie neuronale étaient moins phagocytaires que les microglies sauvages, tandis que la capacité phagocytaire à proximité des plaques restait élevée mais aux dépens de la phagocytose normale du neuropile environnant. Dans toutes les régions du tissu AD, la dégradation extracellulaire et les interactions avec les structures dégénératives étaient aussi réduites. Il est intéressant de noter que les prolongements dans les régions d'apparence saine des modèles de souris AD étaient beaucoup plus susceptibles d'encercler les épines dendritiques par rapport aux autres tissus, y compris les tissus témoins. Nos résultats définissent ensemble l'hétérogénéité de la structure et de la fonction microgliales à haute résolution spatiale dans les tissus de souris et humains en réponse à la pathologie amyloïde.

3.4 Abstract

Alzheimer's disease (AD) is the most common neurodegenerative disease and is characterized by the deposition of extracellular fibrillar amyloid- β (fA β) and intracellular neurofibrillary tangles. As AD progresses, A β drives a robust and prolonged inflammatory response via its recognition by microglia, the brain's resident immune cells. Microglial reactivity to fA β plaques may affect their interactions with neuronal structures, facilitating synaptic loss and neuronal death, the best known correlate to cognitive decline in AD and other neurodegenerative diseases. We identified heterogeneous microglial phenotypes in spatially distinct regions of the CA1 hippocampus using correlative light and electron microscopy, and validated our findings in post-mortem tissue from two human cases of AD. We performed ultrastructural analysis of microglia in healthy tissue, dystrophic tissue, and tissue proximal to fA β plaques in the ventral hippocampus of 14 month old APP^{Swe}-PS1 Δ e9 mice *versus* wild-type littermates. Microglial cell bodies in AD mice had larger cell body areas, perimeters, and displayed ultrastructural signs of cellular stress in the vicinity of fA β . Microglial cell bodies and processes in seemingly healthy AD tissue and in areas of neuronal dystrophy were less phagocytic than wild-type microglia, while phagocytic capacity near the plaques remained high but targeted fA β at the expense of normal phagocytosis of surrounding neuropil. Microglia in all regions of AD tissue displayed reduced extracellular degradation and impaired interactions with degenerating structures. Interestingly, processes in healthy appearing regions of AD mouse models were considerably more likely to encircle dendritic spines compared with any other tissues, including control ones. Our findings together define the heterogeneity of microglial structure and function at high spatial resolution in both mouse and human tissue in response to amyloid pathology.

3.5 Introduction

Alzheimer's disease (AD) is the most common neurodegenerative disease, affecting 47 million people in a demographically aging world (240). The disease causes deficits in memory, learning and thinking abilities (30). The best neuropathological correlates of cognitive decline in AD are neuronal dystrophy and synaptic loss, which are associated with increased network excitability, notably of the hippocampus, and precede neuronal death (241,7). While the hippocampus is pivotal for long-term memory formation in addition to its essential role in memory storage and retrieval (242), hippocampal atrophy is consistent in AD with a mean volume loss ranging from 20-50% (243). The main pathological hallmarks of AD are deposition of extracellular amyloid beta ($A\beta$) plaques comprising insoluble $A\beta$ fibrils (f $A\beta$) and intraneuronal fibrillar tangles of tau protein (244). The prefibrillar soluble amyloid beta (s $A\beta$) that forms a halo around f $A\beta$ plaques was linked to neuronal dystrophy and synaptic loss, both in AD human samples and mouse models of $A\beta$ deposition (79,245,246,247,248,249).

Genome wide association studies (GWAS) uncovered a strong genetic involvement in AD of over 20 gene variants related to the immune system, including triggering receptor expressed on myeloid cells 2 (TREM2) (94,97,250). Microglia, the resident innate immune cells of the brain, recognize and respond to both s $A\beta$ and f $A\beta$ using complexes of pattern recognition receptors (PRRs) (251). Downstream signaling causes increases in $TNF\alpha$ and $IL-1\beta$ secretion which recruits nearby microglia via chemotaxis and can initiate a runaway inflammatory response that injures neurons as well as triggers synaptic loss (252,253,254,255). In the healthy brain the complement cascade mediates microglial pruning of less active synapses while in aging and AD this pathway takes a pathological role and promotes synaptic elimination (253). Microglia are thus firmly connected to brain inflammation and likely contribute to its harmful long-term consequences leading to neurodegeneration (246). Microglia are also instrumental in slowing down plaque growth and reducing synaptic loss by preventing $A\beta$ diffusion and toxicity (256,257), and they perform valuable roles in the clearance of both s $A\beta$ and f $A\beta$ (258,259). Microglial active contribution to $A\beta$ clearance can prevent the precipitation of $A\beta$ into fibrillar plaques and

reduce the brain concentration of harmful sA β species responsible for neurodegenerative effects (260).

Microglial implication in the pathological process of AD is contextual (261,262) and heterogeneous, as illustrated by single cell transcriptomic studies defining different phenotypes (263). For instance, the disease associated microglia (DAM) and microglia neurodegenerative (MGnD) phenotypes showed a reduction in homeostatic genes, but increase in phagocytic genes, and association with fA β plaques in mouse models and human samples (264,265,266). These phenotypes were shown to be regulated by TREM2, an innate immune receptor expressed by microglia which modulates their phagocytic activity, suppresses the production of pro-inflammatory cytokines and is upregulated in plaque-associated microglia (267). However, the functional outcomes of these altered microglial transcriptomes largely remain undetermined. While a role in A β clearance and apoptotic neurons removal was identified, how these new phenotypes impact on neuronal dystrophy and synaptic loss is still unknown. Using electron microscopy, our group recently described the “dark” microglia characterized by their electron-dense cytoplasm and nucleoplasm, among other markers of oxidative stress, and extensive interactions with synapses. These cells which are rare during normal physiological conditions became abundant in aging and AD pathology, in the APP^{Swe}-PS1 Δ e9 model of A β deposition. Dark microglia often associated with plaques, expressed TREM2, contained fA β , and encircled dystrophic neurites as well as synaptic elements (268). Interestingly, intermediate stages between the “dark” and “typical” microglia were also seen, while the “typical” microglia displayed several ultrastructural alterations.

The present study aimed to define the spatial heterogeneity of microglial ultrastructural and functional alterations with relation to neuronal dystrophy and synaptic loss in AD pathology, by comparing APP^{Swe}-PS1 Δ e9 mice (70) with wild-type controls. This well-established mouse model deposits A β forming plaques beginning at four months of age, in the cerebral cortex and hippocampus, with cognitive deficits beginning at six months and robust memory deficits by one year of age (70,269,270). Microglial changes were investigated in hippocampal regions containing plaques, showing neuronal dystrophy, or appearing unaffected by A β pathology ultrastructurally, using a correlative light and electron microscopy method we developed (271). As in our original work defining dark

microglia, the CA1 *strata radiatum* and *lacunosum-moleculare* were targeted, in 14 month old APP^{Swe}-PS1 Δ e9 mice and wild-type littermate controls. In addition, microglial ultrastructural and functional alterations were analyzed in the post-mortem hippocampus of two AD patients. Our results indicate that while some microglial changes in response to A β pathology are conserved across subregions regardless of plaques deposition, such as impairments in extracellular digestion or encirclement of digested cellular elements, other alterations are specific to areas devoid of pathology or neuronal dystrophy, such as impaired phagocytosis but increased contacts with dendritic spines. Taken together, our findings provide data supporting the hypothesis that there are global changes in microglial health in AD but these cells' phenotypes are very much driven by their local environments.

3.6 Materials and methods

3.6.1 Animals

All experimental procedures were performed in agreement with the guidelines of the Institutional Animal Ethics committees, in conformity with the Canadian Council on Animal Care as administered by the Animal Care Committee of Université Laval. The animals were housed under a 12-hour light-dark cycle at 22-25 °C with free access to food and water. Fourteen-month old male APP^{Swe}-PS1Δe9 mice on a C57Bl/6J background (n=4) were compared with age-matched wild-type littermate controls (n=3). The transgenic mice coexpress human presenilin one variant (A246E) and a chimeric mouse/human amyloid precursor protein (APP^{Swe}) (70).

APP^{Swe}-PS1Δe9 mice were injected with Methoxy-X04 (10g/kg; Tocris Bioscience) 24 hours prior to sacrifice as previously described [38]. Methoxy-X04 is Congo Red fluorescent derivative that binds to sheets with high affinity. Mice were anaesthetized with sodium pentobarbital (80 mg/kg, i.p.) and transcardially perfused with ice-cold phosphate saline buffer (PBS; 50 mM at pH 7.4) followed by 3.5% acrolein and 4% paraformaldehyde both diluted in phosphate buffer (PB; 100mM at pH 7.4). Transverse sections of the brain (50-μm thick) were cut in PBS using a vibratome (Leica VT1000S) and kept in cryoprotectant at -20°C until use (236,271).

3.6.2 Brain sections screening for Methoxy-X04-labeled plaques

With the aid of a stereotaxic mouse brain atlas (237), brain sections containing the ventral hippocampus (Bregma -2.75 to -3.5) were selected and placed into a 24-well culture plate. Each section was assigned an individual well. Using an ultraviolet filter with a range of 380-480 nm, an inverted Nikon Eclipse TE300 microscope was used to visualize the methoxy-X04 stained plaques at a magnification of 4X. Pictures of the sections were captured both in bright and fluorescent field modes, naming the images according to the numbering of their position into the 24-well plate (271). Brain sections from the age-matched controls containing the same level of ventral hippocampus as the Methoxy-X04-labeled sections were selected for comparison.

3.6.3 Human tissue

Hippocampal sections containing the dentate gyrus and CA1 from two human cases of AD (C-0032, 76 years of age, 24 hours postmortem delay; H-17, 81 years of age, 6 hours postmortem delay) were obtained from the brain bank established at the CERVO Brain Research Center. Brain banking and postmortem tissue handling procedures were approved by the Ethic Committee of the Institut Universitaire en santé mentale de Québec and by Université Laval. The brain was obtained with written consent and the analyses were performed in conformity with the Code of Ethics of the World Medical Association (Declaration of Helsinki). The brain was first cut in half along the midline and hemibrains were sliced into 2 cm-thick slabs along the coronal plane. These slabs were fixed by immersion in 4% paraformaldehyde at 4°C for 3 days. They were then stored at 4°C in a 0.1M phosphate-buffered saline (PBS, pH 7.4) solution containing 15% sucrose and 0.1% sodium azide. The slabs containing the hippocampus were then cut with a freezing microtome into 50 µm-thick sections that were serially collected in PBS and stored at -20°C in a solution containing glycerol and ethanediol until immunostaining against the microglial marker IBA1.

3.6.4 Brain sections immunostaining and processing for electron microscopy

Hippocampal sections from the human cases, wild-type control and APP^{Swe}-PS1Δe9 mice, containing Aβ plaques in the CA1, were selected. They were washed in PBS, quenched with 0.3 % hydrogen peroxide (H₂O₂) in PBS, and washed again. Sections were then incubated with 0.1 % solution of NaBH₄ for 30 min at room temperature (RT). After washing the tissue was incubated in a blocking buffer of Tris-buffered saline (TBS; 50 mM at pH 8.0) containing 10 % fetal bovine serum, 3 % bovine serum albumin, and 0.01 % Triton X100 for 2 hours at RT. Sections were incubated overnight at 4 °C in rabbit anti-IBA1 antibody (1:1000 in blocking solution; Wako Pure Chemical Industries) and rinsed in TBS. The sections were afterwards incubated for 1.5 hour in goat anti-rabbit IgGs conjugated to biotin (1:200 in TBS; Jackson Immunoresearch) and for 1 hour in A and B reagents of the ABC Vectastain system kit (1:100 in TBS; Vector Laboratories) for immunoperoxidase staining. The staining was revealed using diaminobenzidine (DAB; 0.05 %) and H₂O₂ (0.015 %) in TBS for 8 min. Sections were post-fixed flat in 1 % osmium tetroxide in PB for 30 min and dehydrated in increasing concentrations of ethanol,

immersed in propylene oxide, impregnated in Durcupan resin (Electron Microscopy Sciences; EMS) overnight at RT, and polymerized between ACLAR films (EMS) at 55 °C for 72 hours. Areas of interest were excised from the embedded sections, glued to resin blocks (271), sectioned at 70-80 nm using a Leica UC7 ultramicrotome, and collected on bare square mesh grids (EMS).

3.6.5 Transmission electron microscopy (TEM) imaging

Ultrathin sections were imaged using a FEI Tecnai Spirit G2 microscope running at an accelerated voltage of 80 KV and equipped with an ORCA-HR Hamamatsu (10MP) camera. Microglial cell bodies were identified using a series of distinctive features that comprise their electron density, association with extracellular space pockets, characteristic long stretches of endoplasmic reticulum (ER), numerous vacuoles and intracellular inclusions, irregular contours with obtuse angles, and small elongated nucleus delineated by narrow nuclear cisternae (144,186,272). In most cases, they were also identified by their IBA1 immunoreactivity. This analysis did not distinguish between yolk-sac derived microglia and circulating myeloid cells known to infiltrate the ageing or diseased brain (273).

For qualitative analysis, pictures were acquired at magnifications ranging between 1400X and 13000X. Both mouse and human hippocampal samples were analyzed qualitatively to investigate microglial interactions with the synaptic neuropil, including contacts with dystrophic neurites and dendritic spines, as well as phagocytosis. For quantitative analysis in mouse, pictures of microglial cell bodies and processes were randomly acquired, at 6800X and 9300X respectively. In the APP^{Swe}-PS1 Δ e9 mice, three different subregions were differentiated. The first subregion contained one A β plaque with some rare cases showing two A β plaques, the second region displayed neuronal dystrophy characterized by clusters of swelled neurites containing autophagic vacuoles and electron dense bodies, and the third only comprised ultrastructurally unaffected neuronal compartments with intact delineating plasma membranes and organelles. In the latter subregion, myelinated axons were also surrounded by a compact sheaths of myelin with no signs of alteration. The same number of microglial cell bodies and processes was imaged in the wild-type controls, ranging from 5-20 microglial cell bodies and a minimum of 100

microglial processes.

3.6.6 Quantitative ultrastructural analysis of microglia

The analysis of microglial cells and processes comprised several ultrastructural measures of morphology, phagocytic activity, cellular stress, and physiological function. Experimenters were blinded to the experimental conditions throughout the analysis. For each microglial cell body and process, inclusions (containing partially to completely digested cellular elements *versus* cellular elements still intact), lysosomes (primary, secondary, *versus* tertiary), lipid bodies, fA β , ER dilation, vacuoles (diameter <100 nm), and extracellular digestion were counted, according to the quantitative code 0, 1, 2, and 3+ (designating 3 and more elements). For inclusions, empty versus cellular elements visible were pooled together, in which case the quantitative code 0, 1, 2, 3, 4, 5, and 6+ (designating 6 and more elements) was used instead. Lysosomes were identified by their dense, heterogeneous content made of hydrolytic enzymes and acid phosphatases, enclosed by a membrane (274). Primary lysosomes possessed a homogenous granular content and a diameter ranging from 0.3 to 0.5 μm (275). Secondary lysosomes were 1 to 2 μm across, and their content was heterogeneous showing fusion with intra- or extracellular vacuoles. Tertiary lysosomes ranged in diameter between 1.5 and 2.5 μm and were usually fused to one or two vacuoles associated with lipofuscin granules, as well as lipid bodies showing signs of degradation (276). Lipid bodies were identified as round organelles with an electron dense, either opaque or limpid, cytoplasm enclosed by a monolayer phospholipid layer. Lipofuscin granules were identified by their oval or round shapes, finely granular composition, and association with amorphous materials. They also contained small inclusions and several lipid droplets (276) fA β was identified as densely packed fibrils and filaments, according to previous descriptions (277). ER dilation was recognized by a swelling of the cisternal space ranging from 50 to 300 nm (278). Extracellular digestion, which is also termed “exophagy” and refers to the degradation of cellular constituents by lysosomal enzymes released extracellularly, was defined by the appearance of digested materials (including cellular membranes and other subcellular constituents) in the extracellular space associated with the microglia (279). They were scored using the quantitative code 0, 1, 2, and 3+ (designating 3 and more elements).

Microglial processes were analyzed using the same parameters. Additionally, their encirclement of neuronal compartments (myelinated axons, axon terminals, dendritic spines, synapses between axon terminals and dendritic spines, cellular elements undergoing degradation) was quantified. Encirclement was defined as microglial interactions with these compartments that displayed at least two points of contact, with their juxtaposition sometimes extending over several hundreds of nanometers. They were scored using the quantitative code 0, 1, 2, and 3+ (designating 3 and more elements). The encircled elements were identified according to the following criteria, as described previously (280). Myelinated axons were recognized by their compact myelin sheath. Axon terminals contained synaptic vesicles and were frequently seen branching from axons or making synapses onto dendritic branches and spines. Dendritic spines were identified as extensions from dendrites often forming synapses where a postsynaptic density was seen. Also, microglial processes encirclement of synapses was scored when the process encircling presynaptic terminals and postsynaptic spines extended its contact to the area of synaptic cleft. Moreover, microglial encirclement of partially degraded cellular elements with a shrunk appearance within the extracellular space and/or showing an accumulation of membranes in advanced stage of digestion was determined.

3.6.7 Statistical analysis

GraphPad Prism 7 was used for the analysis. APP^{Swe}-PS1 Δ e9 mice were compared to age-matched wild-type littermate controls using unpaired two-tailed Student's t-test. Microglial cell bodies and processes were compared between plaque-associated, neuronal dystrophy associated, and ultrastructurally healthy tissue of APP^{Swe}-PS1 Δ e9 mice by ordinary one-way ANOVA without matching using Tukey's multiple comparisons *post-hoc* test. Data are expressed as mean +/- SEM. Significant differences are indicated by * $p < 0.05$, ** $p < 0.01$, *** $p < 0.001$, and **** $p < 0.0001$.

3.7 Results

3.7.1 Microglial ultrastructure is altered in proximity to fA β

While several studies have uncovered the intimate relationship between microglia and amyloid plaques in AD human samples and mouse models, as well as changes in microglial function in AD mouse models, we focused on determining how proximity to fA β plaque and neuronal dystrophy affects the phenotypic heterogeneity of microglia. We developed a correlative light and electron microscopy method to characterize at high spatial resolution alterations of microglial ultrastructure and cellular function among subregions containing amyloid plaques (within 113 x 113 microns), displaying neuronal dystrophy, or appearing ultrastructurally healthy in the CA1 *strata radiatum* and *lacunosum-moleculare* of 14 months old APP^{Swe}-PS1 Δ e9 mice *versus* wild-type littermate controls (Figure 3.9.1). Transgenic mice were injected with Methoxy-X04 24 hours prior to tissue collection to label amyloid plaques. Fifty micron thick transverse sections of the brain containing fA β plaques within the ventral hippocampus CA1 were selected and stained for IBA1 to identify microglial cell bodies and processes at the ultrastructural level as described previously (268).

Microglial cell bodies in all four conditions displayed characteristic bean-shaped nuclei containing patches of dense heterochromatin, while their cytoplasm showed immunoreactivity for IBA1 (Figure 3.9.2A-D). In line with previous descriptions of microglial ultrastructure, cell bodies also contained numerous mitochondria often in close apposition to characteristically long stretches of ER, occasional Golgi apparatus, and phagocytic vesicles (281). When investigating whole-region changes in microglial ultrastructure, only cell body area was significantly different between wild-type and transgenic mice, showing an increase in APP^{Swe}-PS1 Δ e9 animals (Table 3.9.11). However, by separating APP^{Swe}-PS1 Δ e9 investigations into three distinct subregions: ultrastructurally healthy, dystrophic, and plaque-associated, we were able to discern region-specific changes in microglial cell bodies and their processes. Microglial cell bodies had larger areas and perimeters when closer to amyloid plaques than any other subregion, implying a response to fA β accumulation (Figure 3.9.2E-F). In contrast, the cell bodies in APP^{Swe}-PS1 Δ e9 hippocampi were significantly rounder than those found in wild-type animals, regardless of their proximity to dystrophic neurons or amyloid plaques (Figure 3.9.2G), implying a

global phenotypic change. Similar microglial morphological changes were previously described *in vivo* in mouse models of amyloid pathology (282).

While microglial cell bodies in WT and APP^{Swe}-PS1 Δ e9 model mice were significantly different in size and shape, the ultrastructure of their processes remained largely unchanged. Numerous *in vivo* two-photon imaging studies have confirmed that microglial processes are incredibly dynamic as they survey the brain neuropil via continuous extension and retraction (126,164). Microglial processes are long, thin, often ramified, discontinuous from cell bodies in ultrathin sections, and are identified by immunocytochemical electron microscopy (immunoEM) staining for IBA1, which labels their cytosol (Figure 3.9.3A-D). They often accumulate phagocytic vesicles, and more proximal processes also contain mitochondria, occasional ER and/or Golgi apparatus, as well as lysosomes. The area and perimeter of microglial processes were relatively unchanged in our analyses when comparing wild-type with APP^{Swe}-PS1 Δ e9 mice (Table 3.9.12).

Although their gross ultrastructural features were not significantly different between wild-type and APP^{Swe}-PS1 Δ e9 tissue, microglial processes interacted differently with the surrounding neuropil depending on their localization and genotype. Unsurprisingly, processes in regions of A β plaques were more likely to encircle amyloid fibrils (Figure 3.9.4F). Processes in APP^{Swe}-PS1 Δ e9 animals were significantly less likely to encircle cellular elements undergoing extracellular digestion compared with wild-type littermates (Figure 3.9.4G). Strikingly, microglial processes in ultrastructurally “healthy” neuropil of APP^{Swe}-PS1 Δ e9 were significantly more likely to encircle dendritic spines than processes in either pathological or wild-type tissues (Figure 3.9.4E). This increase in encirclement was also noted in conjunction with myelinated axons, though the trend did not reach significance. In addition, microglial processes in APP^{Swe}-PS1 Δ e9 mice had significantly rounder and more solid shape descriptors (Figure 3.9.3E and Table 3.9.12). Increases in solidity are considered a readout of reduced plasma membrane ruffling, linked to lower process motility and fewer incidents of macropinocytosis (283) or phagocytosis (284,285). This finding is in agreement with previous observations from *in vivo* two-photon imaging that microglia in AD mouse models display reduced process motility at steady-state and in response to injury (201,282).

3.7.2 Microglial phagocytosis and extracellular degradation is reduced in AD animals

One of microglia's most pivotal roles in the development and maintenance of the brain is their capacity to recognize and actively phagocytose and degrade extraneous synapses, apoptotic cells, and invading pathogens. Microglia often contain phagocytic inclusions in both their cell bodies and processes, associated with the degradation of neuronal compartments and $fA\beta$. Using immunoEM, we are able to identify cargos contained within the phagocytic vesicles of microglia. Completely digested elements appear as electron lucent vesicles, while partially digested or intact elements appear electron dense, and sometimes display recognizable ultrastructural features of cellular membranes, vesicles, myelin sheaths, etc. (Figure 3.9.5A). Interestingly, microglial cell bodies in healthy regions of APP tissue as well as in regions of neuronal dystrophy contained significantly fewer phagocytic inclusions than either microglia in wild-type or within plaque-containing regions of APP tissue (Figure 3.9.5A-D). However, microglial cell bodies from all regions of APP^{Swe}-PS1 Δ e9 tissue investigated contained significantly fewer digested vesicles than wild-type microglia (Figure 3.9.5F) in agreement with previous findings from *in vivo* two-photon imaging (201). In contrast, microglial cell bodies located in regions of neuronal dystrophy or near $fA\beta$ plaques were the only ones to contain amyloid in phagocytic vesicles (Figure 3.9.5G, H), suggesting that microglia in APP^{Swe}-PS1 Δ e9 mice do not migrate, instead they remain in close proximity to amyloid after recognizing it via cell-surface receptor complexes, as supported by previous two-photon *in vivo* imaging observations in cerebral cortex of AD mouse models (282).

Microglial phagocytosis begins with a microglial membrane wrapping and engulfing its phagocytic target. The vesicle is then trafficked to the cell soma through the phagolysosomal pathway, undergoing degradation along the way. As such, depending on the distance from the cell soma, phagosomes within microglial processes are often more likely to contain intact or partially digested elements than phagosomes located within microglial soma (Figure 3.9.6A-D).

Upon investigation, we discovered that microglial processes in healthy regions of APP^{Swe}-PS1 Δ e9 mice as well as regions of neuronal dystrophy were significantly less phagocytic than processes in wild-type animals (Figure 3.9.6E-G). In fact, microglial

processes in healthy tissue of APP^{Swe}-PS1 Δ e9 mice were the least likely to contain phagocytic vesicles (Figure 3.9.6E). However, microglial processes within regions containing fA β contained the same number of phagocytic inclusions as wild-type animals (Figure 3.9.6 E-G). Interestingly, wild-type microglial processes contained nearly twice as many fully digested phagosomes than any processes in APP^{Swe}-PS1 Δ e9 animals, regardless of their proximity to dystrophic neurons or fA β plaques (Figure 3.9.6H). This directly parallels the ratio seen in microglial cell bodies (Figure 3.9.5F), and could imply general impairments among the phagolysosomal system of APP^{Swe}-PS1 Δ e9 animals.

In addition to phagocytosis, microglia contribute to maintaining brain homeostasis by performing extracellular degradation. Extracellular degradation by microglia is recognized in TEM by pockets of extracellular space juxtaposing the microglial membrane containing sparse and degraded cellular elements. These pockets are electron-light, empty of visible contents save partially digested elements (Figure 3.9.7A, E). Occasionally extracellular space is found next to microglial cell bodies and processes in the mature brain without noticeable digestion (144). Extracellular degradation is likely a different process from the one used for process extension and retraction, as it is often visible at the cell soma, which does not move as much as processes except in cases of injury or other stimulus (286), and it is always accompanied by debris. This debris is made up of partially digested elements often recognizable as cellular membranes, sometimes forming myelin sheaths (Figure 3.9.7E). In addition to their phagocytosis impairments, microglia in APP^{Swe}-PS1 Δ e9 animals overall display reduction in extracellular degradation. Microglial cell bodies and their processes in wild-type animals readily perform extracellular degradation, while cell bodies and processes in any region of APP^{Swe}-PS1 Δ e9 animals have impaired levels of extracellular degradation (Figure 3.9.7 I, J, Table 3.9.11, 3.9.12).

To provide additional insights into the alteration of microglial degradation activity, we next investigated the number and stage of lysosomes within microglial cell bodies and their processes. While primary lysosomes are not commonly found in microglial cell soma (0.095 per cell body, Table 3.9.11), secondary and tertiary lysosomes are often present in both wild-type and APP^{Swe}-PS1 Δ e9 animals (between 0.38 and 0.553 per cell body, Table 3.9.11). Although the number of phagosomes per cell was reduced in APP^{Swe}-PS1 Δ e9 animals (Table 3.9.11), the numbers of primary, secondary, and tertiary lysosomes per cell

body and process were not significantly different upon A β pathology (Table 3.9.11). However, upon separating cell soma into ultrastructurally healthy, dystrophic, and plaque-associated subregions, it becomes clear that the number of tertiary lysosomes is decreased in microglial cell bodies only in regions of dystrophy and fA β deposition (Figure 3.9.8). Microglial cell bodies in close proximity to plaques display significantly fewer tertiary lysosomes than those in healthy subregions of APP^{Swe}-PS1 Δ e9 animals (Figure 3.9.8C).

3.7.3 Effects of A β on microglial cell stress

The best characterized ultrastructural marker of cellular stress is ER stress, read out in high spatial resolution as a lumen dilation of ER and Golgi apparatus cisternae. It has been described in several neurodegenerative diseases, including amyotrophic lateral sclerosis (ALS) and AD (287,288). ER dilation is also a characteristic of “dark microglia”, a subtype upregulated in pathology including AD (268). We were interested in investigating intermediate stages between healthy, “typical” microglia, and the dark ones. Various hallmarks of dark microglia were examined in the hippocampus CA1 *strata radiatum* and *lacunosum-moleculare* of wild-type and APP^{Swe}-PS1 Δ e9 animals, including the presence of dilated ER among microglial cell bodies and processes, alterations to various organelles including mitochondria, as well as condensation of cytoplasmic and nucleoplasmic contents (which results in a “dark” electron-dense appearance), and the loss of heterochromatin pattern. Healthy ER in microglial cell bodies and processes is characterized in EM images by long stretches of parallel membranes with very little space between them, and is often located near mitochondria (Figure 3.9.9, white arrowheads). Dilated ER appears as it is described, with the parallel membranes no longer parallel, and containing bloated stretches of electron-light material (Figure 3.9.9, black arrows). Interestingly, microglial cell bodies in the APP^{Swe}-PS1 Δ e9 animals contained nearly twice the dilated stretches of ER that were visualized in wild-type animals (0.834 *versus* 0.425 per cell body, Table 3.9.11). When separating analysis into subregions, healthy, neuronal dystrophy, and fA β plaque, in APP^{Swe}-PS1 Δ e9 animals, it became clear that this increase in dilated ER is only present in the plaque-associated microglial soma (Figure 3.9.9 A-D, I). Cell bodies in subregions near fA β plaques contain significantly higher levels of stressed,

dilated ER (Figure 3.9.9D, I). Interestingly, microglial cell bodies often display reduced levels of IBA1 immunoreactivity in APP^{Swe}-PS1 Δ e9 animals, across the three subregions (see Figure 3.9.9B-D), while it was previously shown that dark microglia downregulate IBA1 in the same hippocampal region of 14 months old APP^{Swe}-PS1 Δ e9 mice (268). Microglial cell bodies endowed with dilated ER, as seen nearby plaques, sometimes appeared “darker” also (see Figure 3.9.9D for an example), suggesting a slight condensation of the cytoplasmic and nucleoplasmic contents. These cells however had a clearly defined heterochromatin pattern as compared with the dark microglia. Furthermore, the increase in ER dilation observed in microglial cell body was recapitulated in processes (Figure 3.9.9 E-H, J), especially striking as most microglial processes do not contain any stretches of ER in ultrathin sections (0.03 dilated ER per process in wild-type animals, Table 3.9.12).

3.7.4 Microglial ultrastructure in human cases of AD

In an effort to determine the clinical relevance of our microglial ultrastructure studies conducted in mouse hippocampus, we investigated tissue gathered from the hippocampus of two postmortem AD cases. 50 micron thick sections within the hippocampal formation were stained against IBA1 to identify microglial cell bodies and processes. As we were not able to perform staining to identify fA β prior to processing for immunoEM staining, it was impossible to focus our investigation on plaque-containing tissues. However, the hippocampal tissue of human AD cases contained abundant numbers of dystrophic neurons, identifiable by the presence of small, regularly packed dense bodies and abundant autophagic vacuoles (289) within their cytoplasm (Figure 3.9.10 B-D). Our identification of dystrophic neurites in human cases of AD is consistent with the literature (290,291,292). As such, the regions of tissues we investigated from AD individuals most closely paralleled that of microglia in regions of neuronal dystrophy in the APP^{Swe}-PS1 Δ e9 animals. Microglia in human AD cases were found to be immunoreactive for IBA1 throughout their processes and cell bodies and display the same characteristic nuclei as those seen in mice (Figure 3.9.10 A). Their heterochromatin pattern nevertheless appears more heterogeneous than that of mouse microglia, with smaller and more numerous pockets of euchromatin (Figure 3.9.10 A). Microglial processes contacted both dystrophic neurites

and dendritic spines (Figure 3.9.10 B-D). Interestingly, one microglial process made many contacts and encircled several sides of a dystrophic neurite containing an accumulation of autophagic vacuoles (Figure 3.9.10 B). Microglia in human tissue were also phagocytic, with many processes comprising one or more phagocytic inclusions (Figure 3.9.10 C-E). The inclusions contained partially degraded membranes and organelles, consistent with the microglial phagocytic inclusions seen in mice. Lysosomes were also frequently seen in microglial processes, showing intact granular structure, and sometimes contacting an inclusion, thus suggesting a probable fusion to produce a phagolysosome (Figure 3.9.10C). In addition, microglial cell bodies and processes frequently associated with pockets of extracellular space containing cellular elements at various stages of digestion, which supports their involvement with the removal of debris (Figure 3.9.10 A-D). It appears microglia in human AD cases recapitulate much of the ultrastructural alterations seen in the mouse model, particularly their intimate interactions with dystrophic neurites and dendritic spines.

3.8 Discussion

Unraveling the role of microglia has been complicated by the heterogeneity displayed by these cells across brain regions, stages of the lifespan, and contexts of health and disease. The past decade has been a boon in the discovery of microglial phenotypic diversity and plasticity, investigated using *in vivo* two-photon microscopy, single cell RNA-sequencing, and positron emission tomography to find hotspots of microglial activity within the human brain (293). These techniques have been invaluable in teasing apart the temporal and molecular mechanisms used by microglia, but were unable to investigate intimate microglial interactions with their surrounding brain environment. We have utilized TEM in order to uncover region-specific roles of microglia in the APP^{Swe}-PS1 Δ e9 mouse model of AD pathology. Our data revealed striking disruptions of microglial function among hippocampal CA1 subregions containing fA β plaques, dystrophic neurons, or appearing healthy in the APP^{Swe}-PS1 Δ e9 mouse model, as well as individuals suffering from AD.

Studies in humans with mild cognitive impairment as well as in mouse models of AD have found links between memory impairment and hyperactive neuronal networks

within the hippocampus (241,294,295,296). The loss of dendritic spines in CA1 *strata radiatum* and *lacunosum-moleculare* was identified as one of the mechanisms leading to neuronal network hyperactivity, in 10 to 14 months old ARTE10 model mice using a combination of super resolution STED microscopy, electrophysiology, and computational modeling (297). Our analyses in healthy subregions of hippocampus devoid of fA β plaque or dystrophic neurons revealed microglial characteristics of impaired phagocytosis and extracellular degradation, together with an increased encirclement of dendritic spines. Interestingly, the encirclement of dendritic spines was validated using our human hippocampal samples. It is thus tempting to hypothesize that impaired functions of microglia could be responding to unhealthy network trafficking within the hippocampus, thus exacerbating cognitive impairment. Numerous *in vitro* and *in vivo* studies in various mouse models of AD have identified profound synaptic alterations in response to small oligomeric and sA β (65,79,298,299,300,301,302). Increased levels of sA β are hypothesized to predispose neurons to hyperactivity and excitotoxicity, accompanied by increases in local microglial response (246,303). Recent human studies have even implicated fA β plaques as amyloid sinks which lower levels of circulating sA β , thus preventing synaptic alterations early in the disease pathology (304). These changes of functional plasticity and excitability are not visible in EM without complex and extensive synaptic analysis and are the focus of future investigations in this area.

While our studies separate plaque-associated tissue from morphologically healthy tissue, we cannot overlook the probability that soluble amyloid is likely present throughout the CA1. Amyloid plaques are electron-dense, but soluble amyloid is not distinguishable ultrastructurally without immunostaining. Three-dimensional EM studies focused on fA β -neuronal interactions found intimate contacts of amyloid with dendritic membranes in the hippocampus of 3XTg model mice and in the prefrontal cortex of aged canines (305). It is possible the phenotypic changes we identified in ‘healthy’ hippocampal regions of our transgenic mice are driven by soluble amyloid. This is particularly interesting when interpreting the increased microglial encirclement of dendritic spines in APP^{Swe}-PS1 Δ e9 mice, and interactions with the synaptic neuropil in human AD hippocampus.

Our studies have shown a nonzero percentage of microglia and their processes found in regions with plaques or dystrophic neurites contain intracellular fA β . This is in

line with numerous *in vitro* and *in vivo* studies demonstrating microglial capacity to phagocytose both soluble and fibrillar forms of A β (306,307,308). While microglia are proficient at phagocytosing amyloid, when presented with chronic high levels of fA β such as those seen in AD animal models and human pathology, their phagolysosomal system becomes overloaded and is unable to properly acidify phagolysosomes in order to degrade the fA β (309). In fact, *in vitro* studies have found intact fA β remains within microglial cell bodies as long as 20 days after incubation with amyloid (310). This may explain both the high prevalence of fA β within microglial soma and processes and the reduced numbers of tertiary lysosomes we reported. It may also explain the differences in phagocytosis seen in healthy *versus* dystrophic *versus* plaque-associated subregions of CA1 – perhaps the increased phagocytosis seen in plaque-associated areas is actually due to impaired digestion of phagocytosed amyloid.

It is important to note, however, because our TEM imaging protocol is on single ultrathin sections, we cannot overlook the possibility that these vacuoles may be pockets of extracellular digestion not yet fully engulfed. Another group has performed 3D EM reconstructions showing no intracellular amyloid in cerebral cortex of the APP23 mouse model (311). However, the differences in mouse model, age of animals, studied region, and sample preparation make it difficult to compare with our own findings. Additionally, this study did not investigate microglial phagocytosis within the synaptic neuropil and instead focused on A β alone, and it is known that microglia readily internalize and degrade numerous targets in healthy and diseased tissue (312,313,314).

Recent transcriptome analysis of tissue from human AD subjects has revealed similarities and differences in the innate immune response when compared to animal models of AD (315). Nearly all amyloid mouse models of AD suffer from overexpression of human APP protein, often with multiple mutations driving A β ₄₂ expression to drive plaque formation (316). These models do not express intracellular tau depositions and often do not recapitulate the extensive neuronal loss seen in human cases of AD. It is thus crucial to verify findings in human studies whenever possible. For the first time, we have investigated microglial interaction with synaptic neuropil at ultrastructural resolution in postmortem hippocampal tissue derived from individuals suffering from AD, which allowed us to validate our findings with respect to microglial extracellular degradation,

encirclement of dystrophic neurites and dendritic spines, as well as functional alterations in the phagolysosomal pathway.

3.9 Figure & legends

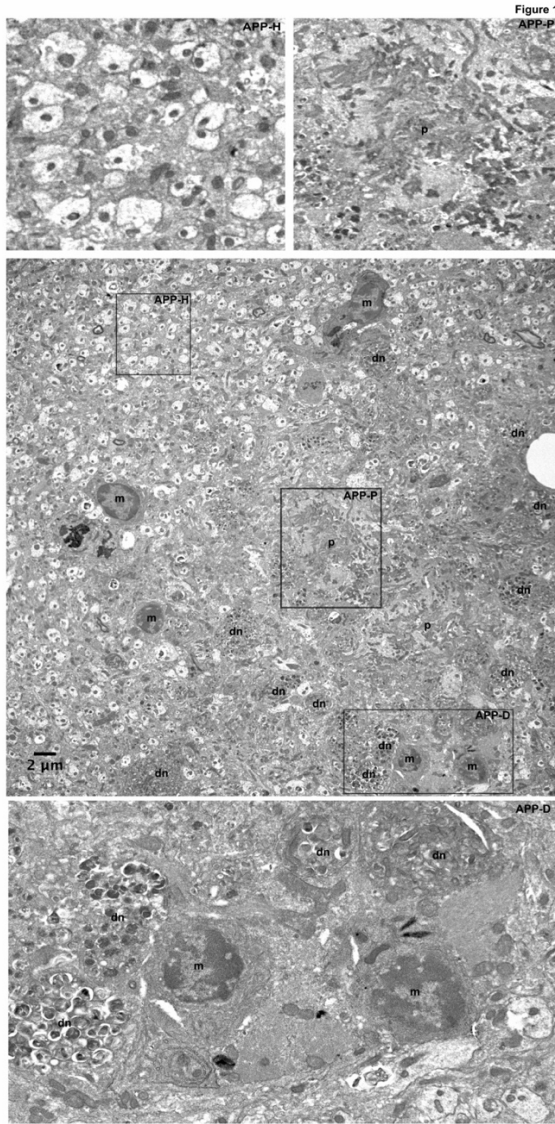


Figure 3.9.1 Defining healthy, dystrophic, and plaque-associated neuropil.

An example EM image displaying several microglial cell bodies in healthy (APP-H), plaque-associated (APP-P), and dystrophic-associated (APP-D) regions of the ventral hippocampus CA1 in APP^{Swe}-PS1Δe9 mice. Abbreviations: m=microglia, p=fAβ plaque, dn= dystrophic neurite.

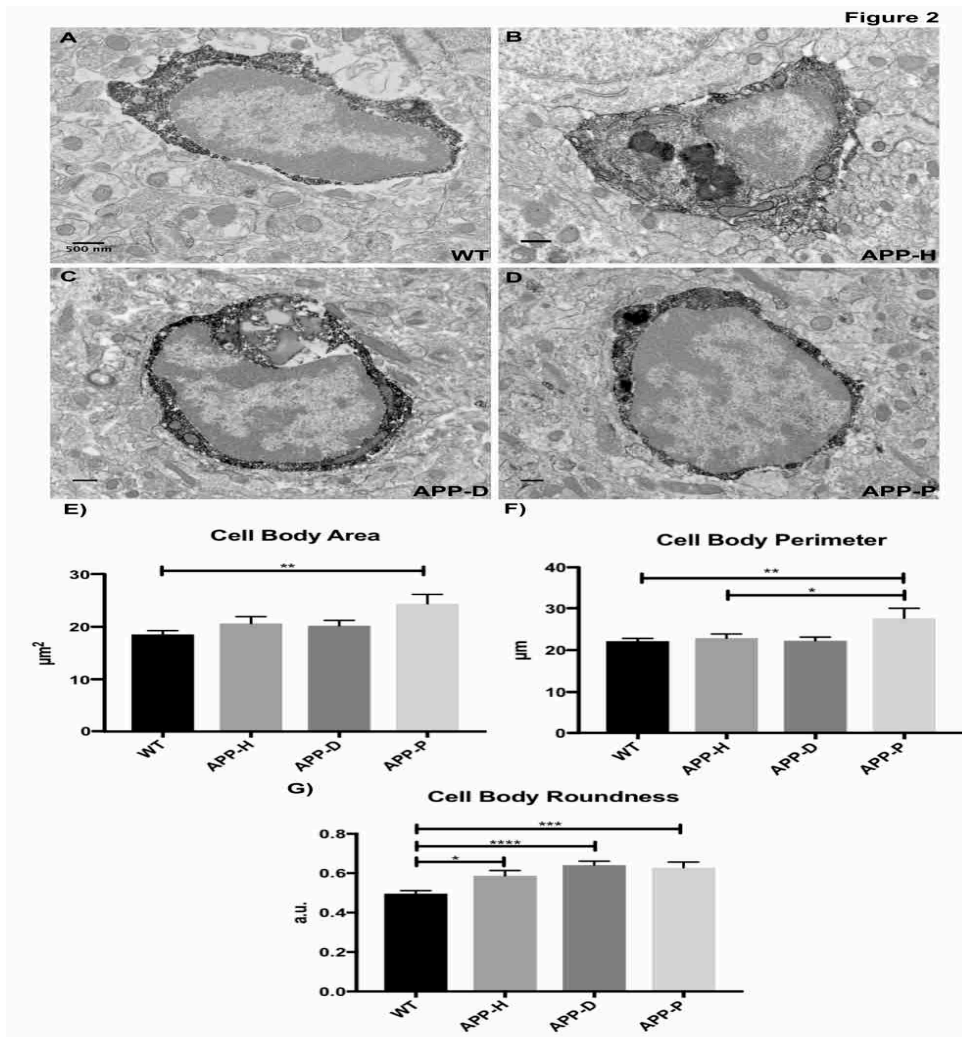


Figure 3.9.2 Microglial ultrastructure is changed by proximity to $\text{fA}\beta$ plaques.

(A) EM image of a wild-type animal showing oval shaped IBA1-positive microglial cell body. (B, C and D) EM images of IBA1-positive microglial cell bodies taken respectively in regions proximal to healthy (B), dystrophic (C) and $\text{fA}\beta$ (D) containing areas in the CA1 of the ventral hippocampus of $\text{APP}^{\text{Swe}}\text{-PS1}\Delta\text{e9}$ mice. Scale bars=500 nm. (E) Change in microglial cell body area of wild-type controls compared to $\text{APP}^{\text{Swe}}\text{-PS1}\Delta\text{e9}$ animals. (F) Change in microglial cell body perimeter in wild-type and $\text{APP}^{\text{Swe}}\text{-PS1}\Delta\text{e9}$ animals. (G) Change in the microglial cell body roundness in wild-type and $\text{APP}^{\text{Swe}}\text{-PS1}\Delta\text{e9}$ animals. All error bars are $\text{mean}\pm\text{SEM}$ *, $p<0.05$; **, $p<0.01$; ***, $p<0.001$; ****, $p<0.0001$.

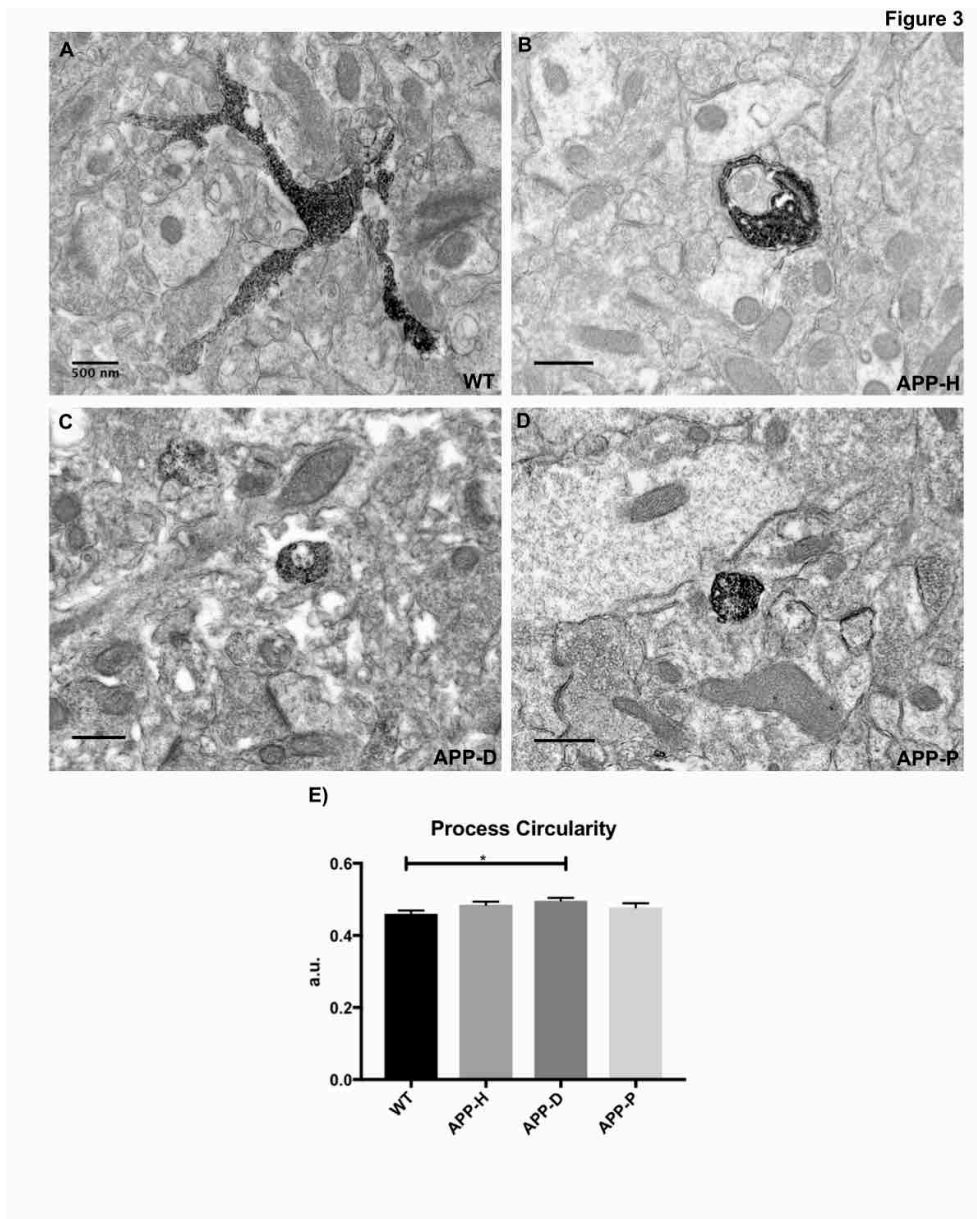


Figure 3.9.3 Microglial processes lose arborization in the presence of dystrophic neurons in APP-PS1 mice.

(A) EM image of a IBA1-positive process in a wild-type control showing a branched structure. (B, C and D) Examples of IBA1-positive processes images in taken respectively in regions proximal to healthy (B), dystrophic (C) and $\text{fA}\beta$ (D) containing areas in the CA1 of the ventral hippocampus of $\text{APP}^{\text{Swe}}\text{-PS1}\Delta\text{e9}$ mice. Scale bars=500 nm. (E)

Quantification of process circularity in wild-type controls compared to APP^{Swe}-PS1Δe9 animals (mean±SEM). *, p<0.05.

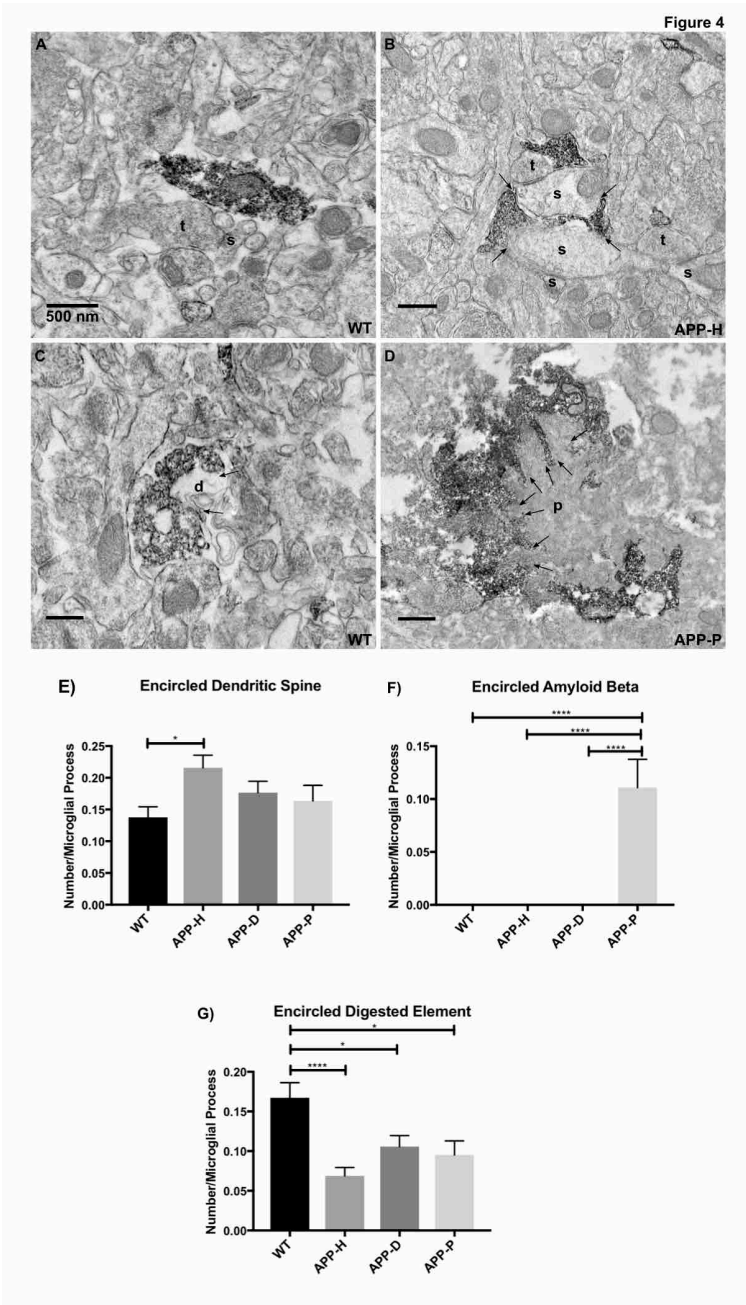


Figure 3.9.4 Distinct changes in process encirclement in APP-PS1 animals

(A) Example image of IBA1-positive microglial process in close proximity to a synaptic terminal (t, synaptic terminal, s, dendritic spine). (B) Example image of a microglial

process in healthy neuropil of APP^{Swe}-PS1 Δ e9 hippocampus encircling synaptic terminals and a dendritic spine (points of contact are shown with black arrows). (C) Example of a microglial process in a WT animal encircling an element undergoing extracellular digestion (d) with points of contact shown by black arrows. Scale bars=500nm. (D) Example image of a microglial process encircling a fA β plaque (p) with various thin ramifications shown in black arrows. (E) Quantification of dendritic spine encirclement by microglial processes. (F) Quantification of fA β encirclement by microglial processes. (G) Quantification of digested element encirclement by microglial processes. Error bars represent mean \pm SEM. *, p<0.05; ****, p<0.0001.

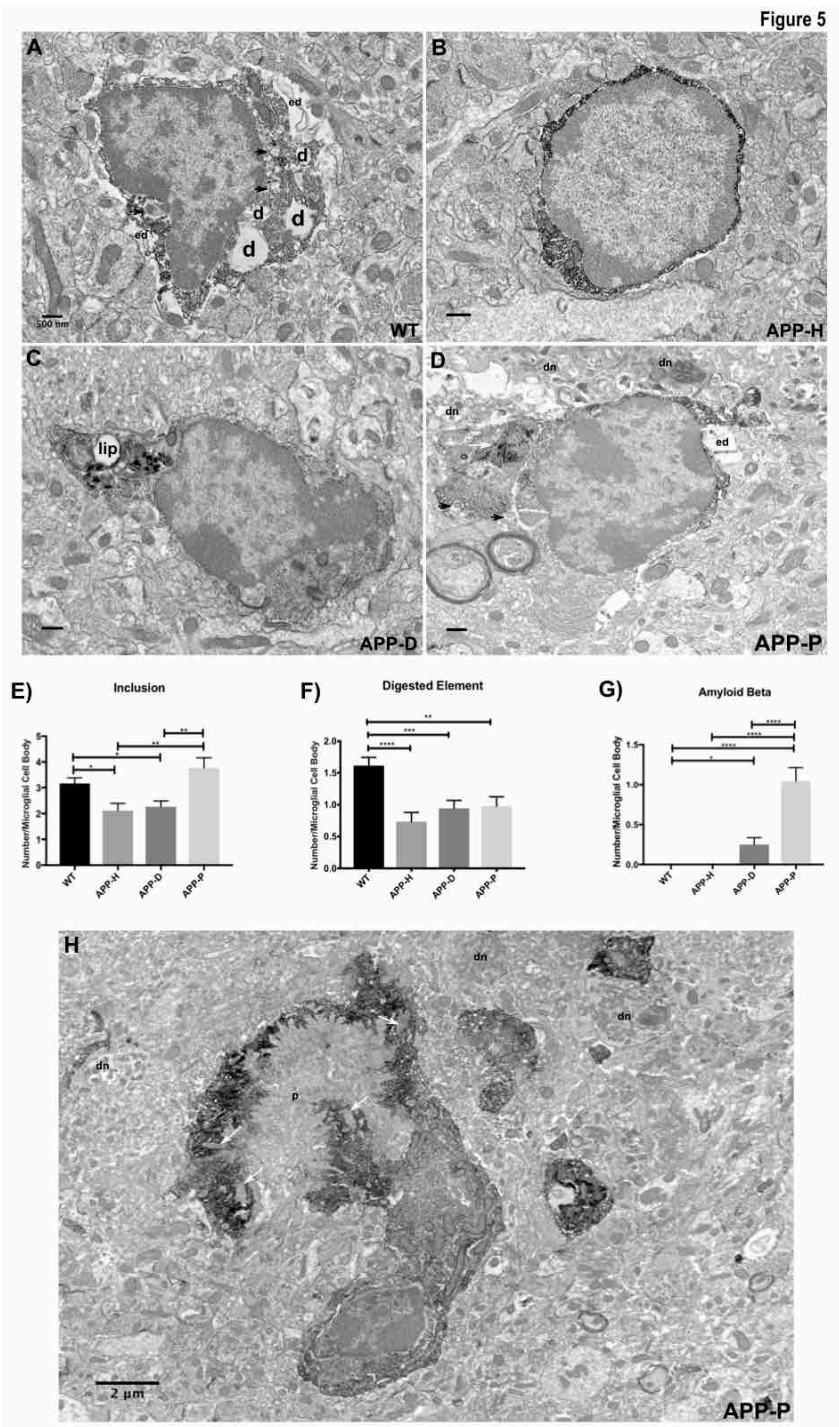


Figure 3.9.5 Microglial cell bodies in APP-PS1 animals show reduced phagocytosis in areas far from plaque deposition.

- (A) Example of IBA1-positive cell body image in a wild-type control performing extracellular digestion (ed) and containing numerous digested inclusions (d) and intact elements (Black arrows). (B, C and D) EM images of IBA1-positive

microglial cell bodies taken respectively in regions proximal to healthy (B), dystrophic, containing lipid bodies (lip) (C) and $fA\beta$ containing contacting dystrophic neurites (dn) and containing $fA\beta$ inclusions (white arrows) (D) areas of APP^{Swe} -PS1 $\Delta e9$ mice. Scale bars=500 nm. (E) Change in total number of inclusions in wild-type and APP^{Swe} -PS1 $\Delta e9$ microglial cell bodies. (F) Change in number of digested elements contained in wild-type and APP^{Swe} -PS1 $\Delta e9$ microglial cell bodies. (G) Change in number of amyloid-beta containing vesicles in wild-type and APP^{Swe} -PS1 $\Delta e9$ microglial cell bodies. (H) Example of IBA1-positive cell body image in plaque region containing numerous inclusions of $A\beta$ (white arrows) and a surrounding a plaque (p), with dystrophic neurites in contact (dn) with various microglial processes. Scale bar=2 μ m. All error bars are mean \pm SEM. *, $p<0.05$; **, $p<0.01$; ***, $p<0.001$; ****, $p<0.0001$.

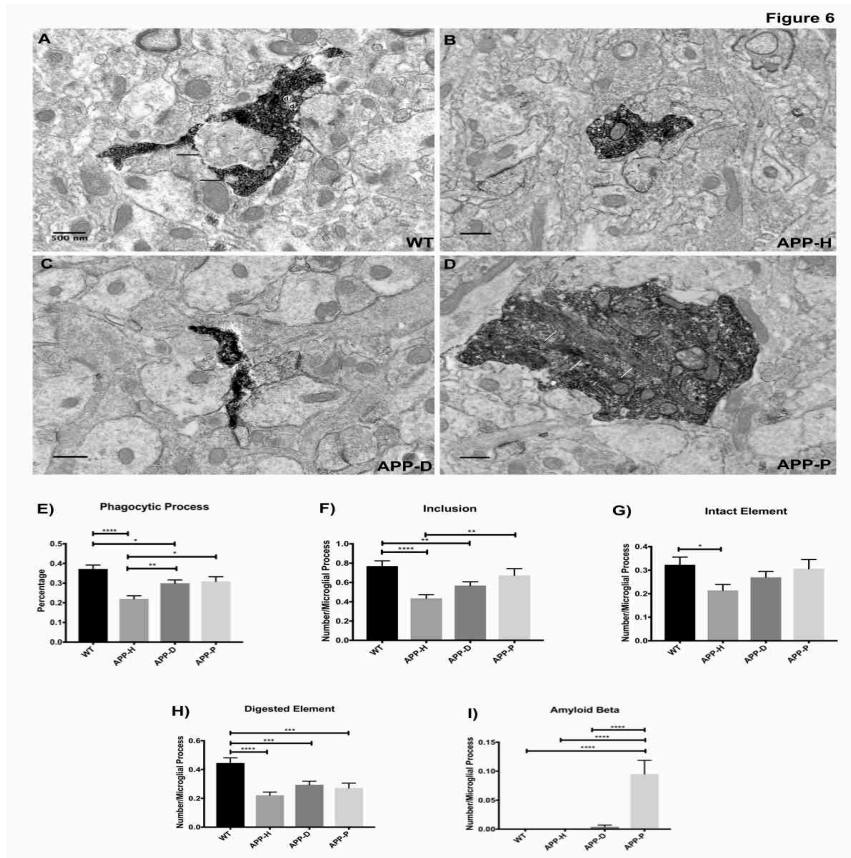


Figure 3.9.6 Microglial processes are less phagocytic and display poorer digestion of inclusions in APP-PS1 animals, even in regions far from A β deposition.

(A) Example of IBA1-positive microglial process in a wild-type control containing multiple digested (d) and intact inclusions (black arrows). (B-D) Example of IBA1-positive microglial process in healthy (B) dystrophic (C), and fA β containing (white arrows) (D) neuropil of APP^{Swe}-PS1 Δ e9 hippocampus. Scale bars=500 nm. (E) Change in percentage of phagocytic microglial processes (F) Change in score of inclusions within processes. (G) Change in score of intact element inclusions within processes. (H) Change in score of digested element inclusions within processes. (I) Change in score of A β inclusions (white arrows, D) in processes. Scale bars display mean \pm SEM. *, p<0.05; **, p<0.01; ***, p<0.001; ****, p<0.0001.

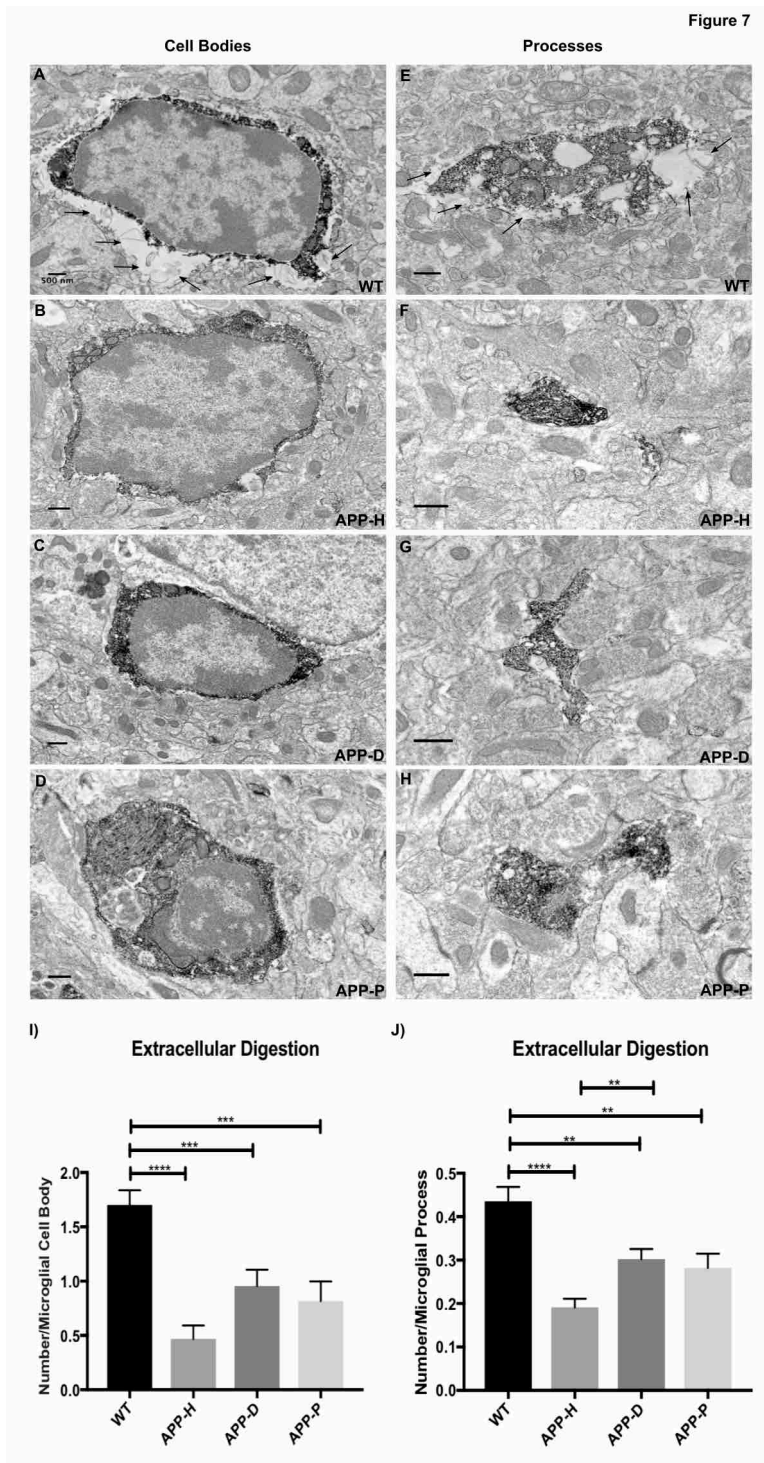
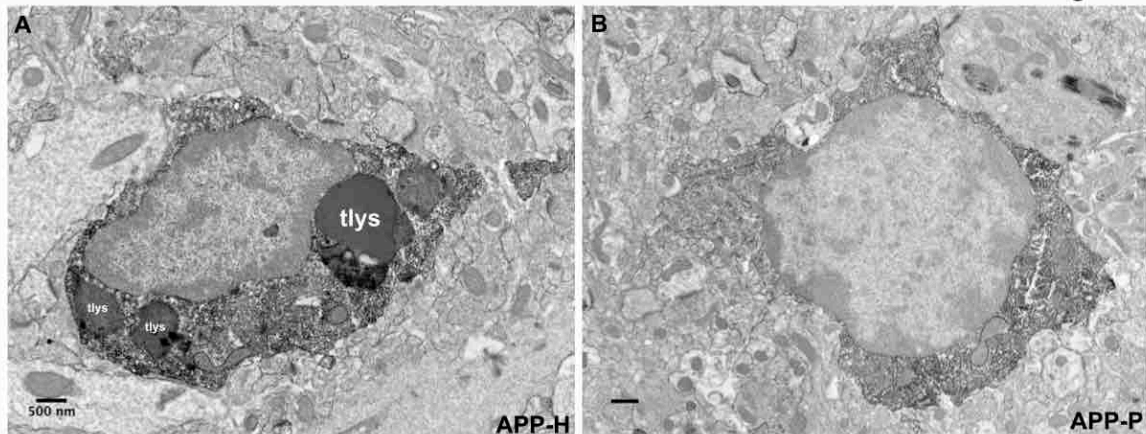


Figure 3.9.7 Microglia in APP-PS1 mice perform less extracellular degradation regardless of their proximity to plaques.

(A) Example of IBA1-positive microglial cell body in a wild-type control performing numerous acts of extracellular digestion (black arrows) at different points between

its plasma membrane and its adjacent neuronal structures. (B, C and D) EM images of IBA1-positive microglial cell bodies taken respectively in regions proximal to healthy (B), dystrophic (C) and $fA\beta$ containing (D) areas of APP^{Swe}-PS1 Δ e9 hippocampus. (E-H) Example images of IBA1-positive microglial processes performing extracellular digestion (black arrows, E) in WT (E), healthy (F), dystrophic (G) and $fA\beta$ containing (H) areas of APP^{Swe}-PS1 Δ e9 hippocampus. Scale bars=500 nm (I) Quantification of extracellular digestion performed by microglial cell bodies. (J) Quantification of extracellular digestion performed by microglial processes. Error bars depict mean \pm SEM. **, $p<0.01$; ***, $p<0.001$; ****, $p<0.0001$.

Figure 8



c) Tertiary Lysosomes

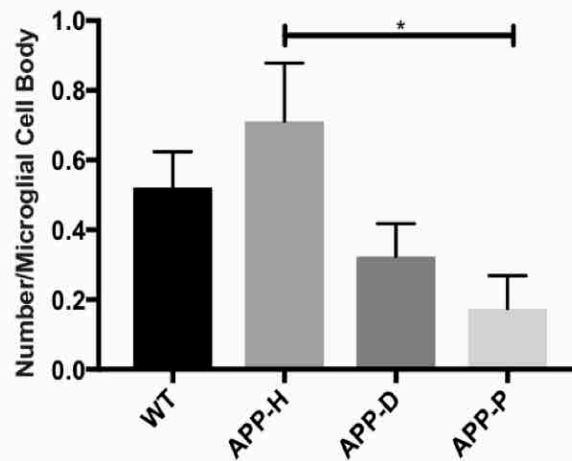


Figure 3.9.8 Microglia in dystrophic and plaque-associated neuropil have reduced numbers of tertiary lysosomes.

(A) Example image of IBA1-positive microglial process in a healthy region of APP^{Swe}-PS1 Δ e9 hippocampus, containing numerous tertiary lysosomes with lipofuscin accompanying lipid bodies (tlys). (B) Example image of IBA1-positive microglial process in a plaque-associated region. Scale bars=500 nm. (C) Change in the score of tertiary lysosomes in microglial cell bodies Error bars represent mean \pm SEM. *, p<0.05.

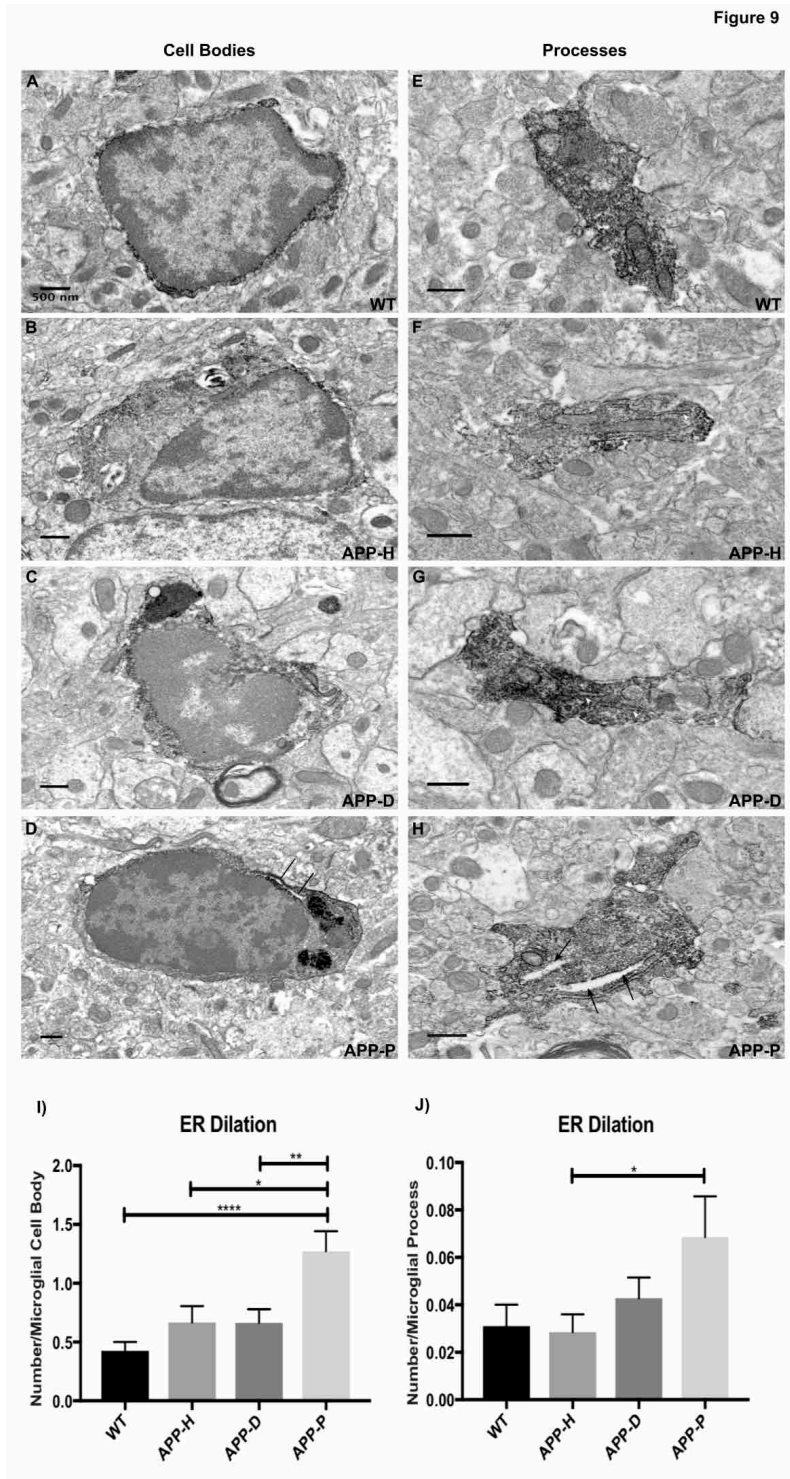


Figure 3.9.9 Proximity to A β plaques correlates with increased ER dilation.

(A) Example of IBA1-positive microglial cell body in a wild-type control. (B-D) Example of IBA1-positive microglial cell bodies containing healthy (white arrowheads) and dilated (black arrows) ER in apparently healthy (B), dystrophic (C), and fA β containing (D) areas

of APP^{Swe}-PS1 Δ e9 hippocampus. (E-H) Example images of IBA1-positive microglial processes in WT (E), healthy (F), dystrophic (G) and fA β containing (H) areas of APP^{Swe}-PS1 Δ e9 hippocampus. Scale bars=500 nm. (I) Quantification of instances of dilated ER in microglial cell bodies. (J) Quantification of instances of dilated ER in microglial processes. Error bars represent mean \pm SEM. *, p<0.05; **, p<0.01; ****, p<0.0001.

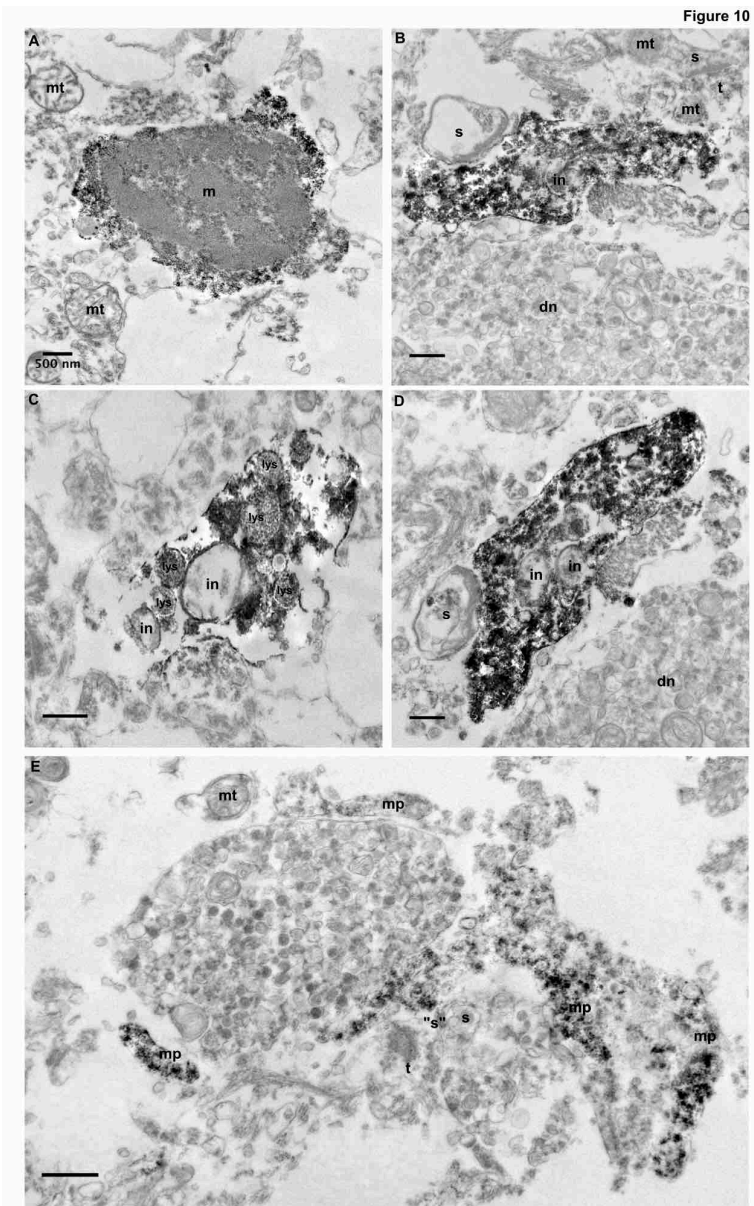


Figure 3.9.10 Microglial ultrastructure in post-mortem samples from human AD patient(s). (A) Image of an IBA1-immunopositive microglial cell body in post-mortem tissue from the hippocampus of an individual diagnosed with AD. m = microglia, mt = mitochondria. (B) Image of an IBA1-positive microglial process making contacts with a dystrophic neurite (d) and synaptic terminal (s). (C) Image of an IBA1-positive microglial process containing numerous inclusions (in) and lysosomes (lys). (D) Image of a microglial process containing numerous inclusions (in) and making contacts with a synaptic terminal (s) and dystrophic

neurite (dn). (E) Microglial process (mp) encircling a dystrophic neurite (dn) and making contacts with a synaptic cleft (“s”). Scale bars=500nm.

Table 3.9.11 Mean comparison of ultrastructural analysis of microglial cell bodies in wild-type and APP-PS1 mice with the depiction of its *p* values. n is number per microglial cell body.

	Wild-type	APP-PS1	
	Mean ± SEM	Mean ± SEM	<i>P</i> value
Area (μm ²)	18513.875 ± 750.061	21544.724 ± 776.927	0.009
Perimeter (μm)	22.186 ± 0.651	23.991 ± 0.839	0.132
Circularity (a.u.)	0.495 ± 0.015	0.511 ± 0.012	0.409
Roundness (a.u.)	0.590 ± 0.016	0.622 ± 0.013	0.163
Solidity (a.u.)	0.844 ± 0.009	0.852 ± 0.007	0.516
Lipid body (n)	0.521 ± 0.094	0.426 ± 0.069	0.414
Aβ (n)	0 ± 0	0.401 ± 0.068	<0.0001
Phagocytic cells (%)	82.8 ± 3.9	0.769 ± 0.033	0.271
Inclusion (n)	3.161 ± 0.223	2.647 ± 0.174	0.071
Intact element (n)	1.548 ± 0.160	1.365 ± 0.119	0.356
Digested element (n)	1.617 ± 0.129	0.891 ± 0.079	<0.0001
ER dilation (n)	0.425 ± 0.074	0.834 ± 0.082	0.0009
Extracellular digestion (n)	1.702 ± 0.1351	0.777 ± 0.090	<0.0001
Primary lysosome (n)	0.095 ± 0.048	0.108 ± 0.038	0.841
Secondary lysosome (n)	0.553 ± 0.107	0.535 ± 0.076	0.888
Tertiary lysosome (n)	0.521 ± 0.102	0.388 ± 0.069	0.267

Table 3.9.12 Mean comparison of ultrastructural analysis of microglial processes in wild-type and APP-PS1 mice with the depiction of its *p* values. n is number per microglial process

	Wild-type	APP-PS1	
	Mean ± SEM	Mean ± SEM	<i>P</i> value
Area (μm ²)	655.163 ± 53.645	678.559 ± 34.591	0.732
Perimeter (μm)	3.986 ± 0.087	4.073 ± 0.148	0.625
Circularity (a.u.)	0.460 ± 0.008	0.488 ± 0.005	0.007
Roundness (a.u.)	0.478 ± 0.007	0.491 ± 0.004	0.168
Solidity (a.u.)	0.756 ± 0.006	0.772 ± 0.003	0.041
Lipid body (n)	0.013 ± 0.005	0.019 ± 0.004	0.492
Aβ (n)	0 ± 0	0.021 ± 0.005	0.019
Phagocytic process (%)	37.18 ± 2.007	27.06 ± 1.039	<0.0001
Inclusion (n)	0.769 ± 0.054	0.538 ± 0.026	<0.0001
Intact element (n)	0.323 ± 0.032	0.255 ± 0.016	0.050
Digested element (n)	0.445 ± 0.035	0.261 ± 0.015	<0.0001
ER dilation (n)	0.030 ± 0.009	0.042 ± 0.005	0.310
Extracellular digestion (n)	0.435 ± 0.033	0.255 ± 0.013	<0.0001
Primary lysosome (n)	0.010 ± 0.004	0.018 ± 0.004	0.284
Secondary lysosome (n)	0.056 ± 0.013	0.051 ± 0.007	0.755
Tertiary lysosome (n)	0.008 ± 0.004	0.020 ± 0.005	0.219
Encirclement (n)	0.617 ± 0.038	0.613 ± 0.021	0.920
Encircled synapse (n)	0.037 ± 0.008	0.040 ± 0.005	0.774
Encircled digested element (n)	0.167 ± 0.018	0.089 ± 0.007	<0.0001
Encircled Aβ (n)	0 ± 0	0.022 ± 0.005	0.022
Encircled myelinated axon (n)	0.003 ± 0.002	0.006 ± 0.001	0.462
Encircled dendritic spine (n)	0.137 ± 0.016	0.188 ± 0.011	0.024
Encircled axonal terminal (n)	0.194 ± 0.020	0.215 ± 0.011	0.391

4. Discussion:

In Chapter 2, we described a new protocol that enabled us to study microglial ultrastructural phenotypes and their interactions with synapses and other neuronal structures in their environment in the presence of A β plaques. Microglia and their interactions were studied in different contexts, covering several areas where microglia were proximal to the A β plaques, proximal to dystrophic elements, and to regions appearing healthy in the APP-PS1 mouse model. The designed approach utilized correlative techniques of light and electron microscopy to localize the dense core A β plaques. Using fluorescent light microscopy, brain sections containing A β plaques in regions and layers of interest to our study, in the hippocampus CA1, *strata radiatum* and *lacunosum-moleculare*, were rapidly selected from samples of mice injected with the congo red derivative Methoxy-X04. The rapid selection and screening made possible by the *in-vivo* injection of Methoxy-X04 were followed by pre-embedding immunostaining for the microglial marker IBA1 to allow localization and visualization of microglial phenotypes and interactions in the presence of A β plaques or neuronal dystrophy at the ultrastructural level (271).

Analysing microglial phenotypes and interactions with relation to A β plaques is extremely important to provide novel insights into microglial involvement in the progression of AD pathology. Microglial inflammatory activity, extensive reactivity, and the release of pro-inflammatory cytokines are implicated in the disruption of normal brain homeostasis and AD pathophysiology (180). In the healthy brain, microglia modulate and mediate neuronal circuits remodeling and synaptic plasticity (143,151). Taking into account that AD is characterized by a progressive synaptic loss in the brain (7,239), microglia are believed to be involved in the pathogenesis and synaptic loss due to the dysregulation in their physiological roles in the remodeling and maintenance of neuronal circuits.

This protocol we established allows better penetration of antibodies to the brain sections due to the improved technique of pre-embedding IBA1 immunostaining method. This improvement renders an enhanced visualization of microglial cell bodies and processes.

Each step of the protocol must be performed thoroughly to avoid any compromise in the integrity of the sample structure and to permit a favorable visualization of cellular membranes and components (271). Also, although this protocol was mainly designed to study microglia in the presence of A β plaques, several cell types can also be targeted by using their complementary antibodies with the utilization of this protocol. Astrocytes, oligodendrocytes, peripheral macrophages and neuronal subdivisions can be studied in the presence of A β plaques. This versatility allows a better understanding of alterations in morphology and cellular interactions due to A β plaques deposition.

However, this protocol can be only used in experiments enabling *in-vivo* injection and can not be used on fixed brain sections. Thus it can not be performed on post-mortem human sections. Moreover, Methoxy-X04 only binds to β -pleated sheets proteins of the plaques and is not able to attach to soluble forms of A β which represents another limitation of the protocol application.

The pathophysiology of AD is deeply linked with A β plaques deposition in multiple regions of the brain (245,246,247,248,249). Microglial cells were seen to surround and interact with these plaques in several studies of AD mouse models (251). Microglia undergo various changes in morphology, function, and gene expression inscriptions during the progression of AD (94,97,250). Also, microglia appear to acquire a heterogeneous response characterized by multiple cellular and functional changes that impact the homeostatic roles that these cells can offer to their brain environment. In our aim to understand better the changes occurring to the resident immune cells of the brain, we employed our specific correlative protocol to study the proposed heterogeneity in microglial phenotype and cellular functions by using high spatial resolution electron microscopy that enabled us to assess those emerging features at the ultrastructural level. Because memory loss is one of the main symptoms of AD which is linked functionally to the alterations taking place in the hippocampus during disease progression (242), we mainly focused on the CA1 region of the hippocampus examining *strata radiatum* and *lacunosum-moleculare* of 14 months old APP-PS1 mice and age-matched controls. We imaged IBA1 immunostained microglial cell bodies and processes in the ventral part of the hippocampus amid regions located near the plaques, among areas of neuronal dystrophy, and in regions appearing healthy regarding neuronal structures' integrity.

In Chapter 3, our study which used this method reported significant changes in the ultrastructure of microglial cell bodies and processes in the vicinity of the plaques. Using quantitative analysis, results showed that the area and perimeter of microglial cell bodies were larger when studied proximal to the plaques than in areas of dystrophy, apparently healthy or in wild-type controls. This finding indicates a microglial response to the $fA\beta$ and is concurrent to the results of a previous study where microglia in the PDAPP transgenic AD model were visualized using *in-vivo* multiphoton microscopy between 14 and 17 months of age. The results revealed that microglia in areas containing $A\beta$ plaques had larger cell body areas and smaller processes when compared to cell bodies from younger (3.5 months) transgenic mice or from the same age group where microglia were in areas devoid and distant from the plaques (282). Also, in a study where an optic nerve crush was performed on wild-type mice, microglial cell bodies showed a significant increase in their areas as a reaction to this procedure when compared to naïve mice (317), suggesting that these morphological changes are linked to their reactivity to damage resulting from mechanical or chemical insults. Moreover, microglia in plaque and dystrophy regions had more round cell bodies compared to wild-type cells, suggesting a decrease in process arborization which is also reported where microglia near plaque had decrease in the size of processes compared to areas devoid from plaques at the light microscopic level in PDAPP mouse model (282). By comparing microglial processes between APP-PS1 and wild-type mice, there was no significant difference in the ultrastructure of these processes. Normally, IBA1-immunostained microglial processes are narrow, long and ramified when examined in ultrathin sections. However, microglial processes in APP-PS1 were significantly rounder and more solid in structure when compared to wild-type controls. This may suggest a decrease in motility of these processes which may impact their normal interactions with neuronal elements and decrease the incidence of macropinocytosis (283). Also, microglial processes in 14 months PDAPP mice were more stable and presented less process movement when compared to 3 month old mice which might also be linked to their rounder and solid shape (282).

One of the essential tasks of microglia is their ability to perform phagocytosis in both standard physiological homeostatic and developmental processes in the healthy brain or in

fighting pathogenic insults. Using our immunoEM protocol, we studied the phagocytic capacity of microglia in wild-type and the already described regions of APP-PS1 mice. The results revealed that microglia in both healthy and dystrophy regions of the APP-PS1 mice were less phagocytic when compared to microglia from wild-type and plaque region cells. Microglial phagocytic capacity in the plaque region of APP-PS1 mice was mainly targeted towards A β plaques where numerous inclusions of A β fibrils were located inside the cell bodies and processes of these cells. Also, the fact that A β fibrils inclusions were mainly restricted to cell bodies and processes located mostly in plaque regions and a lesser extent in dystrophy regions, suggesting that microglia do not relocate after engulfing A β fibrils. Microglial processes in wild-type mice were significantly more phagocytic containing intact, partially digested and fully digested vacuoles. However, microglial processes in healthy APP-PS1 regions were less likely to contain phagocytic inclusions. Digested inclusions were significantly less frequent in all APP-PS1 areas when compared to wild-type. These results indicate alteration of the phagocytosis process in its different steps, starting with the ingestion of those elements and ending in degradation. Microglia in the three regions of APP-PS1 seem to have functional impairments in the phagolysosomal system. Moreover, microglial cell bodies and processes in wild-type animals were significantly linked to and engaged in extracellular degradation that was evident by the presence of partially digested membranes and organelles surrounding microglia. This phenomenon of extracellular degradation was substantially lower in all APP-PS1 studied regions. A study in a rat model of abdominal wall repair showed that the contribution of blood monocytes is essential for the degradation of extracellular matrix scaffolds and is necessary to fulfilling extracellular matrix mediated tissue remodeling (318). The immune cells of the brain may also be a part of the process mediating extracellular matrix degradation to ensure proper neuronal circuits remodeling in the healthy brain which is also seen disrupted in APP-PS1 mouse model.

Cellular stress is an important feature that determines functional status and activity of cells. The signs of stress are usually seen during aging and in pathological conditions such as AD. One of the characteristics of cellular stress is the alteration that takes place in the Golgi apparatus and rough endoplasmic reticulum the organelles which are responsible for

the production and transport of proteins in the cell. Modifications of these organelles are determined by a dilation of the small narrow membranes that are present commonly. Our study of this cellular stress feature revealed that microglial cell bodies and processes in the plaque regions of APP-PS1 showed significant stress features by the presence of numerous dilated structure of endoplasmic reticulum. Microglia in all the APP-PS1 regions combined showed twice the number of dilated endoplasmic reticulum when compared to wild-type, with microglia in the plaque regions having the highest contribution to this score. The phagolysosomal system was another cellular function feature examined in the study. Results from the quantification of primary, secondary and tertiary lysosomes revealed a significant accumulation of tertiary lysosomes in microglial cell bodies from the healthy region of APP-PS1. These tertiary lysosomes collection indicates that those cells are having difficulties in the phagolysosomal pathway which is a complementary part of the process of phagocytosis. This finding can be linked to another result of our study where digested elements inclusions were significantly lower in microglial cell bodies suggesting altered phagocytosis in its different steps in the healthy region of APP-PS1.

Microglial processes interactions with synapses, dendritic spines, axon terminals, myelinated axons, A β and digested extracellular elements were also studied. Processes in APP-PS1 plaque region significantly increased their contact and encirclement of A β plaques. Processes in wild-type animals were considerably encircling digested or degenerating extracellular elements frequently when compared to all regions from APP-PS1. Also, processes in healthy regions of APP-PS1 contacted and encircled the dendritic spine at a higher rate than other studied groups. A recent study on wild-type mice using a light sheet fluorescence microscopy augmented 3D ultrastructural characterization using correlative light, and electron microscopy (CLEM) showed that microglia selectively trogocytose (partially phagocytose) presynaptic elements and contacting postsynaptic elements with no evidence of phagocytosis as an outcome of this contact. Interestingly postsynaptic elements formed filopodial extensions after microglial contacts implicating microglia in development and maturation of neuronal circuits (313). Therefore, significant microglial encirclement of the dendritic spines in the healthy region of APP-PS1 might suggest a prolonged and increased contact compared to other regions

and especially to wild-type which may result in abnormal developmental and remodeling processes.

Microglia were also examined in human post-mortem AD samples. Where IBA1 immunostaining was performed on those samples and then processed for visualization with transmission electron microscopy. Interestingly, microglial cell bodies and processes were seen to contact areas of dystrophic neurites and to contain several inclusions with partially degraded structures which recapitulates the what we have seen in the APP-PS1 mouse model.

Microglia roles in health and disease are diversified depending on the context in which these roles are examined. Developmental stages of microglia, brain region localization and pathological processes in the brain all contribute to the microglial response that shows heterogeneity in morphology, cellular process, and cell to cell interactions. Although many studies were conducted on microglia in health and disease to offer a better understanding of their different physiological roles and using multiple experimental techniques such as single cell RNA-sequencing, *in-vivo* two photon imaging and multiple other methods, there is still a necessity for studying microglia phenotypes and interactions with their environment on a high spatial resolution ultrastructural level in order to delve into the implications of this heterogeneity.

The study we conducted characterised and categorized the some of the different morphological, cellular, and functional processes that microglia undergo in wild-type mice compared with different regions of APP-PS1 animals. The heterogeneity that is evident in the differences of ultrastructure, phagocytic capacity, cellular features and cell interactions through contact between wild-type mice and APP-PS1 and even between different regions of these transgenic mice can further elucidate that microglial diversity in their reactions and interactions may influence physiological and pathological processes.

While microglial ultrastructure and functions were examined in the presence of A β plaques. The contribution of soluble A β was not examined in this study. The implication of soluble A β in the progression of AD is very crucial in further understanding its impact on microglial response that may influence the disease progression.

5. References

1. Stelzmann, R. A., Norman Schnitzlein, H., & Reed Murtagh, F. (1995). An english translation of alzheimer's 1907 paper. "über eine eigenartige erkankung der hirnrinde". *Clinical Anatomy*. <http://doi.org/10.1002/ca.980080612>
2. Alzheimer, A. (1907). Über eine eigenartige Erkrankung der Hirnrinde. *Allg Zeitschr f Psychiatrie u Psych-Gerichtl Med*. <http://doi.org/10.1002/ca.980080612>
3. Alzheimer Association. (2016). 2016 Alzheimer's Disease Facts and Figures. *Alzheimer's & Dementia 2016*. <http://doi.org/10.1016/j.jalz.2016.03.001>
4. Masters, C. L., Bateman, R., Blennow, K., Rowe, C. C., Sperling, R. A., & Cummings, J. L. (2015). Alzheimer's disease. *Nature Reviews Disease Primers*, 1, 15056. Retrieved from <http://dx.doi.org/10.1038/nrdp.2015.56>
5. DeKosky, S. T., & Scheff, S. W. (1990). Synapse loss in frontal cortex biopsies in Alzheimer's disease: Correlation with cognitive severity. *Annals of Neurology*. <http://doi.org/10.1002/ana.410270502>
6. Scheff, S. W., & Price, D. A. (1993). Synapse loss in the temporal lobe in Alzheimer's disease. *Annals of Neurology*. <http://doi.org/10.1002/ana.410330209>
7. Terry, R. D., Masliah, E., Salmon, D. P., Butters, N., DeTeresa, R., Hill, R., Katzman, R. (1991). Physical basis of cognitive alterations in Alzheimer's disease: Synapse loss is the major correlate of cognitive impairment. *Annals of Neurology*. <http://doi.org/10.1002/ana.410300410>

8. Glenner, G. G., & Wong, C. W. (1984). Alzheimer's disease: Initial report of the purification and characterization of a novel cerebrovascular amyloid protein. *Biochemical and Biophysical Research Communications*. [http://doi.org/10.1016/S0006-291X\(84\)80190-4](http://doi.org/10.1016/S0006-291X(84)80190-4)

9. Masters, C. L., Simms, G., Weinman, N. A., Multhaup, G., McDonald, B. L., & Beyreuther, K. (1985). Amyloid plaque core protein in Alzheimer disease and Down syndrome. *Proceedings of the National Academy of Sciences of the United States of America*. <http://doi.org/10.1073/pnas.82.12.4245>

10. Bateman, Randall J, Paul S Aisen, Bart De Strooper, Nick C Fox, Cynthia A Lemere, John M Ringman, Stephen Salloway, Reisa A Sperling, Manfred Windisch, and Chengjie Xiong. "Autosomal-Dominant Alzheimer's Disease: A Review and Proposal for the Prevention of Alzheimer's Disease." *Alzheimer's Research & Therapy* 3, no. 1 (2010): 1. <https://doi.org/10.1186/alzrt59>.

11. Ballard, C., Gauthier, S., Corbett, A., Brayne, C., Aarsland, D., & Jones, E. (2011). Alzheimer's disease. *Lancet*. [http://doi.org/10.1016/s0140-6736\(10\)61349-9](http://doi.org/10.1016/s0140-6736(10)61349-9)

12. Karch, C. M., & Goate, A. M. (2015). Alzheimer's disease risk genes and mechanisms of disease pathogenesis. *Biological Psychiatry*. <http://doi.org/10.1016/j.biopsych.2014.05.006>

13. Xu, W., Tan, L., Wang, H.-F., Jiang, T., Tan, M.-S., Tan, L., ... Yu, J.-T. (2015). Meta-analysis of modifiable risk factors for Alzheimer's disease. *Journal of Neurology, Neurosurgery & Psychiatry*. <http://doi.org/10.1136/jnnp-2015-310548>

14. Serrano-Pozo, A., Frosch, M. P., Masliah, E., & Hyman, B. T. (2011). Neuropathological alterations in Alzheimer disease. *Cold Spring Harbor Perspectives in Medicine*. <http://doi.org/10.1101/cshperspect.a006189>

15. <http://www.brainfacts.org/Diseases-and-Disorders/Neurodegenerative-Disorders/2012/Alzheimers-Disease-Today>

16. Iqbal, K., Liu, F., Gong, C.-X., & Grundke-Iqbal, I. (2010). Tau in Alzheimer Disease and Related Tauopathies. *Current Alzheimer Research*. <http://doi.org/10.2174/156720510793611592>

17. Gao, Y.-L., Wang, N., Sun, F.-R., Cao, X.-P., Zhang, W., & Yu, J.-T. (2018). Tau in neurodegenerative disease. *Annals of Translational Medicine*, 6(10), 175. <http://doi.org/10.21037/atm.2018.04.23>

18. Lee, V. M.-Y., Goedert, M., & Trojanowski, J. Q. (2001). Neurodegenerative Tauopathies. *Annual Review of Neuroscience*. <http://doi.org/10.1146/annurev.neuro.24.1.1121>

19. Lee, V. M. Y., Brunden, K. R., Hutton, M., & Trojanowski, J. Q. (2011). Developing therapeutic approaches to tau, selected kinases, and related neuronal protein targets. *Cold Spring Harbor Perspectives in Medicine*. <http://doi.org/10.1101/cshperspect.a006437>
20. Goedert, M., Spillantini, M. G., Jakes, R., Rutherford, D., & Crowther, R. A. (1989). Multiple isoforms of human microtubule-associated protein tau: sequences and localization in neurofibrillary tangles of Alzheimer's disease. *Neuron*. [http://doi.org/10.1016/0896-6273\(89\)90210-9](http://doi.org/10.1016/0896-6273(89)90210-9)
21. Guerrero-Muñoz, M. J., Gerson, J., & Castillo-Carranza, D. L. (2015). Tau Oligomers: The Toxic Player at Synapses in Alzheimer's Disease. *Frontiers in Cellular Neuroscience*. <http://doi.org/10.3389/fncel.2015.00464>
22. Gómez-Isla, T., Hollister, R., West, H., Mui, S., Growdon, J. H., Petersen, R. C., ... Hyman, B. T. (1997). Neuronal loss correlates with but exceeds neurofibrillary tangles in Alzheimer's disease. *Annals of Neurology*. <http://doi.org/10.1002/ana.410410106>
23. Scheltens, P., Blennow, K., Breteler, M. M. B., de Strooper, B., Frisoni, G. B., Salloway, S., & Van der Flier, W. M. (2016). Alzheimer's disease. *The Lancet*, 388(10043), 505–517. [http://doi.org/10.1016/S0140-6736\(15\)01124-1](http://doi.org/10.1016/S0140-6736(15)01124-1)
24. Ittner, Lars M., Yazici D. Ke, Fabien Delerue, Mian Bi, Amadeus Gladbach, Janet van Eersel, Heidrun Wölfling, et al. "Dendritic Function of Tau Mediates Amyloid- β Toxicity in Alzheimer's Disease Mouse Models." *Cell* 142, no. 3 (August 2010): 387–97. <https://doi.org/10.1016/j.cell.2010.06.036>.
25. Gotz, J. (2001). Formation of Neurofibrillary Tangles in P301L Tau Transgenic Mice Induced by A β 42 Fibrils. *Science*. <http://doi.org/10.1126/science.1062097>
26. Roberson, E. D., Scarce-Levie, K., Palop, J. J., Yan, F., Cheng, I. H., Wu, T., ... Mucke, L. (2007). Reducing endogenous tau ameliorates amyloid beta-induced deficits in an Alzheimer's disease mouse model. *Science (New York, N.Y.)*. <http://doi.org/10.1126/science.1141736>
27. Glenner, G. G., & Wong, C. W. (1984). Alzheimer's disease: Initial report of the purification and characterization of a novel cerebrovascular amyloid protein. *Biochemical and Biophysical Research Communications*. [http://doi.org/10.1016/S0006-291X\(84\)80190-4](http://doi.org/10.1016/S0006-291X(84)80190-4)
28. Glenner, G. G., & Wong, C. W. (1984). Alzheimer's disease and Down's syndrome: Sharing of a unique cerebrovascular amyloid fibril protein. *Biochemical and Biophysical Research Communications*, 122(3), 1131–1135. [http://doi.org/https://doi.org/10.1016/0006-291X\(84\)91209-9](http://doi.org/https://doi.org/10.1016/0006-291X(84)91209-9)

29. Oh, Esther S., Alena V. Savonenko, Julie F. King, Stina M. Fangmark Tucker, Gay L. Rudow, Guilian Xu, David R. Borchelt, and Juan C. Troncoso. "Amyloid Precursor Protein Increases Cortical Neuron Size in Transgenic Mice." *Neurobiology of Aging* 30, no. 8 (August 2009): 1238–44. <http://doi.org/10.1016/j.neurobiolaging.2007.12.024>.
30. Selkoe, D. J. (2001). Alzheimer's Disease: Genes, Proteins, and Therapy. *Perspective*. [http://doi.org/10.1016/0092-8674\(88\)90462-x](http://doi.org/10.1016/0092-8674(88)90462-x)
31. Thinakaran, G., & Koo, E. H. (2008). Amyloid precursor protein trafficking, processing, and function. *The Journal of Biological Chemistry*. <http://doi.org/10.1074/jbc.R800019200>
32. Shepherd, C., McCann, H., & Halliday, G. M. (2009). Variations in the neuropathology of familial Alzheimer's disease. *Acta Neuropathologica*. <http://doi.org/10.1007/s00401-009-0521-4>
33. Shen, J., & Kelleher, R. J. (2007). The presenilin hypothesis of Alzheimer's disease: Evidence for a loss-of-function pathogenic mechanism. *Proceedings of the National Academy of Sciences*. <http://doi.org/10.1073/pnas.0608332104>
34. Tiraboschi, P., Hansen, L. A., Masliah, E., Alford, M., Thal, L. J., & Corey-Bloom, J. (2004). Impact of APOE genotype on neuropathologic and neurochemical markers of Alzheimer disease. *Neurology*. <http://doi.org/10.1212/01.WNL.0000128091.92139.0F>
35. Holtzman, D. M., Bales, K. R., Wu, S., Bhat, P., Parsadanian, M., Fagan, A. M., ... Paul, S. M. (1999). Expression of human apolipoprotein E reduces amyloid-B deposition in a mouse model of Alzheimer's disease. *Journal of Clinical Investigation*. <http://doi.org/10.1172/JCI6179>
36. Yankner, B. A., Dawes, L. R., Fisher, S., Villa-Komaroff, L., Oster-Granite, M. Lou, & Neve, R. L. (1989). Neurotoxicity of a fragment of the amyloid precursor associated with Alzheimer's disease. *Science*. <http://doi.org/10.1126/science.2474201>
37. Irizarry, Michael C., Ferdie Soriano, Megan McNamara, Keith J. Page, Dale Schenk, Dora Games, and Bradley T. Hyman. "A β Deposition Is Associated with Neuropil Changes, but Not with Overt Neuronal Loss in the Human Amyloid Precursor Protein V717F (PDAPP) Transgenic Mouse." *The Journal of Neuroscience* 17, no. 18 (September 15, 1997): 7053–59. <https://doi.org/10.1523/JNEUROSCI.17-18-07053.1997>.
38. Spires, T. L. (2005). Dendritic Spine Abnormalities in Amyloid Precursor Protein Transgenic Mice Demonstrated by Gene Transfer and Intravital Multiphoton

Microscopy. *Journal of Neuroscience*. <http://doi.org/10.1523/JNEUROSCI.1879-05.2005>

39. Chen, Guiquan, Karen S. Chen, Jane Knox, Jennifer Inglis, Andrew Bernard, Stephen J. Martin, Alan Justice, et al. "A Learning Deficit Related to Age and β -Amyloid Plaques in a Mouse Model of Alzheimer's Disease." *Nature* 408, no. 6815 (December 2000): 975–79. <https://doi.org/10.1038/35050103>.
40. El Khoury, J., Toft, M., Hickman, S. E., Means, T. K., Terada, K., Geula, C., & Luster, A. D. (2007). Ccr2 deficiency impairs microglial accumulation and accelerates progression of Alzheimer-like disease. *Nature Medicine*. <http://doi.org/10.1038/nm1555>
41. Wang, D. S., Dickson, D. W., & Malter, J. S. (2006). β -Amyloid degradation and Alzheimer's disease. *Journal of Biomedicine & Biotechnology*. <http://doi.org/10.1155/JBB/2006/58406>
42. Yasojima, K., McGeer, E. G., & McGeer, P. L. (2001). Relationship between beta amyloid peptide generating molecules and neprilysin in Alzheimer disease and normal brain. *Brain Research*. [http://doi.org/10.1016/S0006-8993\(01\)03008-6](http://doi.org/10.1016/S0006-8993(01)03008-6)
43. Da Mesquita, Sandro, Antoine Louveau, Andrea Vaccari, Igor Smirnov, R. Chase Cornelison, Kathryn M. Kingsmore, Christian Contarino, et al. "Functional Aspects of Meningeal Lymphatics in Ageing and Alzheimer's Disease." *Nature* 560, no. 7717 (August 2018): 185–91. <https://doi.org/10.1038/s41586-018-0368-8>.
44. Zlokovic, B. V. (2011). Neurovascular pathways to neurodegeneration in Alzheimer's disease and other disorders. *Nature Reviews Neuroscience*. <http://doi.org/10.1038/nrn3114>
45. Braak, H., & Del Tredici, K. (2011). Alzheimer's pathogenesis: Is there neuron-to-neuron propagation? *Acta Neuropathologica*. <http://doi.org/10.1007/s00401-011-0825-z>
46. Miners, J. S., Baig, S., Tayler, H., Kehoe, P. G., & Love, S. (2009). Neprilysin and insulin-degrading enzyme levels are increased in Alzheimer disease in relation to disease severity. *Journal of Neuropathology and Experimental Neurology*. <http://doi.org/10.1097/NEN.0b013e3181afe475>
47. Caccamo, A., Oddo, S., Billings, L. M., Green, K. N., Martinez-Coria, H., Fisher, A., & LaFerla, F. M. (2006). M1 receptors play a central role in modulating AD-like pathology in transgenic mice. *Neuron*. <http://doi.org/10.1016/j.neuron.2006.01.020>

48. Lin, M. T., & Beal, M. F. (2006). Mitochondrial dysfunction and oxidative stress in neurodegenerative diseases. *Nature*. <http://doi.org/10.1038/nature05292>
49. Gandhi, S., & Abramov, A. Y. (2012). Mechanism of oxidative stress in neurodegeneration. *Oxidative Medicine and Cellular Longevity*. <http://doi.org/10.1155/2012/428010>
50. Praticò, D. (2008). Oxidative stress hypothesis in Alzheimer's disease: a reappraisal. *Trends in Pharmacological Sciences*, 29(12), 609–615. <http://doi.org/10.1016/j.tips.2008.09.001>
51. Makhaeva, Galina F., Sofya V. Lushchekina, Natalia P. Boltneva, Vladimir B. Sokolov, Vladimir V. Grigoriev, Olga G. Serebryakova, Ekaterina A. Vikhareva, et al. "Conjugates of γ -Carbolines and Phenothiazine as New Selective Inhibitors of Butyrylcholinesterase and Blockers of NMDA Receptors for Alzheimer Disease." *Scientific Reports* 5, no. 1 (October 2015). <https://doi.org/10.1038/srep13164>.
52. Mhatre, Molina, Robert A. Floyd, and Kenneth Hensley. "Oxidative Stress and Neuroinflammation in Alzheimer's Disease and Amyotrophic Lateral Sclerosis: Common Links and Potential Therapeutic Targets." Edited by M. Cristina Polidori. *Journal of Alzheimer's Disease* 6, no. 2 (April 13, 2004): 147–57. <https://doi.org/10.3233/JAD-2004-6206>.
53. Zhao, Y., & Zhao, B. (2013). Oxidative stress and the pathogenesis of alzheimer's disease. *Oxidative Medicine and Cellular Longevity*. <http://doi.org/10.1155/2013/316523>
54. Grivennikova, V. G., & Vinogradov, A. D. (2006). Generation of superoxide by the mitochondrial Complex I. *Biochimica et Biophysica Acta - Bioenergetics*. <http://doi.org/10.1016/j.bbabi.2006.03.013>
55. Koffie, R. M., Hyman, B. T., & Spires-Jones, T. L. (2011). Alzheimer's disease: Synapses gone cold. *Molecular Neurodegeneration*. <http://doi.org/10.1186/1750-1326-6-63>
56. Wang, J. M., & Sun, C. (2010). Calcium and neurogenesis in Alzheimer's disease. *Frontiers in Neuroscience*. <http://doi.org/10.3389/fnins.2010.00194>
57. Green, K.N., I.F. Smith, and F.M. Laferla. "Role of Calcium in the Pathogenesis of Alzheimer's Disease and Transgenic Models." In *Calcium Signalling and Disease*, edited by Ernesto Carafoli and Marisa Brini, 45:507–21. Dordrecht: Springer Netherlands, 2007. https://doi.org/10.1007/978-1-4020-6191-2_19.

58. Kelliher, M., J. Fastbom, R.F. Cowburn, W. Bonkale, T.G. Ohm, R. Ravid, V. Sorrentino, and C. O'Neill. "Alterations in the Ryanodine Receptor Calcium Release Channel Correlate with Alzheimer's Disease Neurofibrillary and β -Amyloid Pathologies." *Neuroscience* 92, no. 2 (May 1999): 499–513. [https://doi.org/10.1016/S0306-4522\(99\)00042-1](https://doi.org/10.1016/S0306-4522(99)00042-1).
59. Baumgärtel, K., & Mansuy, I. M. (2012). Neural functions of calcineurin in synaptic plasticity and memory. *Learning and Memory*. <http://doi.org/10.1101/lm.027201.112>
60. Lisman, J., Schulman, H., & Cline, H. (2002). The molecular basis of CaMKII function in synaptic and behavioural memory. *Nature Reviews Neuroscience*. <http://doi.org/10.1038/nrn753>
61. Megill, A., T. Tran, K. Eldred, N. J. Lee, P. C. Wong, H.-S. Hoe, A. Kirkwood, and H.-K. Lee. "Defective Age-Dependent Metaplasticity in a Mouse Model of Alzheimer's Disease." *Journal of Neuroscience* 35, no. 32 (August 12, 2015): 11346–57. <https://doi.org/10.1523/JNEUROSCI.5289-14.2015>.
62. Games, Dora, David Adams, Ree Alessandrini, Robin Barbour, Patricia Borthette, Catherine Blackwell, Tony Carr, et al. "Alzheimer-Type Neuropathology in Transgenic Mice Overexpressing V717F β -Amyloid Precursor Protein." *Nature* 373, no. 6514 (February 1995): 523–27. <https://doi.org/10.1038/373523a0>.
63. Hsiao, K., P. Chapman, S. Nilsen, C. Eckman, Y. Harigaya, S. Younkin, F. Yang, and G. Cole. "Correlative Memory Deficits, A Elevation, and Amyloid Plaques in Transgenic Mice." *Science* 274, no. 5284 (October 4, 1996): 99–103. <https://doi.org/10.1126/science.274.5284.99>.
64. Sturchler-Pierrat, C., Abramowski, D., Duke, M., Wiederhold, K. H., Mistl, C., Rothacher, S., ... Sommer, B. (1997). Two amyloid precursor protein transgenic mouse models with Alzheimer disease-like pathology. *Proceedings of the National Academy of Sciences of the United States of America*. <http://doi.org/10.1073/pnas.94.24.13287>
65. Mucke, Lennart, Eliezer Masliah, Gui-Qiu Yu, Margaret Mallory, Edward M. Rockenstein, Gwen Tatsuno, Kang Hu, Dora Kholodenko, Kelly Johnson-Wood, and Lisa McConlogue. "High-Level Neuronal Expression of A β ₁₋₄₂ in Wild-Type Human Amyloid Protein Precursor Transgenic Mice: Synaptotoxicity without Plaque Formation." *The Journal of Neuroscience* 20, no. 11 (June 1, 2000): 4050–58. <https://doi.org/10.1523/JNEUROSCI.20-11-04050.2000>.

66. Chishti, M. Azhar, Dun-Shen Yang, Christopher Janus, Amie L. Phinney, Patrick Horne, Jacqueline Pearson, Robert Strome, et al. "Early-Onset Amyloid Deposition and Cognitive Deficits in Transgenic Mice Expressing a Double Mutant Form of Amyloid Precursor Protein 695." *Journal of Biological Chemistry* 276, no. 24 (June 15, 2001): 21562–70. <https://doi.org/10.1074/jbc.M100710200>.
67. Citron, Martin, Tilman Oltersdorf, Christian Haass, Lisa McConlogue, Albert Y. Hung, Peter Seubert, Carmen Vigo-Pelfrey, Ivan Lieberburg, and Dennis J. Selkoe. "Mutation of the β -Amyloid Precursor Protein in Familial Alzheimer's Disease Increases β -Protein Production." *Nature* 360, no. 6405 (December 1992): 672–74. <https://doi.org/10.1038/360672a0>.
68. De Strooper, Bart, Paul Saftig, Katleen Craessaerts, Hugo Vanderstichele, Gundula Guhde, Wim Annaert, Kurt Von Figura, and Fred Van Leuven. "Deficiency of Presenilin-1 Inhibits the Normal Cleavage of Amyloid Precursor Protein." *Nature* 391, no. 6665 (January 1998): 387–90. <https://doi.org/10.1038/34910>.
69. Holcomb, Leigh, Marcia N. Gordon, Eileen McGowan, Xin Yu, Stan Benkovic, Paul Jantzen, Kristal Wright, et al. "Accelerated Alzheimer-Type Phenotype in Transgenic Mice Carrying Both Mutant Amyloid Precursor Protein and Presenilin 1 Transgenes." *Nature Medicine* 4, no. 1 (January 1998): 97–100. <https://doi.org/10.1038/nm0198-097>.
70. Borchelt, David R, Tamara Ratovitski, Judy van Lare, Michael K Lee, Vicki Gonzales, Nancy A Jenkins, Neal G Copeland, Donald L Price, and Sangram S Sisodia. "Accelerated Amyloid Deposition in the Brains of Transgenic Mice Coexpressing Mutant Presenilin 1 and Amyloid Precursor Proteins." *Neuron* 19, no. 4 (October 1997): 939–45. [https://doi.org/10.1016/S0896-6273\(00\)80974-5](https://doi.org/10.1016/S0896-6273(00)80974-5).
71. Schmitz, Christoph, Bart P.F. Rutten, Andrea Pielen, Stephanie Schäfer, Oliver Wirths, Günter Tremp, Christian Czech, et al. "Hippocampal Neuron Loss Exceeds Amyloid Plaque Load in a Transgenic Mouse Model of Alzheimer's Disease." *The American Journal of Pathology* 164, no. 4 (April 2004): 1495–1502. [https://doi.org/10.1016/S0002-9440\(10\)63235-X](https://doi.org/10.1016/S0002-9440(10)63235-X).
72. Casas, Caty, Nicolas Sergeant, Jean-Michel Itier, Véronique Blanchard, Oliver Wirths, Nicolien van der Kolk, Valérie Vingtdeux, et al. "Massive CA1/2 Neuronal Loss with Intraneuronal and N-Terminal Truncated A β 42 Accumulation in a Novel Alzheimer Transgenic Model." *The American Journal of Pathology* 165, no. 4 (October 2004): 1289–1300. [https://doi.org/10.1016/S0002-9440\(10\)63388-3](https://doi.org/10.1016/S0002-9440(10)63388-3).

73. Hardy, J., and G. Higgins. "Alzheimer's Disease: The Amyloid Cascade Hypothesis." *Science* 256, no. 5054 (April 10, 1992): 184–85. <https://doi.org/10.1126/science.1566067>.
74. Thomas, A., Ballard, C., Kenny, R. A., O'Brien, J., Oakley, A., & Kalaria, R. (2005). Correlation of entorhinal amyloid with memory in Alzheimer's and vascular but not Lewy body dementia. *Dementia and Geriatric Cognitive Disorders*. <http://doi.org/10.1159/000082349>
75. Prasher, V. P., Farrer, M. J., Kessling, a M., Fisher, E. M., West, R. J., Barber, P. C., & Butler, a C. (1998). Molecular mapping of Alzheimer-type dementia in Down's syndrome. *Annals of Neurology*. <http://doi.org/10.1002/ana.410430316>
76. Jonsson, Thorlakur, Jasvinder K. Atwal, Stacy Steinberg, Jon Snaedal, Palmi V. Jonsson, Sigurbjorn Bjornsson, Hreinn Stefansson, et al. "A Mutation in APP Protects against Alzheimer's Disease and Age-Related Cognitive Decline." *Nature* 488, no. 7409 (August 2012): 96–99. <https://doi.org/10.1038/nature11283>.
77. Castellano, J. M., J. Kim, F. R. Stewart, H. Jiang, R. B. DeMattos, B. W. Patterson, A. M. Fagan, et al. "Human ApoE Isoforms Differentially Regulate Brain Amyloid-Peptide Clearance." *Science Translational Medicine* 3, no. 89 (June 29, 2011): 89ra57-89ra57. <https://doi.org/10.1126/scitranslmed.3002156>.
78. Shankar, Ganesh M, Shaomin Li, Tapan H Mehta, Amaya Garcia-Munoz, Nina E Shepardson, Imelda Smith, Francesca M Brett, et al. "Amyloid- β Protein Dimers Isolated Directly from Alzheimer's Brains Impair Synaptic Plasticity and Memory." *Nature Medicine* 14, no. 8 (August 2008): 837–42. <https://doi.org/10.1038/nm1782>.
79. Koffie, R. M., M. Meyer-Luehmann, T. Hashimoto, K. W. Adams, M. L. Mielke, M. Garcia-Alloza, K. D. Micheva, et al. "Oligomeric Amyloid Associates with Postsynaptic Densities and Correlates with Excitatory Synapse Loss near Senile Plaques." *Proceedings of the National Academy of Sciences* 106, no. 10 (March 10, 2009): 4012–17. <https://doi.org/10.1073/pnas.0811698106>.
80. Jin, M., Shepardson, N., Yang, T., Chen, G., Walsh, D., & Selkoe, D. J. (2011). Soluble amyloid -protein dimers isolated from Alzheimer cortex directly induce Tau hyperphosphorylation and neuritic degeneration. *Proceedings of the National Academy of Sciences*. <http://doi.org/10.1073/pnas.1017033108>

81. Jack, C. R., & Holtzman, D. M. (2013). Biomarker modeling of alzheimer's disease. *Neuron*. <http://doi.org/10.1016/j.neuron.2013.12.003>
82. Jack, Clifford R, David S Knopman, William J Jagust, Ronald C Petersen, Michael W Weiner, Paul S Aisen, Leslie M Shaw, et al. "Tracking Pathophysiological Processes in Alzheimer's Disease: An Updated Hypothetical Model of Dynamic Biomarkers." *The Lancet Neurology* 12, no. 2 (February 2013): 207–16. [https://doi.org/10.1016/S1474-4422\(12\)70291-0](https://doi.org/10.1016/S1474-4422(12)70291-0).
83. Kim, Jungsu, Paramita Chakrabarty, Amanda Hanna, Amelia March, Dennis W Dickson, David R Borchelt, Todd Golde, and Christopher Janus. "Normal Cognition in Transgenic BRI2-A β Mice." *Molecular Neurodegeneration* 8, no. 1 (2013): 15. <https://doi.org/10.1186/1750-1326-8-15>.
84. Kim, J., L. Onstead, S. Randle, R. Price, L. Smithson, C. Zwizinski, D. W. Dickson, T. Golde, and E. McGowan. "A 40 Inhibits Amyloid Deposition In Vivo." *Journal of Neuroscience* 27, no. 3 (January 17, 2007): 627–33. <https://doi.org/10.1523/JNEUROSCI.4849-06.2007>.
85. Salloway, Stephen, Reisa Sperling, Nick C. Fox, Kaj Blennow, William Klunk, Murray Raskind, Marwan Sabbagh, et al. "Two Phase 3 Trials of Bapineuzumab in Mild-to-Moderate Alzheimer's Disease." *New England Journal of Medicine* 370, no. 4 (January 23, 2014): 322–33. <https://doi.org/10.1056/NEJMoa1304839>.
86. Doody, Rachelle S., Ronald G. Thomas, Martin Farlow, Takeshi Iwatsubo, Bruno Vellas, Steven Joffe, Karl Kieburtz, et al. "Phase 3 Trials of Solanezumab for Mild-to-Moderate Alzheimer's Disease." *New England Journal of Medicine* 370, no. 4 (January 23, 2014): 311–21. <https://doi.org/10.1056/NEJMoa1312889>.
87. Edison, P., H. A. Archer, R. Hinz, A. Hammers, N. Pavese, Y. F. Tai, G. Hotton, et al. "Amyloid, Hypometabolism, and Cognition in Alzheimer Disease: An [11C]PIB and [18F]FDG PET Study." *Neurology* 68, no. 7 (February 13, 2007): 501–8. <https://doi.org/10.1212/01.wnl.0000244749.20056.d4>.

88. Li, Yi, Juha O. Rinne, Lisa Mosconi, Elizabeth Pirraglia, Henry Rusinek, Susan DeSanti, Nina Kemppainen, et al. "Regional Analysis of FDG and PIB-PET Images in Normal Aging, Mild Cognitive Impairment, and Alzheimer's Disease." *European Journal of Nuclear Medicine and Molecular Imaging* 35, no. 12 (December 2008): 2169–81. <https://doi.org/10.1007/s00259-008-0833-y>.
89. Chételat, Gaël. "A β -Independent Processes—Rethinking Preclinical AD: Alzheimer Disease." *Nature Reviews Neurology* 9, no. 3 (March 2013): 123–24. <https://doi.org/10.1038/nrneurol.2013.21>.
90. Selkoe, D. J., & Hardy, J. (2016). The amyloid hypothesis of Alzheimer's disease at 25 years. *EMBO Molecular Medicine*. <http://doi.org/10.15252/emmm.201606210>
91. Zotova, Elina, Viraj Bharambe, Matthew Cheaveau, William Morgan, Clive Holmes, Scott Harris, James W. Neal, Seth Love, James A. R. Nicoll, and Delphine Boche. "Inflammatory Components in Human Alzheimer's Disease and after Active Amyloid-B42 Immunization." *Brain* 136, no. 9 (September 2013): 2677–96. <https://doi.org/10.1093/brain/awt210>.
92. Matarin, Mar, Dervis A. Salih, Marina Yasvoina, Damian M. Cummings, Sebastian Guelfi, Wenfei Liu, Muzammil A. Nahaboo Solim, et al. "A Genome-Wide Gene-Expression Analysis and Database in Transgenic Mice during Development of Amyloid or Tau Pathology." *Cell Reports* 10, no. 4 (February 2015): 633–44. <https://doi.org/10.1016/j.celrep.2014.12.041>.
93. Wang, Jun, Lan Tan, Hui-Fu Wang, Chen-Chen Tan, Xiang-Fei Meng, Chong Wang, Shao-Wen Tang, and Jin-Tai Yu. "Anti-Inflammatory Drugs and Risk of Alzheimer's Disease: An Updated Systematic Review and Meta-Analysis." *Journal of Alzheimer's Disease* 44, no. 2 (January 22, 2015): 385–96. <https://doi.org/10.3233/JAD-141506>.
94. European Alzheimer's Disease Initiative (EADI), Genetic and Environmental Risk in Alzheimer's Disease (GERAD), Alzheimer's Disease Genetic Consortium (ADGC), Cohorts for Heart and Aging Research in Genomic Epidemiology (CHARGE), Jean-Charles Lambert, Carla A Ibrahim-Verbaas, Denise Harold, et al. "Meta-Analysis of 74,046 Individuals Identifies 11 New Susceptibility Loci for Alzheimer's Disease." *Nature Genetics* 45, no. 12 (December 2013): 1452–58. <https://doi.org/10.1038/ng.2802>.

95. The Alzheimer's Disease Neuroimaging Initiative, CHARGE consortium, EADI1 consortium, Paul Hollingworth, Denise Harold, Rebecca Sims, Amy Gerrish, et al. "Common Variants at ABCA7, MS4A6A/MS4A4E, EPHA1, CD33 and CD2AP Are Associated with Alzheimer's Disease." *Nature Genetics* 43, no. 5 (May 2011): 429–35. <https://doi.org/10.1038/ng.803>.
96. Naj, Adam C, Gyungah Jun, Gary W Beecham, Li-San Wang, Badri Narayan Vardarajan, Jacqueline Buross, Paul J Gallins, et al. "Common Variants at MS4A4/MS4A6E, CD2AP, CD33 and EPHA1 Are Associated with Late-Onset Alzheimer's Disease." *Nature Genetics* 43, no. 5 (May 2011): 436–41. <https://doi.org/10.1038/ng.801>.
97. Jonsson, T., Stefansson, H., Steinberg, S., Jonsdottir, I., Jonsson, P. V., Snaedal, J., ... Stefansson, K. (2013). Variant of TREM2 associated with the risk of Alzheimer's disease. *The New England Journal of Medicine*. <https://doi.org/10.1056/NEJMoa1211103>
98. Pottier, Cyril, Thomas A. Ravenscroft, Patricia H. Brown, NiCole A. Finch, Matt Baker, Meeia Parsons, Yan W. Asmann, et al. "TYROBP Genetic Variants in Early-Onset Alzheimer's Disease." *Neurobiology of Aging* 48 (December 2016): 222.e9-222.e15. <https://doi.org/10.1016/j.neurobiolaging.2016.07.028>.
99. Harold, Denise, Richard Abraham, Paul Hollingworth, Rebecca Sims, Amy Gerrish, Marian L Hamshere, Jaspreet Singh Pahwa, et al. "Genome-Wide Association Study Identifies Variants at CLU and PICALM Associated with Alzheimer's Disease." *Nature Genetics* 41, no. 10 (October 2009): 1088–93. <https://doi.org/10.1038/ng.440>.
100. The European Alzheimer's Disease Initiative Investigators, Jean-Charles Lambert, Simon Heath, Gael Even, Dominique Campion, Kristel Sleegers, Mikko Hiltunen, et al. "Genome-Wide Association Study Identifies Variants at CLU and CR1 Associated with Alzheimer's Disease." *Nature Genetics* 41, no. 10 (October 2009): 1094–99. <https://doi.org/10.1038/ng.439>.
101. Bolós, Marta, Juan Ramón Perea, and Jesús Avila. "Alzheimer's Disease as an Inflammatory Disease." *Biomolecular Concepts* 8, no. 1 (January 1, 2017). <https://doi.org/10.1515/bmc-2016-0029>.

102. Heneka, M. T., Golenbock, D. T., & Latz, E. (2015). Innate immunity in Alzheimer's disease. *Nat Immunol.* <http://doi.org/10.1038/ni.3102>
103. Zuroff, L., Daley, D., Black, K. L., & Koronyo-Hamaoui, M. (2017). Clearance of cerebral A β in Alzheimer's disease: reassessing the role of microglia and monocytes. *Cellular and Molecular Life Sciences.* <http://doi.org/10.1007/s00018-017-2463-7>
104. Bagyinszky, E., Giau, V. Van, Shim, K., Suk, K., An, S. S. A., & Kim, S. Y. (2017). Role of inflammatory molecules in the Alzheimer's disease progression and diagnosis. *Journal of the Neurological Sciences.* <http://doi.org/10.1016/j.jns.2017.03.031>
105. Hui, C. W., Zhang, Y., & Herrup, K. (2016). Non-Neuronal Cells Are Required to Mediate the Effects of Neuroinflammation: Results from a Neuron-Enriched Culture System. *PLoS ONE.* <http://doi.org/10.1371/journal.pone.0147134>
106. Su, F., Bai, F., Zhou, H., & Zhang, Z. (2016). Microglial toll-like receptors and Alzheimer's disease. *Brain, Behavior, and Immunity.* <http://doi.org/10.1016/j.bbi.2015.10.010>
107. Yogendra, S., Gaurav, G., Birendra, S., Rajiv, D., Juhi, T., Madhu, A., ... Kamal, D. (2017). Calcitonin gene-related peptide (CGRP): A novel target for Alzheimer's disease. *CNS Neuroscience & Therapeutics*, 23(6), 457–461. <http://doi.org/10.1111/cns.12696>
108. Schwartz, M., & Deczkowska, A. (2016). Neurological Disease as a Failure of Brain–Immune Crosstalk: The Multiple Faces of Neuroinflammation. *Trends in Immunology.* <http://doi.org/10.1016/j.it.2016.08.001>
109. Busse, M., Michler, E., Von Hoff, F., Dobrowolny, H., Hartig, R., Frodl, T., & Busse, S. (2017). Alterations in the Peripheral Immune System in Dementia. *Journal of Alzheimer's Disease.* <http://doi.org/10.3233/JAD-161304>
110. Virchow, R. (1856). Phlogose und Thrombose im Gefasssystem. *Gesammelte Abhandlungen Zur Wissenschaftlichen Medicin, Fankfurt.*
111. Lenhossek, M. (1895). Der feinere Bau des Nervensystems im Lichte neuester Forschungen.
112. Navarrete, M., & Araque, A. (2014). The Cajal school and the physiological role of astrocytes: a way of thinking. *Frontiers in Neuroanatomy*, 8, 33. <http://doi.org/10.3389/fnana.2014.00033>
113. Alzheimer, A., & Nissl, F. (1904). Histologische und histopathologische Arbeiten über die Grosshirnrinde: Mit besonderer Berücksichtigung der pathologischen Anatomie der Geisteskrankheiten ... Erster-sechter Band. pp. 401–562. Jena: G. Fischer

114. Alzheimer, A., & Nissl, F. (1904). Histologische und histopathologische Arbeiten über die Grosshirnrinde: Mit besonderer Berücksichtigung der pathologischen Anatomie der Geisteskrankheiten ... Erster-sechster Band. Jena: G. Fischer
115. Robertson, Ford. "A Microscopic Demonstration of the Normal and Pathological Histology of Mesoglia Cells." *Journal of Mental Science* 46, no. 195 (October 1900): 724. <http://doi.org/10.1192/bjp.46.195.724>.
116. Sierra, A., de Castro, F., del Río-Hortega, J., Rafael Iglesias-Rozas, J., Garrosa, M., & Kettenmann, H. (2016). The "Big-Bang" for modern glial biology: Translation and comments on Pío del Río-Hortega 1919 series of papers on microglia. *GLIA*. <http://doi.org/10.1002/glia.23046>
117. Aguzzi, A., Barres, B. A., & Bennett, M. L. (2013). Microglia: Scapegoat, saboteur, or something else? *Science*. <http://doi.org/10.1126/science.1227901>
118. Prinz, M., Erny, D., & Hagemeyer, N. (2017). Ontogeny and homeostasis of CNS myeloid cells. *Nature Immunology*. <http://doi.org/10.1038/ni.3703>
119. Kierdorf, Katrin, Daniel Erny, Tobias Goldmann, Victor Sander, Christian Schulz, Elisa Gomez Perdiguero, Peter Wieghofer, et al. "Microglia Emerge from Erythromyeloid Precursors via Pu.1- and Irf8-Dependent Pathways." *Nature Neuroscience* 16, no. 3 (March 2013): 273–80. <https://doi.org/10.1038/nn.3318>.
120. Alliot, F., Godin, I., & Pessac, B. (1999). Microglia derive from progenitors, originating from the yolk sac, and which proliferate in the brain. *Developmental Brain Research*. [http://doi.org/10.1016/S0165-3806\(99\)00113-3](http://doi.org/10.1016/S0165-3806(99)00113-3)
121. Cunningham, C. L., Martinez-Cerdeno, V., & Noctor, S. C. (2013). Microglia Regulate the Number of Neural Precursor Cells in the Developing Cerebral Cortex. *Journal of Neuroscience*. <http://doi.org/10.1523/JNEUROSCI.3441-12.2013>
122. Ginhoux, F., Lim, S., Hoeffel, G., Low, D., & Huber, T. (2013). Origin and differentiation of microglia. *Frontiers in Cellular Neuroscience*. <http://doi.org/10.3389/fncel.2013.00045>
123. Ginhoux, F., M. Greter, M. Leboeuf, S. Nandi, P. See, S. Gokhan, M. F. Mehler, et al. "Fate Mapping Analysis Reveals That Adult Microglia Derive from Primitive Macrophages." *Science* 330, no. 6005 (November 5, 2010): 841–45. <http://doi.org/10.1126/science.1194637>.

124. Ajami, B., Bennett, J. L., Krieger, C., Tetzlaff, W., & Rossi, F. M. V. (2007). Local self-renewal can sustain CNS microglia maintenance and function throughout adult life. *Nature Neuroscience*. <http://doi.org/10.1038/nn2014>
125. Ransohoff, R. M., & Perry, V. H. (2009). Microglial Physiology: Unique Stimuli, Specialized Responses. *Annual Review of Immunology*. <http://doi.org/10.1146/annurev.immunol.021908.132528>
126. Nimmerjahn, A., Kirchhoff, F., & Helmchen, F. (2005). Neuroscience: Resting microglial cells are highly dynamic surveillants of brain parenchyma in vivo. *Science*. <http://doi.org/10.1126/science.1110647>
127. Oppenheim, R. W. (1991). Cell Death During Development of the Nervous System. *Annual Review of Neuroscience*. <http://doi.org/10.1146/annurev.ne.14.030191.002321>
128. Yeo, W., & Gautier, J. (2004). Early neural cell death: Dying to become neurons. *Dev Biol*. <http://doi.org/10.1016/j.ydbio.2004.07.026>
129. Dailey, M. E., Eyo, U., Fuller, L., Hass, J., & Kurpius, D. (2013). Imaging microglia in brain slices and slice cultures. *Cold Spring Harbor Protocols*. <http://doi.org/10.1101/pdb.prot079483>
130. Dalmau, I., Finsen, B., Zimmer, J., González, B., & Castellano, B. (1998). Development of microglia in the postnatal rat hippocampus. *Hippocampus*. [http://doi.org/10.1002/\(SICI\)1098-1063\(1998\)8:5<458::AID-HIPO6>3.0.CO;2-N](http://doi.org/10.1002/(SICI)1098-1063(1998)8:5<458::AID-HIPO6>3.0.CO;2-N)
131. Sierra, A., Abiega, O., Shahraz, A., & Neumann, H. (2013). Janus-faced microglia: beneficial and detrimental consequences of microglial phagocytosis. *Frontiers in Cellular Neuroscience*. <http://doi.org/10.3389/fncel.2013.00006>
132. Chamak, B., Morandi, V., & Mallat, M. (1994). Brain macrophages stimulate neurite growth and regeneration by secreting thrombospondin. *Journal of Neuroscience Research*. <http://doi.org/10.1002/jnr.490380213>
133. Morgan, S. C., Taylor, D. L., & Pockock, J. M. (2004). Microglia release activators of neuronal proliferation mediated by activation of mitogen-activated protein kinase, phosphatidylinositol-3-kinase/ Akt and delta-Notch signalling cascades. *Journal of Neurochemistry*. <http://doi.org/10.1111/j.1471-4159.2004.02461.x>
134. Antony, J. M., Paquin, A., Nutt, S. L., Kaplan, D. R., & Miller, F. D. (2011). Endogenous microglia regulate development of embryonic cortical precursor cells. *Journal of Neuroscience Research*. <http://doi.org/10.1002/jnr.22533>

135. Ueno, M., Fujita, Y., Tanaka, T., Nakamura, Y., Kikuta, J., Ishii, M., & Yamashita, T. (2013). Layer v cortical neurons require microglial support for survival during postnatal development. *Nature Neuroscience*. <http://doi.org/10.1038/nn.3358>
136. Swinnen, Nina, Sophie Smolders, Ariel Avila, Kristof Notelaers, Rik Paesen, Marcel Ameloot, Bert Brône, Pascal Legendre, and Jean-Michel Rigo. “Complex Invasion Pattern of the Cerebral Cortex By microglial Cells during Development of the Mouse Embryo.” *Glia* 61, no. 2 (February 2013): 150–63. <https://doi.org/10.1002/glia.22421>.
137. Squarzoni, Paola, Guillaume Oller, Guillaume Hoeffel, Lorena Pont-Lezica, Philippe Rostaing, Donovan Low, Alain Bessis, Florent Ginhoux, and Sonia Garel. “Microglia Modulate Wiring of the Embryonic Forebrain.” *Cell Reports* 8, no. 5 (September 2014): 1271–79. <https://doi.org/10.1016/j.celrep.2014.07.042>.
138. Pont-Lezica, L., Béchade, C., Belarif-Cantaut, Y., Pascual, O., & Bessis, A. (2011). Physiological roles of microglia during development. *Journal of Neurochemistry*. <http://doi.org/10.1111/j.1471-4159.2011.07504.x>
139. Hua, J. Y., & Smith, S. J. (2004). Neural activity and the dynamics of central nervous system development. *Nature Neuroscience*. <http://doi.org/10.1038/nn1218>
140. Zhan, Yang, Rosa C Paolicelli, Francesco Sforazzini, Laetitia Weinhard, Giulia Bolasco, Francesca Pagani, Alexei L Vyssotski, et al. “Deficient Neuron-Microglia Signaling Results in Impaired Functional Brain Connectivity and Social Behavior.” *Nature Neuroscience* 17, no. 3 (March 2014): 400–406. <https://doi.org/10.1038/nn.3641>.
141. Schafer, D. P., Lehrman, E. K., Kautzman, A. G., Koyama, R., Mardinly, A. R., Yamasaki, R., ... Stevens, B. (2012). Microglia Sculpt Postnatal Neural Circuits in an Activity and Complement-Dependent Manner. *Neuron*. <http://doi.org/10.1016/j.neuron.2012.03.026>
142. Yamada, J., Hayashi, Y., Jinno, S., Wu, Z., Inoue, K., Kohsaka, S., & Nakanishi, H. (2008). Reduced synaptic activity precedes synaptic stripping in vagal motoneurons after axotomy. *GLIA*. <http://doi.org/10.1002/glia.20711>
143. Šišková, Z., & Tremblay, M. È. (2013). Microglia and synapse: Interactions in health and neurodegeneration. *Neural Plasticity*. <http://doi.org/10.1155/2013/425845>
144. Tremblay, M. È., Lowery, R. L., & Majewska, A. K. (2010). Microglial interactions with synapses are modulated by visual experience. *PLoS Biology*. <http://doi.org/10.1371/journal.pbio.1000527>

145. Paolicelli, R. C., Bisht, K., & Tremblay, M.-È. (2014). Fractalkine regulation of microglial physiology and consequences on the brain and behavior. *Frontiers in Cellular Neuroscience*. <http://doi.org/10.3389/fncel.2014.00129>
146. Stevens, Beth, Nicola J. Allen, Luis E. Vazquez, Gareth R. Howell, Karen S. Christopherson, Navid Nouri, Kristina D. Micheva, et al. "The Classical Complement Cascade Mediates CNS Synapse Elimination." *Cell* 131, no. 6 (December 2007): 1164–78. <https://doi.org/10.1016/j.cell.2007.10.036>.
147. Stephan, A. H., Barres, B. A., & Stevens, B. (2012). The complement system: an unexpected role in synaptic pruning during development and disease. *Annual Review of Neuroscience*. <http://doi.org/10.1146/annurev-neuro-061010-113810>
148. Kolodziejczak, Marta, Catherine Béchade, Nicolas Gervasi, Theano Irinopoulou, Sophie M. Banas, Corinne Cordier, Alexandra Rebsam, Anne Roumier, and Luc Maroteaux. "Serotonin Modulates Developmental Microglia via 5-HT_{2B} Receptors: Potential Implication during Synaptic Refinement of Retinogeniculate Projections." *ACS Chemical Neuroscience* 6, no. 7 (July 15, 2015): 1219–30. <https://doi.org/10.1021/cn5003489>.
149. Lee, Hanmi, Barbara K. Brott, Lowry A. Kirkby, Jaimie D. Adelson, Sarah Cheng, Marla B. Feller, Akash Datwani, and Carla J. Shatz. "Synapse Elimination and Learning Rules Co-Regulated by MHC Class I H2-Db." *Nature* 509, no. 7499 (May 2014): 195–200. <https://doi.org/10.1038/nature13154>.
150. Salter, M. W., & Beggs, S. (2014). Sublime microglia: Expanding roles for the guardians of the CNS. *Cell*. <http://doi.org/10.1016/j.cell.2014.06.008>
151. Tremblay, M.-È., Stevens, B., Sierra, A., Wake, H., Bessis, A., & Nimmerjahn, A. (2011). The role of microglia in the healthy brain. *The Journal of Neuroscience : The Official Journal of the Society for Neuroscience*. <http://doi.org/10.1523/JNEUROSCI.4158-11.2011>
152. Miyamoto, Akiko, Hiroaki Wake, Ayako Wendy Ishikawa, Kei Eto, Keisuke Shibata, Hideji Murakoshi, Schuichi Koizumi, Andrew J. Moorhouse, Yumiko Yoshimura, and Junichi Nabekura. "Microglia Contact Induces Synapse Formation in Developing Somatosensory Cortex." *Nature Communications* 7, no. 1 (December 2016). <https://doi.org/10.1038/ncomms12540>.

153. Lim, So-Hee, Eunha Park, Boram You, Youngseob Jung, A-Reum Park, Sung Goo Park, and Jae-Ran Lee. "Neuronal Synapse Formation Induced by Microglia and Interleukin 10." Edited by Laurent Groc. *PLoS ONE* 8, no. 11 (November 22, 2013): e81218. <https://doi.org/10.1371/journal.pone.0081218>.
154. Parkhurst, Christopher N., Guang Yang, Ipe Ninan, Jeffrey N. Savas, John R. Yates, Juan J. Lafaille, Barbara L. Hempstead, Dan R. Littman, and Wen-Biao Gan. "Microglia Promote Learning-Dependent Synapse Formation through Brain-Derived Neurotrophic Factor." *Cell* 155, no. 7 (December 2013): 1596–1609. <https://doi.org/10.1016/j.cell.2013.11.030>.
155. Hoshiko, M., Arnoux, I., Avignone, E., Yamamoto, N., & Audinat, E. (2012). Deficiency of the microglial receptor CX3CR1 impairs postnatal functional development of thalamocortical synapses in the barrel cortex. *Journal of Neuroscience*. <http://doi.org/10.1523/JNEUROSCI.1167-12.2012>
156. Poon, V. Y., Choi, S., & Park, M. (2013). Growth factors in synaptic function. *Frontiers in Synaptic Neuroscience*. <http://doi.org/10.3389/fnsyn.2013.00006>
157. Stellwagen, D., Beattie, E. C., Seo, J. Y., & Malenka, R. C. (2005). Differential regulation of AMPA receptor and GABA receptor trafficking by tumor necrosis factor-alpha. *The Journal of Neuroscience: The Official Journal of the Society for Neuroscience*. <http://doi.org/10.1523/JNEUROSCI.4486-04.2005>
158. Kawasaki, Y., Zhang, L., Cheng, J.-K., & Ji, R.-R. (2008). Cytokine mechanisms of central sensitization: distinct and overlapping role of interleukin-1beta, interleukin-6, and tumor necrosis factor-alpha in regulating synaptic and neuronal activity in the superficial spinal cord. *Journal of Neuroscience*. <http://doi.org/10.1523/JNEUROSCI.3338-07.2008>
159. Tan, H., Cao, J., Zhang, J., & Zuo, Z. (2014). Critical role of inflammatory cytokines in impairing biochemical processes for learning and memory after surgery in rats. *Journal of Neuroinflammation*. <http://doi.org/10.1186/1742-2094-11-93>
160. Rogers, J. T., J. M. Morganti, A. D. Bachstetter, C. E. Hudson, M. M. Peters, B. A. Grimmig, E. J. Weeber, P. C. Bickford, and C. Gemma. "CX3CR1 Deficiency Leads to Impairment of Hippocampal Cognitive Function and Synaptic Plasticity." *Journal of Neuroscience* 31, no. 45 (November 9, 2011): 16241–50. <https://doi.org/10.1523/JNEUROSCI.3667-11.2011>.
161. Rachal Pugh, C., Fleshner, M., Watkins, L. R., Maier, S. F., & Rudy, J. W. (2001). The immune system and memory consolidation: A role for the cytokine IL-1 β .

162. Pascual, O., Ben Achour, S., Rostaing, P., Triller, A., & Bessis, A. (2012). Microglia activation triggers astrocyte-mediated modulation of excitatory neurotransmission. *Proceedings of the National Academy of Sciences.* <http://doi.org/10.1073/pnas.1111098109>
163. Gomez-Nicola, D., & Perry, V. H. (2015). Microglial dynamics and role in the healthy and diseased brain: A paradigm of functional plasticity. *Neuroscientist.* <http://doi.org/10.1177/1073858414530512>
164. Davalos, Dimitrios, Jaime Grutzendler, Guang Yang, Jiyun V Kim, Yi Zuo, Steffen Jung, Dan R Littman, Michael L Dustin, and Wen-Biao Gan. "ATP Mediates Rapid Microglial Response to Local Brain Injury in Vivo." *Nature Neuroscience* 8, no. 6 (June 2005): 752–58. <https://doi.org/10.1038/nm1472>.
165. Wake, H., A. J. Moorhouse, S. Jinno, S. Kohsaka, and J. Nabekura. "Resting Microglia Directly Monitor the Functional State of Synapses In Vivo and Determine the Fate of Ischemic Terminals." *Journal of Neuroscience* 29, no. 13 (April 1, 2009): 3974–80. <https://doi.org/10.1523/JNEUROSCI.4363-08.2009>.
166. Dissing-Olesen, L., LeDue, J. M., Rungta, R. L., Hefendehl, J. K., Choi, H. B., & MacVicar, B. A. (2014). Activation of Neuronal NMDA Receptors Triggers Transient ATP-Mediated Microglial Process Outgrowth. *Journal of Neuroscience.* <http://doi.org/10.1523/JNEUROSCI.0405-14.2014>
167. Sipe, G. O., Lowery, R. L., Tremblay, M., Kelly, E. A., Lamantia, C. E., & Majewska, A. K. (2016). Microglial P2Y12 is necessary for synaptic plasticity in mouse visual cortex. *Nature Communications.* <http://doi.org/10.1038/ncomms10905>
168. Stephan, A. H., D. V. Madison, J. M. Mateos, D. A. Fraser, E. A. Lovelett, L. Coutellier, L. Kim, et al. "A Dramatic Increase of C1q Protein in the CNS during Normal Aging." *Journal of Neuroscience* 33, no. 33 (August 14, 2013): 13460–74. <https://doi.org/10.1523/JNEUROSCI.1333-13.2013>.
169. Sierra, Amanda, Juan M. Encinas, Juan J.P. Deudero, Jessica H. Chancey, Grigori Enikolopov, Linda S. Overstreet-Wadiche, Stella E. Tsirka, and Mirjana Maletic-Savatic. "Microglia Shape Adult Hippocampal Neurogenesis through Apoptosis-Coupled Phagocytosis." *Cell Stem Cell* 7, no. 4 (October 2010): 483–95. <http://doi.org/10.1016/j.stem.2010.08.014>.

170. Kempermann, G., Jessberger, S., Steiner, B., & Kronenberg, G. (2004). Milestones of neuronal development in the adult hippocampus. *Trends in Neurosciences*. <http://doi.org/10.1016/j.tins.2004.05.013>
171. Kempermann, G. (2008). The neurogenic reserve hypothesis: what is adult hippocampal neurogenesis good for? *Trends in Neurosciences*. <http://doi.org/10.1016/j.tins.2008.01.002>
172. Fourgeaud, Lawrence, Paqui G. Través, Yusuf Tufail, Humberto Leal-Bailey, Erin D. Lew, Patrick G. Burrola, Perri Callaway, et al. "TAM Receptors Regulate Multiple Features of Microglial Physiology." *Nature* 532, no. 7598 (April 2016): 240–44. <https://doi.org/10.1038/nature17630>.
173. Yin, Zhuoran, Divya Raj, Nasrin Saiepour, Debby Van Dam, Nieske Brouwer, Inge R. Holtman, Bart J.L. Eggen, et al. "Immune Hyperreactivity of A β Plaque-Associated Microglia in Alzheimer's Disease." *Neurobiology of Aging* 55 (July 2017): 115–22. <https://doi.org/10.1016/j.neurobiolaging.2017.03.021>.
174. Hanisch, U. K., & Kettenmann, H. (2007). Microglia: Active sensor and versatile effector cells in the normal and pathologic brain. *Nature Neuroscience*. <http://doi.org/10.1038/nn1997>
175. Tang, Y., & Le, W. (2016). Differential Roles of M1 and M2 Microglia in Neurodegenerative Diseases. *Molecular Neurobiology*. <http://doi.org/10.1007/s12035-014-9070-5>
176. Franco, R., & Fernández-Suárez, D. (2015). Alternatively activated microglia and macrophages in the central nervous system. *Progress in Neurobiology*. <http://doi.org/10.1016/j.pneurobio.2015.05.003>
177. Chen, Z., & Trapp, B. D. (2016). Microglia and neuroprotection. *Journal of Neurochemistry*. <http://doi.org/10.1111/jnc.13062>
178. Wolf, S. A., Boddeke, H. W. G. M., & Kettenmann, H. (2017). Microglia in Physiology and Disease. *Annual Review of Physiology*. <http://doi.org/10.1146/annurev-physiol-022516-034406>
179. Perry, V. H., & Holmes, C. (2014). Microglial priming in neurodegenerative disease. *Nature Reviews Neurology*. <http://doi.org/10.1038/nrneurol.2014.38>
180. Norden, D. M., & Godbout, J. P. (2013). Review: Microglia of the aged brain: Primed to be activated and resistant to regulation. *Neuropathology and Applied Neurobiology*. <http://doi.org/10.1111/j.1365-2990.2012.01306.x>

181. Heneka, M. T., Kummer, M. P., & Latz, E. (2014). Innate immune activation in neurodegenerative disease. *Nature Reviews Immunology*. <http://doi.org/10.1038/nri3705>
182. Santoni, G., Cardinali, C., Morelli, B. B., Santoni, M., Nabissi, M., & Amantini, C. (2015). Danger- and pathogen-associated molecular patterns recognition by pattern-recognition receptors and ion channels of the transient receptor potential family triggers the inflammasome activation in immune cells and sensory neurons. *Journal of Neuroinflammation*. <http://doi.org/10.1186/s12974-015-0239-2>
183. Lehnardt, S. (2010). Innate immunity and neuroinflammation in the CNS: The role of microglia in toll-like receptor-mediated neuronal injury. *GLIA*. <http://doi.org/10.1002/glia.20928>
184. Lawson, L. J., Perry, V. H., & Gordon, S. (1992). Turnover of resident microglia in the normal adult mouse brain. *Neuroscience*. [http://doi.org/10.1016/0306-4522\(92\)90500-2](http://doi.org/10.1016/0306-4522(92)90500-2)
185. Long, Jeffrey M, Audrey N Kalehua, Nancy J Muth, Michael E Calhoun, Mathias Jucker, John M Hengemihle, Donald K Ingram, and Peter R Mouton. "Stereological Analysis of Astrocyte and Microglia in Aging Mouse Hippocampus." *Neurobiology of Aging* 19, no. 5 (September 1998): 497–503. [https://doi.org/10.1016/S0197-4580\(98\)00088-8](https://doi.org/10.1016/S0197-4580(98)00088-8).
186. Tremblay, M.-È., Zettel, M. L., Ison, J. R., Allen, P. D., & Majewska, A. K. (2012). Effects of aging and sensory loss on glial cells in mouse visual and auditory cortices. *Glia*. <http://doi.org/10.1002/glia.22287>
187. Streit, W. J., & Xue, Q.-S. (2010). The Brain's Aging Immune System. *Aging Dis*. <http://doi.org/10.1038/nature09191.Pathogenic>
188. Kamphuis, W., Orre, M., Kooijman, L., Dahmen, M., & Hol, E. M. (2012). Differential cell proliferation in the cortex of the APP^{swe}PS1^{dE9} Alzheimer's disease mouse model. *GLIA*. <http://doi.org/10.1002/glia.22295>
189. Jørgensen, M. B., Finsen, B. R., Jensen, M. B., Castellano, B., Diemer, N. H., & Zimmer, J. (1993). Microglial and astroglial reactions to ischemic and kainic acid-induced lesions of the adult rat hippocampus. *Experimental Neurology*. <http://doi.org/10.1006/exnr.1993.1041>
190. Streit, W. J. (2004). Microglia and Alzheimer's disease pathogenesis. *Journal of Neuroscience Research*. <http://doi.org/10.1002/jnr.20093>
191. Itagaki, S., McGeer, P. L., Akiyama, H., Zhu, S., & Selkoe, D. (1989). Relationship of microglia and astrocytes to amyloid deposits of Alzheimer disease. *Journal of Neuroimmunology*. [http://doi.org/10.1016/0165-5728\(89\)90115-X](http://doi.org/10.1016/0165-5728(89)90115-X)

192. Koenigsknecht-Talboo, J., M. Meyer-Luehmann, M. Parsadanian, M. Garcia-Alloza, M. B. Finn, B. T. Hyman, B. J. Bacskai, and D. M. Holtzman. "Rapid Microglial Response Around Amyloid Pathology after Systemic Anti-A Antibody Administration in PDAPP Mice." *Journal of Neuroscience* 28, no. 52 (December 24, 2008): 14156–64. <https://doi.org/10.1523/JNEUROSCI.4147-08.2008>.
193. Damani, M. R., Zhao, L., Fontainhas, A. M., Amaral, J., Fariss, R. N., & Wong, W. T. (2011). Age-related alterations in the dynamic behavior of microglia. *Aging Cell*. <http://doi.org/10.1111/j.1474-9726.2010.00660.x>
194. Hefendehl, J. K., Neher, J. J., Sühs, R. B., Kohsaka, S., Skodras, A., & Jucker, M. (2014). Homeostatic and injury-induced microglia behavior in the aging brain. *Aging Cell*. <http://doi.org/10.1111/acer.12149>
195. Orre, Marie, Willem Kamphuis, Lana M. Osborn, Jeroen Melief, Lieneke Kooijman, Inge Huitinga, Jan Klooster, Koen Bossers, and Elly M. Hol. "Acute Isolation and Transcriptome Characterization of Cortical Astrocytes and Microglia from Young and Aged Mice." *Neurobiology of Aging* 35, no. 1 (January 2014): 1–14. <https://doi.org/10.1016/j.neurobiolaging.2013.07.008>.
196. McLarnon, James G. "Microglial Chemotactic Signaling Factors in Alzheimer's Disease." *American Journal of Neurodegenerative Disease* 1, no. 3 (2012): 199–204.
197. Rogers, J., & Lue, L. F. (2001). Microglial chemotaxis, activation, and phagocytosis of amyloid β -peptide as linked phenomena in Alzheimer's disease. *Neurochemistry International*. [http://doi.org/10.1016/S0197-0186\(01\)00040-7](http://doi.org/10.1016/S0197-0186(01)00040-7)
198. Ryu, J. K., T. Cho, H. B. Choi, Y. T. Wang, and J. G. McLarnon. "Microglial VEGF Receptor Response Is an Integral Chemotactic Component in Alzheimer's Disease Pathology." *Journal of Neuroscience* 29, no. 1 (January 7, 2009): 3–13. <https://doi.org/10.1523/JNEUROSCI.2888-08.2009>.
199. Yates, Stephen L., Loyd H. Burgess, June Kocsis-Angle, Joyce M. Antal, Michael D. Dority, Paula B. Embury, Anthony M. Piotrkowski, and Kurt R. Brunden. "Amyloid β and Amylin Fibrils Induce Increases in Proinflammatory Cytokine and Chemokine Production by THP-1 Cells and Murine Microglia." *Journal of Neurochemistry* 74, no. 3 (March 2000): 1017–25. <https://doi.org/10.1046/j.1471-4159.2000.0741017.x>.

200. Vaughan, D. W., and A. Peters. "Neuroglial Cells in the Cerebral Cortex of Rats from Young Adulthood to Old Age: An Electron Microscope Study." *Journal of Neurocytology* 3, no. 4 (October 1974): 405–29.
201. Krabbe, Grietje, Annett Halle, Vitali Matyash, Jan L. Rinnenthal, Gina D. Eom, Ulrike Bernhardt, Kelly R. Miller, Stefan Prokop, Helmut Kettenmann, and Frank L. Heppner. "Functional Impairment of Microglia Coincides with Beta-Amyloid Deposition in Mice with Alzheimer-Like Pathology." Edited by Josef Priller. *PLoS ONE* 8, no. 4 (April 8, 2013): e60921. <https://doi.org/10.1371/journal.pone.0060921>.
202. Solito, E., & Sastre, M. (2012). Microglia function in Alzheimer's disease. *Frontiers in Pharmacology*. <http://doi.org/10.3389/fphar.2012.00014>
203. Hickman, S. E., Allison, E. K., & El Khoury, J. (2008). Microglial dysfunction and defective-amyloid clearance pathways in aging Alzheimer's disease mice. *Journal of Neuroscience*. <http://doi.org/10.1523/JNEUROSCI.0616-08.2008>
204. Taylor, R. C., & Dillin, A. (2011). Aging as an event of proteostasis collapse. *Cold Spring Harbor Perspectives in Biology*. <http://doi.org/10.1101/cshperspect.a004440>
205. Prokop, S., Miller, K. R., & Heppner, F. L. (2013). Microglia actions in Alzheimer's disease. *Acta Neuropathologica*. <http://doi.org/10.1007/s00401-013-1182-x>
206. Heppner, F. L., Ransohoff, R. M., & Becher, B. (2015). Immune attack: The role of inflammation in Alzheimer disease. *Nature Reviews Neuroscience*. <http://doi.org/10.1038/nrn3880>
207. Zhang, Bin, Chris Gaiteri, Liviu-Gabriel Bodea, Zhi Wang, Joshua McElwee, Alexei A. Podtelezhnikov, Chunsheng Zhang, et al. "Integrated Systems Approach Identifies Genetic Nodes and Networks in Late-Onset Alzheimer's Disease." *Cell* 153, no. 3 (April 2013): 707–20. <https://doi.org/10.1016/j.cell.2013.03.030>.
208. McEwen, B. S., & Seeman, T. (1999). Protective and damaging effects of mediators of stress. Elaborating and testing the concepts of allostasis and allostatic load. In *Annals of the New York Academy of Sciences*. <http://doi.org/10.1111/j.1749-6632.1999.tb08103.x>
209. McCormick, C. M., & Hodges, T. E. (2017). Stress, Glucocorticoids, and Brain Development in Rodent Models. In *Stress: Neuroendocrinology and Neurobiology*. <http://doi.org/10.1016/B978-0-12-802175-0.00019-X>
210. Liu, Y.-Z., Wang, Y.-X., & Jiang, C.-L. (2017). Inflammation: the common pathway of stress-related diseases. *Frontiers in Human Neuroscience*. <http://doi.org/10.3389/fnhum.2017.00316>

211. Smith, S. M., & Vale, W. W. (2006). The role of the hypothalamic-pituitary-adrenal axis in neuroendocrine responses to stress. *Dialogues in Clinical Neuroscience*. <http://doi.org/10.1038/nrendo.2011.222>
212. Scheuer, D. A. (2010). Adrenal corticosteroid effects in the central nervous system on long-term control of blood pressure. *Experimental Physiology*. <http://doi.org/10.1113/expphysiol.2008.045484>
213. Sierra, A., Gottfried-Blackmore, A., Milner, T. A., McEwen, B. S., & Bulloch, K. (2008). Steroid hormone receptor expression and function in microglia. *GLIA*. <http://doi.org/10.1002/glia.20644>
214. Vyas, S., Rodrigues, A. J., Silva, J. M., Tronche, F., Almeida, O. F. X., Sousa, N., & Sotiropoulos, I. (2016). Chronic stress and glucocorticoids: From neuronal plasticity to neurodegeneration. *Neural Plasticity*. <http://doi.org/10.1155/2016/6391686>
215. Sapolsky, R. M., Krey, L. C., & McEwen, B. S. (1985). Prolonged glucocorticoid exposure reduces hippocampal neuron number: implications for aging. *Journal of Neuroscience*. <http://doi.org/10.1016/j.cmet.2007.09.011>
216. Green, K. N., Billings, L. M., Roozendaal, B., McGaugh, J. L., & LaFerla, F. M. (2006). Glucocorticoids increase amyloid β and tau pathology in a mouse model of Alzheimer's disease. *Journal of Neuroscience*. <http://doi.org/10.1523/JNEUROSCI.2797-06.2006>
217. Swaab, D. F., Raadsheer, F. C., Endert, E., Hofman, M. A., Kamphorst, W., & Ravid, R. (1994). Increased Cortisol Levels in Aging and Alzheimer's Disease in Postmortem Cerebrospinal Fluid. *Journal of Neuroendocrinology*. <http://doi.org/10.1111/j.1365-2826.1994.tb00635.x>
218. Ownby, R. L., Crocco, E., Acevedo, A., John, V., & Loewenstein, D. (2006). Depression and risk for Alzheimer disease: Systematic review, meta-analysis, and metaregression analysis. *Archives of General Psychiatry*. <http://doi.org/10.1001/archpsyc.63.5.530>
219. Devi, L., Alldred, M. J., Ginsberg, S. D., & Ohno, M. (2010). Sex- and brain region-specific acceleration of β -amyloidogenesis following behavioral stress in a mouse model of Alzheimer's disease. *Molecular Brain*. <http://doi.org/10.1186/1756-6606-3-34>
220. Huang, H.-J., Liang, K.-C., Ke, H.-C., Chang, Y.-Y., & Hsieh-Li, H. M. (2011). Long-term social isolation exacerbates the impairment of spatial working memory in APP/PS1 transgenic mice. *Brain Research*, 1371, 150–160. <http://doi.org/https://doi.org/10.1016/j.brainres.2010.11.043>

221. Rothman, Sarah M., Nathan Herdener, Simonetta Camandola, Sarah J. Texel, Mohamed R. Mughal, Wei-Na Cong, Bronwen Martin, and Mark P. Mattson. “3xTgAD Mice Exhibit Altered Behavior and Elevated A β after Chronic Mild Social Stress.” *Neurobiology of Aging* 33, no. 4 (April 2012): 830.e1-830.e12. <https://doi.org/10.1016/j.neurobiolaging.2011.07.005>.
222. Santos, L. E., Beckman, D., & Ferreira, S. T. (2016). Microglial dysfunction connects depression and Alzheimer’s disease. *Brain, Behavior, and Immunity*. <https://doi.org/10.1016/j.bbi.2015.11.011>
223. Milior, Giampaolo, Cynthia Lecours, Louis Samson, Kanchan Bisht, Silvia Poggini, Francesca Pagani, Cristina Deflorio, et al. “Fractalkine Receptor Deficiency Impairs Microglial and Neuronal Responsiveness to Chronic Stress.” *Brain, Behavior, and Immunity* 55 (July 2016): 114–25. <https://doi.org/10.1016/j.bbi.2015.07.024>.
224. McKim, D B, M D Weber, A Niraula, C M Sawicki, X Liu, B L Jarrett, K Ramirez-Chan, et al. “Microglial Recruitment of IL-1 β -Producing Monocytes to Brain Endothelium Causes Stress-Induced Anxiety.” *Molecular Psychiatry* 23, no. 6 (June 2018): 1421–31. <https://doi.org/10.1038/mp.2017.64>.
225. Hinwood, M., Morandini, J., Day, T. A., & Walker, F. R. (2012). Evidence that microglia mediate the neurobiological effects of chronic psychological stress on the medial prefrontal cortex. *Cerebral Cortex*. <http://doi.org/10.1093/cercor/bhr229>
226. Heneka, Michael T, Monica J Carson, Joseph El Khoury, Gary E Landreth, Frederic Brosseron, Douglas L Feinstein, Andreas H Jacobs, et al. “Neuroinflammation in Alzheimer’s Disease.” *The Lancet Neurology* 14, no. 4 (April 2015): 388–405. [https://doi.org/10.1016/S1474-4422\(15\)70016-5](https://doi.org/10.1016/S1474-4422(15)70016-5).
227. Herrup, Karl. “The Case for Rejecting the Amyloid Cascade Hypothesis.” *Nature Neuroscience* 18, no. 6 (June 2015): 794–99. <https://doi.org/10.1038/nn.4017>.
228. Klunk, William E., Brian J. Bacsikai, Chester A. Mathis, Stephen T. Kajdasz, Megan E. McLellan, Matthew P. Frosch, Manik L. Debnath, Daniel P. Holt, Yanming Wang, and Bradley T. Hyman. “Imaging A β Plaques in Living Transgenic Mice with Multiphoton Microscopy and Methoxy-X04, a Systemically Administered Congo Red Derivative.” *Journal of Neuropathology & Experimental Neurology* 61, no. 9 (September 2002): 797–805. <https://doi.org/10.1093/jnen/61.9.797>.

229. Liebscher, S., & Meyer-Luehmann, M. (2012). A peephole into the brain: Neuropathological features of Alzheimer's disease revealed by in vivo two-photon imaging. *Frontiers in Psychiatry*. <http://doi.org/10.3389/fpsy.2012.00026>
230. Fuhrmann, Martin, Tobias Bittner, Christian K E Jung, Steffen Burgold, Richard M Page, Gerda Mitteregger, Christian Haass, Frank M LaFerla, Hans Kretzschmar, and Jochen Herms. "Microglial Cx3cr1 Knockout Prevents Neuron Loss in a Mouse Model of Alzheimer's Disease." *Nature Neuroscience* 13, no. 4 (April 2010): 411–13. <https://doi.org/10.1038/nn.2511>.
231. Ly, P. T. T., Cai, F., & Song, W. (2011). Detection of neuritic plaques in Alzheimer's disease mouse model. *Journal of Visualized Experiments : JoVE*. <http://doi.org/10.3791/2831>
232. Sadowski, Marcin, Joanna Pankiewicz, Henrieta Scholtzova, Julia Tsai, Yongsheng Li, Richard I. Carp, Harry C. Meeker, et al. "Targeting Prion Amyloid Deposits In Vivo." *Journal of Neuropathology & Experimental Neurology* 63, no. 7 (July 2004): 775–84. <https://doi.org/10.1093/jnen/63.7.775>.
233. Bussière, T., Bard, F., Barbour, R., Grajeda, H., Guido, T., Khan, K., ... Buttini, M. (2004). Morphological characterization of Thioflavin-S-positive amyloid plaques in transgenic Alzheimer mice and effect of passive A β immunotherapy on their clearance. *American Journal of Pathology*. [http://doi.org/10.1016/S0002-9440\(10\)63360-3](http://doi.org/10.1016/S0002-9440(10)63360-3)
234. Rajamohamedsait, H. B., & Sigurdsson, E. M. (2012). Histological staining of amyloid and pre-amyloid peptides and proteins in mouse tissue. *Methods in Molecular Biology*. http://doi.org/10.1007/978-1-61779-551-0_28
235. Afkhami, A., & Moosavi, R. (2010). Adsorptive removal of Congo red, a carcinogenic textile dye, from aqueous solutions by maghemite nanoparticles. *Journal of Hazardous Materials*. <http://doi.org/10.1016/j.jhazmat.2009.09.066>
236. Tremblay, M.-E., Riad, M., & Majewska, A. (2010). Preparation of mouse brain tissue for immunoelectron microscopy. *Journal of Visualized Experiments : JoVE*. <http://doi.org/10.3791/2021>
237. Paxinos, G., & Franklin, K. B. J. (2004). *The mouse brain in stereotaxic coordinates*. Academic Press. [http://doi.org/10.1016/S0306-4530\(03\)00088-X](http://doi.org/10.1016/S0306-4530(03)00088-X)
238. Norden, Diana M., Megan M. Muccigrosso, and Jonathan P. Godbout. "Microglial Priming and Enhanced Reactivity to Secondary Insult in Aging, and Traumatic CNS Injury, and Neurodegenerative Disease." *Neuropharmacology* 96 (September 2015): 29–41. <https://doi.org/10.1016/j.neuropharm.2014.10.028>.

239. DeKosky, S. T., Scheff, S. W., & Styren, S. D. (1996). Structural correlates of cognition in dementia: quantification and assessment of synapse change. *Neurodegeneration*. <http://doi.org/10.1006/neur.1996.0056>
240. Prince, M., Comas-Herrera, A., Knapp, M., Guerchet, M., & Karagiannidou, M. (2016). World Alzheimer Report 2016 Improving healthcare for people living with dementia. Coverage, Quality and costs now and in the future. *Alzheimer's Disease International (ADI)*. <http://doi.org/10.13140/RG.2.2.22580.04483>
241. Šišková, Zuzana, Daniel Justus, Hiroshi Kaneko, Detlef Friedrichs, Niklas Henneberg, Tatjana Beutel, Julika Pitsch, et al. "Dendritic Structural Degeneration Is Functionally Linked to Cellular Hyperexcitability in a Mouse Model of Alzheimer's Disease." *Neuron* 84, no. 5 (December 2014): 1023–33. <https://doi.org/10.1016/j.neuron.2014.10.024>.
242. O'Sullivan, Mike, Elmar Ngo, Anand Viswanathan, Eric Jouvent, Andreas Gschwendtner, Philipp G. Saemann, Marco Duering, et al. "Hippocampal Volume Is an Independent Predictor of Cognitive Performance in CADASIL." *Neurobiology of Aging* 30, no. 6 (June 2009): 890–97. <https://doi.org/10.1016/j.neurobiolaging.2007.09.002>.
243. Mega, M. S., Small, G. W., Xu, M. L., Felix, J., Manese, M., Tran, N. P., ... Toga, A. W. (2002). Hippocampal atrophy in persons with age-associated memory impairment: Volumetry within a common space. *Psychosomatic Medicine*. <http://doi.org/10.1097/00006842-200205000-00013>
244. Schuitemaker, Alie, Marc A. Kropholler, Ronald Boellaard, Wiesje M. van der Flier, Reina W. Kloet, Thalia F. van der Doef, Dirk L. Knol, et al. "Microglial Activation in Alzheimer's Disease: An (R)-[11C]PK11195 Positron Emission Tomography Study." *Neurobiology of Aging* 34, no. 1 (January 2013): 128–36. <https://doi.org/10.1016/j.neurobiolaging.2012.04.021>.
245. Mucke, L., & Selkoe, D. J. (2012). Neurotoxicity of Amyloid β -Protein: Synaptic and Network Dysfunction. *Cold Spring Harbor Perspectives in Medicine*, 2(7), a006338. <http://doi.org/10.1101/cshperspect.a006338>
246. Ferreira, S. T., Lourenco, M. V., Oliveira, M. M., & De Felice, F. G. (2015). Soluble amyloid- β oligomers as synaptotoxins leading to cognitive impairment in Alzheimer's disease. *Frontiers in Cellular Neuroscience*. <http://doi.org/10.3389/fncel.2015.00191>

247. Selkoe, Dennis J. “Soluble Oligomers of the Amyloid β -Protein Impair Synaptic Plasticity and Behavior.” *Behavioural Brain Research* 192, no. 1 (September 2008): 106–13. <https://doi.org/10.1016/j.bbr.2008.02.016>.
248. Cummings, B. J., Su, J. H., Geddes, J. W., Van Nostrand, W. E., Wagner, S. L., Cunningham, D. D., & Cotman, C. W. (1992). Aggregation of the amyloid precursor protein within degenerating neurons and dystrophic neurites in Alzheimer’s disease. *Neuroscience*. [http://doi.org/10.1016/0306-4522\(92\)90265](http://doi.org/10.1016/0306-4522(92)90265)
249. Adalbert, Robert, Antal Nogradi, Elisabetta Babetto, Lucie Janeckova, Simon A. Walker, Martin Kerschensteiner, Thomas Misgeld, and Michael P. Coleman. “Severely Dystrophic Axons at Amyloid Plaques Remain Continuous and Connected to Viable Cell Bodies.” *Brain* 132, no. 2 (February 2009): 402–16. <https://doi.org/10.1093/brain/awn312>.
250. Griciuc, Ana, Alberto Serrano-Pozo, Antonio R. Parrado, Andrea N. Lesinski, Caroline N. Asselin, Kristina Mullin, Basavaraj Hooli, Se Hoon Choi, Bradley T. Hyman, and Rudolph E. Tanzi. “Alzheimer’s Disease Risk Gene CD33 Inhibits Microglial Uptake of Amyloid Beta.” *Neuron* 78, no. 4 (May 2013): 631–43. <https://doi.org/10.1016/j.neuron.2013.04.014>.
251. Doens, D., & Fernández, P. L. (2014). Microglia receptors and their implications in the response to amyloid β for Alzheimer’s disease pathogenesis. *Journal of Neuroinflammation*. <http://doi.org/10.1186/1742-2094-11-48>
252. Meda, Lucia, Marco A. Cassatella, Gyorgyi I. Szendrei, Laszlo Otvos, Pierluigi Baron, Martin Villalba, Davide Ferrari, and Filippo Rossi. “Activation of Microglial Cells by β -Amyloid Protein and Interferon- γ .” *Nature* 374, no. 6523 (April 1995): 647–50. <https://doi.org/10.1038/374647a0>.
253. Tan, J. “Microglial Activation Resulting from CD40-CD40L Interaction After - Amyloid Stimulation.” *Science* 286, no. 5448 (December 17, 1999): 2352–55. <https://doi.org/10.1126/science.286.5448.2352>.
254. Hong, S., V. F. Beja-Glasser, B. M. Nfonoyim, A. Frouin, S. Li, S. Ramakrishnan, K. M. Merry, et al. “Complement and Microglia Mediate Early Synapse Loss in Alzheimer Mouse Models.” *Science* 352, no. 6286 (May 6, 2016): 712–16. <https://doi.org/10.1126/science.aad8373>.

255. El Khoury, Joseph B., Kathryn J. Moore, Terry K. Means, Josephine Leung, Kinya Terada, Michelle Toft, Mason W. Freeman, and Andrew D. Luster. "CD36 Mediates the Innate Host Response to β -Amyloid." *The Journal of Experimental Medicine* 197, no. 12 (June 16, 2003): 1657–66. <https://doi.org/10.1084/jem.20021546>.
256. Zhao, R., Hu, W., Tsai, J., Li, W., & Gan, W.-B. (2017). Microglia limit the expansion of β -amyloid plaques in a mouse model of Alzheimer's disease. *Molecular Neurodegeneration*, 12(1), 47. <http://doi.org/10.1186/s13024-017-0188-6>
257. Wang, Yaming, Tyler K. Ulland, Jason D. Ulrich, Wilbur Song, John A. Tzaferis, Justin T. Hole, Peng Yuan, et al. "TREM2-Mediated Early Microglial Response Limits Diffusion and Toxicity of Amyloid Plaques." *The Journal of Experimental Medicine* 213, no. 5 (May 2, 2016): 667–75. <https://doi.org/10.1084/jem.20151948>.
258. Wildsmith, Kristin R, Monica Holley, Julie C Savage, Rebecca Skerrett, and Gary E Landreth. "Evidence for Impaired Amyloid β Clearance in Alzheimer's Disease." *Alzheimer's Research & Therapy* 5, no. 4 (2013): 33. <https://doi.org/10.1186/alzrt187>.
259. Elali, A., & Rivest, S. (2013). The role of ABCB1 and ABCA1 in beta-amyloid clearance at the neurovascular unit in Alzheimer's disease. *Frontiers in Physiology*. <http://doi.org/10.3389/fphys.2013.00045>
260. Ries, M., & Sastre, M. (2016). Mechanisms of A β clearance and degradation by glial cells. *Frontiers in Aging Neuroscience*. <http://doi.org/10.3389/fnagi.2016.00160>
261. Gosselin, David, Verena M. Link, Casey E. Romanoski, Gregory J. Fonseca, Dawn Z. Eichenfield, Nathanael J. Spann, Joshua D. Stender, et al. "Environment Drives Selection and Function of Enhancers Controlling Tissue-Specific Macrophage Identities." *Cell* 159, no. 6 (December 2014): 1327–40. <https://doi.org/10.1016/j.cell.2014.11.023>.
262. Gosselin, David, Dylan Skola, Nicole G. Coufal, Inge R. Holtman, Johannes C. M. Schlachetzki, Eniko Sajti, Baptiste N. Jaeger, et al. "An Environment-Dependent Transcriptional Network Specifies Human Microglia Identity." *Science* 356, no. 6344 (June 23, 2017): eaal3222. <https://doi.org/10.1126/science.aal3222>.
263. Bisht, K., Sharma, K., & Tremblay, M.-È. (2018). Chronic stress as a risk factor for Alzheimer's disease: Roles of microglia-mediated synaptic remodeling, inflammation, and oxidative stress. *Neurobiology of Stress*. <http://doi.org/10.1016/j.ynstr.2018.05.003>

264. Keren-Shaul, Hadas, Amit Spinrad, Assaf Weiner, Orit Matcovitch-Natan, Raz Dvir-Szternfeld, Tyler K. Ulland, Eyal David, et al. "A Unique Microglia Type Associated with Restricting Development of Alzheimer's Disease." *Cell* 169, no. 7 (June 2017): 1276-1290.e17. <https://doi.org/10.1016/j.cell.2017.05.018>.
265. Krasemann, Susanne, Charlotte Madore, Ron Cialic, Caroline Baufeld, Narghes Calcagno, Rachid El Fatimy, Lien Beckers, et al. "The TREM2-APOE Pathway Drives the Transcriptional Phenotype of Dysfunctional Microglia in Neurodegenerative Diseases." *Immunity* 47, no. 3 (September 2017): 566-581.e9. <https://doi.org/10.1016/j.immuni.2017.08.008>.
266. Mathys, Hansruedi, Chinnakkaruppan Adaikkan, Fan Gao, Jennie Z. Young, Elodie Manet, Martin Hemberg, Philip L. De Jager, Richard M. Ransohoff, Aviv Regev, and Li-Huei Tsai. "Temporal Tracking of Microglia Activation in Neurodegeneration at Single-Cell Resolution." *Cell Reports* 21, no. 2 (October 2017): 366–80. <https://doi.org/10.1016/j.celrep.2017.09.039>.
267. Hsieh, C. L., Koike, M., Spusta, S. C., Niemi, E. C., Yenari, M., Nakamura, M. C., & Seaman, W. E. (2009). A role for TREM2 ligands in the phagocytosis of apoptotic neuronal cells by microglia. *Journal of Neurochemistry*. <http://doi.org/10.1111/j.1471-4159.2009.06042.x>
268. Bisht, Kanchan, Kaushik P. Sharma, Cynthia Lecours, Maria Gabriela Sánchez, Hassan El Hajj, Giampaolo Miliore, Adrián Olmos-Alonso, et al. "Dark Microglia: A New Phenotype Predominantly Associated with Pathological States: A New Microglial Phenotype." *Glia* 64, no. 5 (May 2016): 826–39. <https://doi.org/10.1002/glia.22966>.
269. Puoliväli, J., Wang, J., Heikkinen, T., Heikkilä, M., Tapiola, T., van Groen, T., & Tanila, H. (2002). Hippocampal A beta 42 levels correlate with spatial memory deficit in APP and PS1 double transgenic mice. *Neurobiology of Disease*. <http://doi.org/10.1006/nbdi.2002.0481>
270. Malm, T., Koistinaho, J., & Kanninen, K. (2011). Utilization of APP^{swe}/PS1^{dE9} transgenic mice in research of Alzheimer's disease: Focus on gene therapy and cell-based therapy applications. *International Journal of Alzheimer's Disease*. <http://doi.org/10.4061/2011/517160>
271. Bisht, K., El Hajj, H., Savage, J. C., Sánchez, M. G., & Tremblay, M.-È. (2016). Correlative light and electron microscopy to study microglial interactions with β -Amyloid Plaques. *Journal of Visualized Experiments*. <http://doi.org/10.3791/54060>
272. Tremblay, M. È., Marker, D. F., Puccini, J. M., Muly, E. C., Lu, S. M., & Gelbard, H. A. (2013). Ultrastructure of microglia-synapse interactions in the HIV-1 Tat-injected

- murine central nervous system. *Communicative and Integrative Biology*. <http://doi.org/10.4161/cib.27670>
273. Simard, A. R., Soulet, D., Gowing, G., Julien, J. P., & Rivest, S. (2006). Bone marrow-derived microglia play a critical role in restricting senile plaque formation in Alzheimer's disease. *Neuron*. <http://doi.org/10.1016/j.neuron.2006.01.022>
274. Duve, Christian de. "The Lysosome Concept." In *Novartis Foundation Symposia*, edited by A. V. S. de Reuck and Margrate P. Cameron, 1–35. Chichester, UK: John Wiley & Sons, Ltd, 1963. <https://doi.org/10.1002/9780470715314.ch1>.
275. Holtzman, E., Novikoff, A. B., & Villaverde, H. (1967). Lysosomes and GERL in normal and chromatolytic neurons of the rat ganglion nodosum. *The Journal of Cell Biology*. <http://doi.org/10.1083/jcb.33.2.419>
276. Nandy, K. (1971). Properties of neuronal lipofuscin pigment in mice. *Acta Neuropathologica*. <http://doi.org/10.1007/BF00690951>
277. Perlmutter, L. S., Barron, E., & Chui, H. C. (1990). Morphologic association between microglia and senile plaque amyloid in Alzheimer's disease. *Neuroscience Letters*. [http://doi.org/10.1016/0304-3940\(90\)90748-X](http://doi.org/10.1016/0304-3940(90)90748-X)
278. Chavez-Valdez, R., Flock, D. L., Martin, L. J., & Northington, F. J. (2016). Endoplasmic reticulum pathology and stress response in neurons precede programmed necrosis after neonatal hypoxia-ischemia. *International Journal of Developmental Neuroscience*. <http://doi.org/10.1016/j.ijdevneu.2015.11.007>
279. Haka, A. S., Barbosa-Lorenzi, V. C., Lee, H. J., Falcone, D. J., Hudis, C. A., Dannenberg, A. J., & Maxfield, F. R. (2016). Exocytosis of macrophage lysosomes leads to digestion of apoptotic adipocytes and foam cell formation. *Journal of Lipid Research*. <http://doi.org/10.1194/jlr.M064089>
280. Peters A, Palay SL, Webster H. 1991. The fine structure of the nervous system: the neurons and supporting cells. Philadelphia: W.B. Saunders
281. Savage, J. C., Picard, K., González-Ibáñez, F., & Tremblay, M.-È. (2018). A brief history of microglial ultrastructure: Distinctive features, phenotypes, and functions discovered over the past 60 years by electron microscopy. *Frontiers in Immunology*. <http://doi.org/10.3389/fimmu.2018.00803>
282. Koenigsknecht-Talboo, J., Meyer-Luehmann, M., Parsadanian, M., Garcia-Alloza, M., Finn, M. B., Hyman, B. T., ... Holtzman, D. M. (2008). Rapid microglial response around amyloid pathology after systemic anti-A antibody administration in PDAPP mice. *Journal of Neuroscience*. <http://doi.org/10.1523/JNEUROSCI.4147-08.2008>

283. Conner, S. D., & Schmid, S. L. (2003). Regulated portals of entry into the cell. *Nature*. <http://doi.org/10.1038/nature01451>
284. Ohsawa, K., Y. Imai, H. Kanazawa, Y. Sasaki, and S. Kohsaka. "Involvement of Iba1 in Membrane Ruffling and Phagocytosis of Macrophages/Microglia." *Journal of Cell Science* 113 (Pt 17) (September 2000): 3073–84.
285. Kanazawa, H., Ohsawa, K., Sasaki, Y., Kohsaka, S., & Imai, Y. (2002). Macrophage/microglia-specific protein Iba1 enhances membrane ruffling and Rac activation via phospholipase C- β -dependent pathway. *Journal of Biological Chemistry*. <http://doi.org/10.1074/jbc.M109218200>
286. Eyo, Ukpong B., Mingshu Mo, Min-Hee Yi, Madhuvika Murugan, Junting Liu, Rohan Yarlagadda, David J. Margolis, Pingyi Xu, and Long-Jun Wu. "P2Y12R-Dependent Translocation Mechanisms Gate the Changing Microglial Landscape." *Cell Reports* 23, no. 4 (April 2018): 959–66. <https://doi.org/10.1016/j.celrep.2018.04.001>.
287. Sasaki, Shoichi. "Endoplasmic Reticulum Stress in Motor Neurons of the Spinal Cord in Sporadic Amyotrophic Lateral Sclerosis." *Journal of Neuropathology & Experimental Neurology* 69, no. 4 (April 2010): 346–55. <https://doi.org/10.1097/NEN.0b013e3181d44992>.
288. <http://doi.org/10.1097/NEN.0b013e3181d44992>Li, J. Q., Yu, J. T., Jiang, T., & Tan, L. (2015). Endoplasmic reticulum dysfunction in Alzheimer's disease. *Molecular Neurobiology*. <http://doi.org/10.1007/s12035-014-8695-8>
289. Sanchez-Varo, R., Trujillo-Estrada, L., Sanchez-Mejias, E., Torres, M., Baglietto-Vargas, D., Moreno-Gonzalez, I., ... Gutierrez, A. (2012). Abnormal accumulation of autophagic vesicles correlates with axonal and synaptic pathology in young Alzheimer's mice hippocampus. *Acta Neuropathologica*. <http://doi.org/10.1007/s00401-011-0896-x>
290. Nixon, R. A. (2007). Autophagy, amyloidogenesis and Alzheimer disease. *Journal of Cell Science*. <http://doi.org/10.1242/jcs.019265>
291. Nixon, R. A., Wegiel, J., Kumar, A., Yu, W. H., Peterhoff, C., Cataldo, A., & Cuervo, A. M. (2005). Extensive involvement of autophagy in Alzheimer disease: An immunoelectron microscopy study. *Journal of Neuropathology and Experimental Neurology*. <http://doi.org/10.1093/jnen/64.2.113>
292. Nixon, R. A., & Yang, D. S. (2011). Autophagy failure in Alzheimer's disease-locating the primary defect. *Neurobiology of Disease*. <http://doi.org/10.1016/j.nbd.2011.01.021>

293. Ransohoff, Richard M., and Joseph El Khoury. "Microglia in Health and Disease." *Cold Spring Harbor Perspectives in Biology* 8, no. 1 (January 2016): a020560. <https://doi.org/10.1101/cshperspect.a020560>.
294. Nestor, Peter J., Tim D. Fryer, and John R. Hodges. "Declarative Memory Impairments in Alzheimer's Disease and Semantic Dementia." *NeuroImage* 30, no. 3 (April 2006): 1010–20. <https://doi.org/10.1016/j.neuroimage.2005.10.008>.
295. Palop, Jorge J., Jeannie Chin, Erik D. Roberson, Jun Wang, Myo T. Thwin, Nga Bien-Ly, Jong Yoo, et al. "Aberrant Excitatory Neuronal Activity and Compensatory Remodeling of Inhibitory Hippocampal Circuits in Mouse Models of Alzheimer's Disease." *Neuron* 55, no. 5 (September 2007): 697–711. <https://doi.org/10.1016/j.neuron.2007.07.025>.
296. Sperling, Reisa A., Paul S. Aisen, Laurel A. Beckett, David A. Bennett, Suzanne Craft, Anne M. Fagan, Takeshi Iwatsubo, et al. "Toward Defining the Preclinical Stages of Alzheimer's Disease: Recommendations from the National Institute on Aging-Alzheimer's Association Workgroups on Diagnostic Guidelines for Alzheimer's Disease." *Alzheimer's & Dementia* 7, no. 3 (May 2011): 280–92. <https://doi.org/10.1016/j.jalz.2011.03.003>.
297. Putcha, D., M. Brickhouse, K. O'Keefe, C. Sullivan, D. Rentz, G. Marshall, B. Dickerson, and R. Sperling. "Hippocampal Hyperactivation Associated with Cortical Thinning in Alzheimer's Disease Signature Regions in Non-Demented Elderly Adults." *Journal of Neuroscience* 31, no. 48 (November 30, 2011): 17680–88. <https://doi.org/10.1523/JNEUROSCI.4740-11.2011>.
298. Hsia, A. Y., E. Masliah, L. McConlogue, G.-Q. Yu, G. Tatsuno, K. Hu, D. Kholodenko, R. C. Malenka, R. A. Nicoll, and L. Mucke. "Plaque-Independent Disruption of Neural Circuits in Alzheimer's Disease Mouse Models." *Proceedings of the National Academy of Sciences* 96, no. 6 (March 16, 1999): 3228–33. <https://doi.org/10.1073/pnas.96.6.3228>.
299. Walsh, Dominic M., Igor Klyubin, Julia V. Fadeeva, William K. Cullen, Roger Anwyl, Michael S. Wolfe, Michael J. Rowan, and Dennis J. Selkoe. "Naturally Secreted Oligomers of Amyloid β Protein Potently Inhibit Hippocampal Long-Term Potentiation in Vivo." *Nature* 416, no. 6880 (April 2002): 535–39. <https://doi.org/10.1038/416535a>.

300. Kamenetz, Flavio, Taisuke Tomita, Helen Hsieh, Guy Seabrook, David Borchelt, Takeshi Iwatsubo, Sangram Sisodia, and Roberto Malinow. "APP Processing and Synaptic Function." *Neuron* 37, no. 6 (March 2003): 925–37. [https://doi.org/10.1016/S0896-6273\(03\)00124-7](https://doi.org/10.1016/S0896-6273(03)00124-7).
301. Shankar, G. M., B. L. Bloodgood, M. Townsend, D. M. Walsh, D. J. Selkoe, and B. L. Sabatini. "Natural Oligomers of the Alzheimer Amyloid- Protein Induce Reversible Synapse Loss by Modulating an NMDA-Type Glutamate Receptor-Dependent Signaling Pathway." *Journal of Neuroscience* 27, no. 11 (March 14, 2007): 2866–75. <https://doi.org/10.1523/JNEUROSCI.4970-06.2007>.
302. Li, Shaomin, Soyon Hong, Nina E. Shepardson, Dominic M. Walsh, Ganesh M. Shankar, and Dennis Selkoe. "Soluble Oligomers of Amyloid β Protein Facilitate Hippocampal Long-Term Depression by Disrupting Neuronal Glutamate Uptake." *Neuron* 62, no. 6 (June 2009): 788–801. <https://doi.org/10.1016/j.neuron.2009.05.012>.
303. Fan, Z., Okello, A. A., Brooks, D. J., & Edison, P. (2015). Longitudinal influence of microglial activation and amyloid on neuronal function in Alzheimer's disease. *Brain*. <http://doi.org/10.1093/brain/awv288>
304. Esparza, T. J., Gangolli, M., Cairns, N. J., & Brody, D. L. (2018). Soluble amyloid-beta buffering by plaques in Alzheimer disease dementia versus high-pathology controls. *PLoS ONE*. <http://doi.org/10.1371/journal.pone.0200251>
305. Nuntagij, Paworn, Salvatore Oddo, Frank M. LaFerla, Naiphinich Kotchabhakdi, Ole P. Ottersen, and Reidun Torp. "Amyloid Deposits Show Complexity and Intimate Spatial Relationship with Dendrosomatic Plasma Membranes: An Electron Microscopic 3D Reconstruction Analysis in 3xTg-AD Mice and Aged Canines." *Journal of Alzheimer's Disease* 16, no. 2 (February 16, 2009): 315–23. <https://doi.org/10.3233/JAD-2009-0962>.
306. Paresce, D. M., Chung, H., & Maxfield, F. R. (1997). Slow degradation of aggregates of the Alzheimer's disease amyloid β -protein by microglial cells. *Journal of Biological Chemistry*. <http://doi.org/10.1074/jbc.272.46.29390>
307. Koenigsknecht, J. "Microglial Phagocytosis of Fibrillar β -Amyloid through a 1 Integrin-Dependent Mechanism." *Journal of Neuroscience* 24, no. 44 (November 3, 2004): 9838–46. <https://doi.org/10.1523/JNEUROSCI.2557-04.2004>.
308. Boissonneault, V., M. Filali, M. Lessard, J. Relton, G. Wong, and S. Rivest. "Powerful Beneficial Effects of Macrophage Colony-Stimulating Factor on β -Amyloid Deposition and Cognitive Impairment in Alzheimer's Disease." *Brain* 132, no. 4 (May 21, 2008): 1078–92. <https://doi.org/10.1093/brain/awn331>.

309. Majumdar, A., Capetillo-Zarate, E., Cruz, D., Gouras, G. K., & Maxfield, F. R. (2011). Degradation of Alzheimer's amyloid fibrils by microglia requires delivery of CIC-7 to lysosomes. *Molecular Biology of the Cell*. <http://doi.org/10.1091/mbc.E10-09-0745>
310. Frackowiak, J., Wisniewski, H. M., Wegiel, J., Merz, G. S., Iqbal, K., & Wang, K. C. (1992). Ultrastructure of the microglia that phagocytose amyloid and the microglia that produce β -amyloid fibrils. *Acta Neuropathologica*. <http://doi.org/10.1007/BF00227813>
311. Stalder, M., Deller, T., Staufenbiel, M., & Jucker, M. (2001). 3D-Reconstruction of microglia and amyloid in APP23 transgenic mice: No evidence of intracellular amyloid. *Neurobiology of Aging*. [http://doi.org/10.1016/S0197-4580\(01\)00209-3](http://doi.org/10.1016/S0197-4580(01)00209-3)
312. Brown, G. C., & Neher, J. J. (2014). Microglial phagocytosis of live neurons. *Nature Reviews Neuroscience*. <http://doi.org/10.1038/nrn3710>
313. Weinhard, Laetitia, Giulia di Bartolomei, Giulia Bolasco, Pedro Machado, Nicole L. Schieber, Urte Neniskyte, Melanie Exiga, et al. "Microglia Remodel Synapses by Presynaptic Trophocytosis and Spine Head Filopodia Induction." *Nature Communications* 9, no. 1 (December 2018). <https://doi.org/10.1038/s41467-018-03566-5>.
314. Paolicelli, Rosa C., Ali Jawaaid, Christopher M. Henstridge, Andrea Valeri, Mario Merlini, John L. Robinson, Edward B. Lee, et al. "TDP-43 Depletion in Microglia Promotes Amyloid Clearance but Also Induces Synapse Loss." *Neuron* 95, no. 2 (July 2017): 297-308.e6. <https://doi.org/10.1016/j.neuron.2017.05.037>.
315. Friedman, Brad A., Karpagam Srinivasan, Gai Ayalon, William J. Meilandt, Han Lin, Melanie A. Huntley, Yi Cao, et al. "Diverse Brain Myeloid Expression Profiles Reveal Distinct Microglial Activation States and Aspects of Alzheimer's Disease Not Evident in Mouse Models." *Cell Reports* 22, no. 3 (January 2018): 832-47. <https://doi.org/10.1016/j.celrep.2017.12.066>.
316. Sasaguri, Hiroki, Per Nilsson, Shoko Hashimoto, Kenichi Nagata, Takashi Saito, Bart De Strooper, John Hardy, Robert Vassar, Bengt Winblad, and Takaomi C Saido. "APP Mouse Models for Alzheimer's Disease Preclinical Studies." *The EMBO Journal* 36, no. 17 (September 1, 2017): 2473-87. <https://doi.org/10.15252/emboj.201797397>.
317. Davis, B. M., Salinas-Navarro, M., Cordeiro, M. F., Moons, L., & Groef, L. De. (2017). Characterizing microglia activation: A spatial statistics approach to maximize information extraction. *Scientific Reports*. <http://doi.org/10.1038/s41598-017-01747-8>

318. Valentin, Jolene E., Ann M. Stewart-Akers, Thomas W. Gilbert, and Stephen F. Badylak. "Macrophage Participation in the Degradation and Remodeling of Extracellular Matrix Scaffolds." *Tissue Engineering Part A* 15, no. 7 (July 2009): 1687–94. <https://doi.org/10.1089/ten.tea.2008.0419>.